NTNU – Trondheim
Norwegian University of
Science and Technology

Stability assessment of underground parking cavern in Hammerfest

Martin Dyhrberg Pettersen

Geotechnology
Submission date: June 2014
Supervisor: Krishna Kanta Panthi, IGB
Co-supervisor: Harald Sverre Arntsen, SWECO Narvik

Norwegian University of Science and Technology
Department of Geology and Mineral Resources Engineering

NTNU
Norwegian University of
Science and Technology

Department of Geology
and Mineral Resources Engineering

Your ref.: MS/N17T28/IGB/MDPKKP

Date: 13.01.2014

TGB4930 INGGEOL/BERGMEK - MSc thesis

for

Eng. geo. student Martin Dyhrberg Pettersen

STABILITY ASSESSMENT OF UNDERGROUND PARKING CAVERN IN HAMMERFEST

Background

Underground caverns and tunnels used for day to day public must full fill high level of safety standards. Any failures on the walls and roof of the underground structures must be avoided including failure to the applied rock support, rock fall and water ingress. Therefore, it is important that these underground structures must be investigated and assessed with high degree of accuracy before excavation started and during the construction phase.

An underground parking cavern is planned to be constructed at Hammerfest. The candidate has carried out pre-feasibility study as a project work. In addition to the information gathered from earlier studies, the candidate himself was engaged to carry out engineering geological field mapping and laboratory assessment of the rock samples. The evaluation on the placement of underground cavern is also carried out. However, more study is needed to be carried out covering stability assessment of the cavern and analysis on the needed rock support requirement.

MSc thesis task

Therefore, this MSc thesis is intended to carry out detail stability assessment of the proposed underground parking cavern in Hammerfest and shall address following issues:

- Through theoretical review on the stability issues for underground caverns
- Present two large scale caverns that were built in Norway during last 30 years. Discuss major challenges related to the stability and safety, investigations, use of rock supports and monitoring installations;
- Present size requirement, topographic and geological conditions of the case under study in this thesis.

- Carry out kinematic assessment of the cavern to identify possible areas with wedge fall.
- Carry out stability assessment using empirical and analytical approaches. Estimate and optimize permanent rock support requirement including mitigations related to water inflow.
- Carry out 2D numerical assessment consisting both wedge un-wedge and Phase 2.
- Assess potential groundwater drawdown mitigation and discuss on the frost protection measures.
- Finalize the rock support requirement, estimate quantities of different rock supports.
- Discuss construction aspect of the underground cavern and estimate required construction time.

Relevant computer software packages

Candidate shall use *roc-science package* and other relevant computer software for the master study.

Background information for the study

- The information provided by the supervisors.
- Information, field and laboratory test data collected by the candidate during autumn 2013.
- Scientific papers, reports and books related to hydrogeology, engineering geology and tunnelling

Cooperating partner

Sweco Narvik is the cooperating partner. Mr. Knut Karlsen is the contact person for needed further information for the project.

The project work is to start on January 13, 2014 and to be completed by June 10, 2014.

The Norwegian University of Science and Technology (NTNU)
Department of Geology and Mineral Resources Engineering

January 13, 2014

Krishna Panthi

Dr.ing. Krishna K. Panthi
Associate Professor of geological engineering, main supervisor

Acknowledgment

Foremost, i would like to sincerely thank Dr. Krishna Panthi for Supervising the work with this Master thesis.

Additionally a great thank you is given to cooperating partners SWECO AS Narvik, especially Harald Sverre Arntsen and Knut Karlsen Norway for making the project possible.

Finally I would like to thank the class of 2009-2014 in engineering geology at NTNU for contributing with comfortable work environment, enlightening discussions and many great moments up to this point.

M.D.P

Summary

This thesis addresses in detail the stability of the planned parking cavern in Hammerfest. It includes a review on recognized literature of support design for underground constructions, frost issues in tunnels, water inflow and mitigation, numerical modelling, and general stability of underground caverns. Studying the local and regional geology reviled that the rock mass is mainly composed of gneiss, with some small amount of quartzite. The rock mass is expected to be strong (RMR>60, Q>10) but encountering a zone of weak rock mass(Q<0.01) is anticipated. Two cases of underground facilities in Norway are reviewed with emphasis on key experiences, support requirement, and monitoring.

Support needed for the Hammerfest parking cavern is suggested by analytical, empirical approaches. Finalized rock support measures are quantified and tested with numerical modelling. The cavern is expected to be sufficiently supported with rock bolts and shotcrete. However, if weak rock is encountered, reinforced shotcrete arches and spiling bolts will be needed.

Kinematic assessment is carried out identifying possible failing wedges in the roof and walls. Leakage of water is discussed and consequences of draining surface ponds are evaluated. Some leakage is expected in the cavern based on field observations however, levels are generally anticipated as dripping. Ahead-of-face investigations are concluded necessary to identify possible high water conduction near the weak rock mass zone. There will be need for grouting should the water leakage exceed quantified limits given in the thesis.

Frost intrusion to the cavern is modelled and discussed. It has been recognized that frost will enter the cavern and sufficient mitigation is suggested.

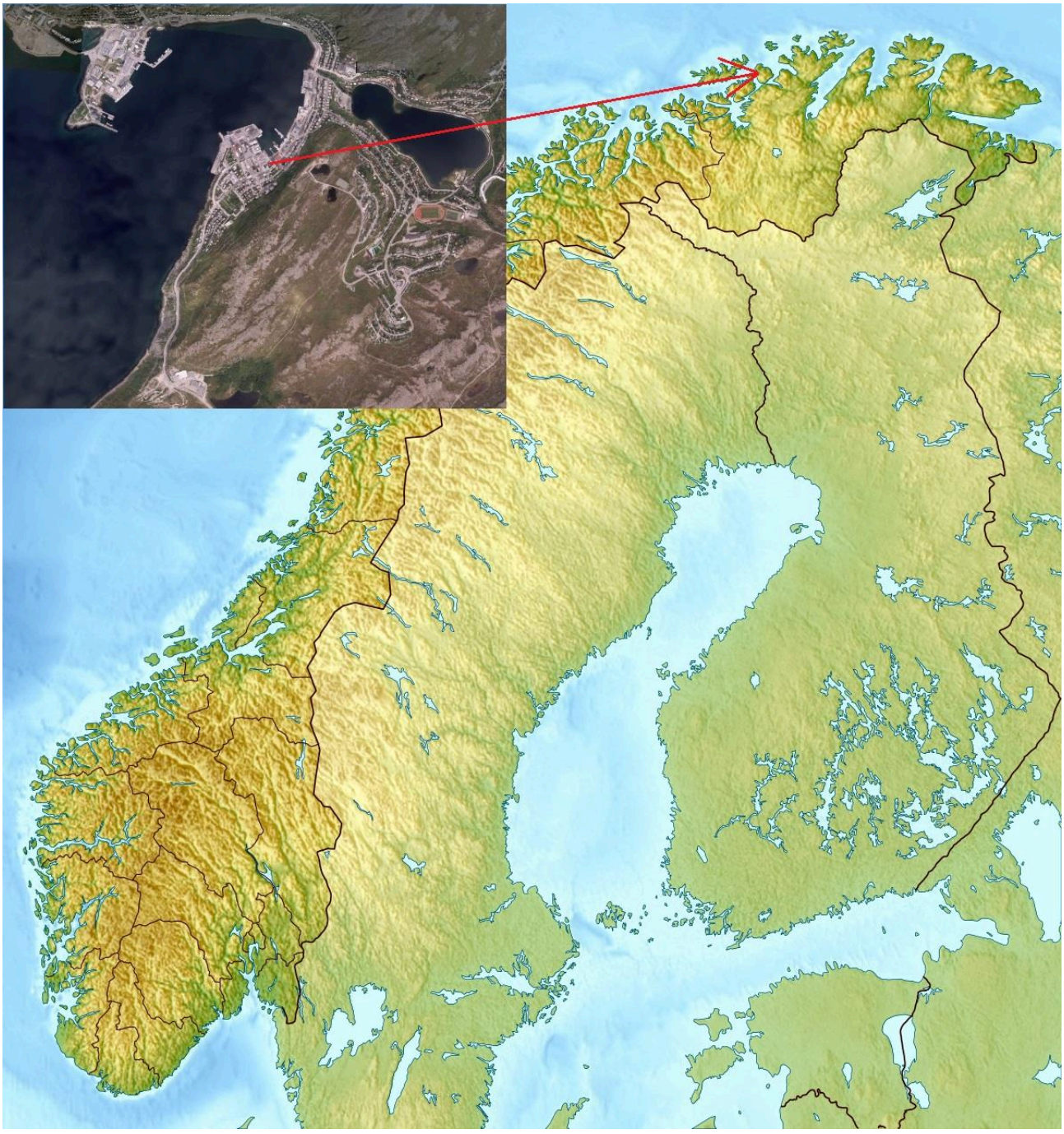

Sammendrag

I oppgaven har det blitt gjennomgått faglitteratur om numerisk moddelering, ingeniørgeologiske metoder for dimensjonering av sikring, frost problematikk, vanntiltak, og stabilitet av fjellanlegg. Områdets geologi er studert og kartlagt på befaring, og består i hovedsak av av gneis og mindre deler kvartsitt, der største delen av berget er av god kvalitet, dvs. RMR>60, og bergklasse B. Det forventes påmøte av svakhetssone som skissert i vedlegg A. Sonens oppførsel i fjellet er usikkert og burde kontrolleres med sonderboringer. Det har blitt studert to eksempler av undergrunnsanlegg i Norge, og viktig problematikk, sikring, og overvåkning har blitt drøftet.

Sikring er foreslått og diskutert med bagrunn i analytiske, og empiriske metoder, og er modellert med numerisk verktøy. Det forventes å kunne sikres med bolter og sprøytebetong, og for dårlig berg vil det vil bli behov for sprøytebetongbuer og forbolting. Analyser er blitt utført som bekrefter sikringens egnethet.

Kinematisk analyse har identifisert mulige blokker i heng og vegger. Vannlekkasje til anlegget er diskutert og følgende konsekvens for drenasje av overflatevann er blitt drøftet. Det forventes behov for injeksjon i områder rundt svakt berg skulle sonderbringer vise sterk vannlekkasje. Noe vann er ventet å være tilstede i bergmassen. Tidsbetraktninger er diskutert med bakgrunn i erfaringstall.

Det har blitt gjort vurdering av frostinntrenging til hallene. Undersøkelsen viser at frost er påventet med ventilasjon som beskrevet i forprosjektet. Det er i tillegg foreslått nødvendig frostsirking for annlegget.

Contents

List of Figures

List of Tables

1. Introduction

1.1 Background

One characteristic of today's large construction projects in urban districts is that demand for vacant areas are increasing. This is very much the case in down-town Hammerfest, a city in Northern Norway of about 10.000 inhabitants, where demand for available parking is at a high in a city centre lacking available area for spacious facilities such as large parking lots.

To meet the increasing need for parking space, Hammerfest commune has completed a pre-feasibility study on the construction of a large underground cavern located in the small mountain Salsfjellet just south end of the city centre. The study was carried out in May-June 2013, by SWECO AS Norway. The target of the study was to create solutions for a parking cavern located in Salsfjellet based on clients suggestions, develop main principles for design of the cavern, investigate geological and constructional conditions in the project area, and estimate the costs of the project. When built, the full scale cavern will be able to house 1038 regular vehicles in addition to 33 reduced mobility spaces, spread out over a 28 000m^2 area.

1.2 Thesis Tasks

The overall task of this master thesis is to carry out detailed stability assessment of the proposed underground parking cavern in Hammerfest. The thesis will present and discuss two large caverns of built in the last 30 years in Norway with emphasis on

major stability challenges, safety, investigations, need for support and monitoring. The Hammerfest parking cavern will be presented in terms of geometry and size, geological and tectonic conditions.

The study involves carrying out multiple analysis on the stability of the cavern through the various approaches stated below.

- Conduct an evaluation of block fall problems through software code Unwedge.
- Present a stability assessment with the use of empirical and analytical approaches that includes suggestions rock support and water mitigation.
- Analyse the cavern stability in weakness zone using code Rocsupport.
- Investigate support performance in 2D finite element numerical modelling with software $Phase^2$. Finalize support requirements and estimating amounts of rock support.
- Investigate the level of frost that will enter the cavern based on proposed ventilation scheme and determine how much frost insulation will be needed.
- Assessing the impact of draining the pond Salsvannet will have on the surroundings.
- Further discuss the constructional aspects and assess construction time.

1.3 Available data

Data available for the study is:

- Engineering geological report from may 2013.
- The project thesis, used as background for the Master thesis.
- Note from field visit performed by Sweco in May 2013.
- National and internationally relevant and recognized literature.
- Digital maps, sketches and drawings provided by SWECO AS.

- The pre-feasibility study carried out by SWECO AS may 2013, including ventilation concept for the facility.

2. Factors that contribute to stability of underground constructions

2.1 Rock mass as a building material

Anticipating rock mass behaviour is complex. Principally one wishes to benefit from the ground's ability to support itself. Since rock is a very abundant material, achieving the goal means vast cost savings when considering many underground constructions. This method of design approach proves crucial in sparsely populated Norway, which has difficult topography but geology much suited for underground construction. Sufficient knowledge of factors that impacts the stability of constructions is the only way one can successfully apply this principle and be left with a cost effective underground alternative competitive to surface based solutions.

2.2 Jointing and fracturing

Often one tends to rely on the results from lab tests when describing the characteristics of a rock in a project area, but not only intact rock strength dictates the conditions from a constructional point of view. Rock mass is in most cases not at all intact, but intersected with one or more sets of discontinuities, joints or fractures. Discontinuities are often created by large scale geological processes or follow planar attributes within the rock and hence tend to make up repetitive sets. Several geological processes happening over large periods of time give the possibility for mutliple fracture sets carving the rock mass. The rock is in most cases weaker along

discontinuities which impacts the stability when excavating in it, requiring mitigation in most cases where human activity is anticipated. Investigation of an areas fracture properties is important for the design and construction of the underground facility. Such investigations are usually made in field by a geologist before detailed planning of a project is commenced where the features of the rock mass is mapped in detail. Field mapping is used for in all cases where it is applicable but there are instances where rock outcrops are not accessible. Projects concerning underwater tunnels or landscapes completely covered in soil are two instances requiring alternative methods of investigation such as seismic surveys or borehole logging.

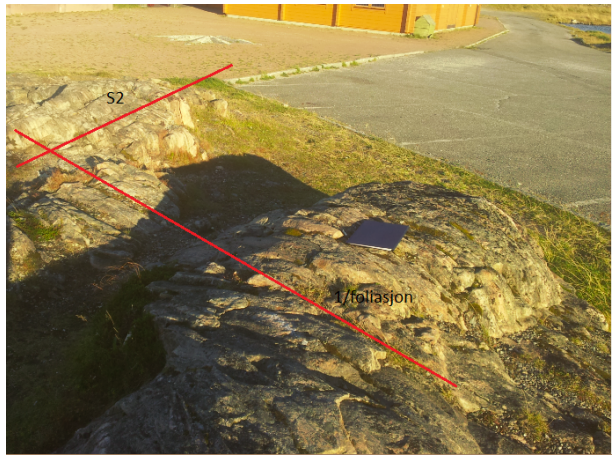

Figure 2.1: Example of jointed rock mass in Hammerfest, Norway.

A large advantage with surface exploration is the low cost and the easy nature along with good classification schemes and large amounts of literature on how to interpret structures in field. The challenge is that the rock characteristics naturally varies from exposed outcrops to tunnel elevation. In most cases there is worse rock quality at the surface where weathering has been occurring however, the opposite has been observed. Strong and resisting rock mass may be accessible as outcrops but worse conditions is found during construction if weathering is extensive. An example is the Vaere Tunnel in Trondelag, Norway (Adresseavisen[online], 2004).

2.3 Weakness zones

Weakness zones are larger scale zones characterized by impaired quality rock mass. The structures may vary in thickness and lengthwise range from a few metres to several kilometres. They are typically detected as lineaments or depressions in the terrain and is usually be identified by studying aerial photos. Field exploration is crucial in analysing the zones and investigating traits such as presence of clay, geometrical features and character of the material. Such formations is often caused by faults, geological boundaries, weathering of weak minerals or increased joining as a result of tectonics. Material impairment can vary from being lower strength rock mass to act completely as a soil. Weakness zones pose a direct threat to the stability of an underground construction and mapping of them is important before excavation is initiated. It is experienced that weakness zones traditionally contributes to most problems in underground constructions in Norway (Palmstrom et al., 2003). Therefore when planning it is favourable to avoid them. Weakness zones has in the past caused problems as severe as face collapse during construction when not handled properly. Further they may contain high water pressures or weak material that can fall into an excavation in progress. Chemically they may contain sub-tropical deep weathering layers harbouring swelling clay which is problematic for traditional mitigation used in Norway.

2.4 Stresses in the subsurface

Unfavourable or high stresses around and underground opening will enhance problem aspects throughout construction. High stresses are mostly an issue in deep excavations where weight of overlaying rock mass results in high vertical stresses. Tangential stresses around the excavation opening may challenge the stability of the rock mass and could produce hazardous phenomena such as rock burst, spalling, scaling, or squeezing. Myrvang (2001).

Vertical stresses at a certain depth in the subsurface can be estimated as a function of

depth with the following formula (Myrvang, 2001), e.g the weight of the overburden:

$$\sigma_v = \rho \times g \times h$$

where
σ_v is the vertical stress.
h is the depth below surface.
g is the gravitational constant.
ρ is the rock density.

Based on Hooke's law and the deformation modulus E one can estimate the according horizontal stress for the given depth caused directly by the vertical stress.

$$\sigma_h = \sigma_v \times \frac{\upsilon}{1-\upsilon}$$

where
σ_h is the horizontal stress.
and υ is poisson's number.

The formula above estimates theoretical horizontal stress induced by the overburden and the elastic properties of the rock. Realistically many other factors contributes to further accumulation of horizontal stresses as discussed in Myrvang (2001). In Norway for instance, geological conditions tend to dominate the horizontal stress regime in old Precambrian rock types. Factors resulting in elevated magnitudes of horizontal stress can be a result of isostatic uplift, tectonics, or tension related to folding structures. Practically one usually investigates stresses by doing in-situ testing such as hydrofracturing or the Doorstopper method, if data from nearby excavations is not at hand. High stresses may however also be discovered in cores from boreholes by a phenomena called core-discing where rock breaks when brought to the surface relieved of the subsurface stress, or by studying borehole offsets in fresh road cuts (Pascala et al., 2005).

2.5 Groundwater and environmental impacts

An advantage of building under ground is the reduced visibility from human intervention when comparing to surface facilities. Should an underground facility influence the environment around it negatively, many of the obvious benefits from building under ground loose their purpose. Unfortunate effects could be groundwater lowering resulting in dried out creeks and rivers, increased landslide activity, and loss of flora and fauna. The first point embodying the possibility for surface settlement and damage to vulnerable buildings in soil, and for deep constructions also rock (Loew et al., 2010). Effects could also be creating problems for an excavation in process. Water inflows could damage personnel, equipment and cause great delays along with additional cost. Some facilities require no water present in the excavation for safety reasons in the operational phase. In Norway, injection of cement-based solutions into the rock mass, called grouting, is used to control the water leakage.

Predicting rock conductivity in regard to water has proven very hard due to unpredictable behaviour of water inside a given rock mass along with large areas of investigation (Loew et al., 2010). Usually the most reliable method of gaining knowledge is by in-situ testing such as the Lugeon test however, there are ways of early predicting water inflows.

From Snow (1965) water carrying channels in a rock mass may be viewed as flow between two parallel smooth plates where flow can happen freely as a function of difference in hydraulic head.

$$Q = \frac{g \times a_h^3}{12v} \times \frac{dp}{dl} \times w$$

where Q is the rate of laminar flow, g is the gravitational constant, a_h is the dilation of the plates, v is fluid viscosity, dp/dl is the hydraulic gradient, and w is the width of the fracture.

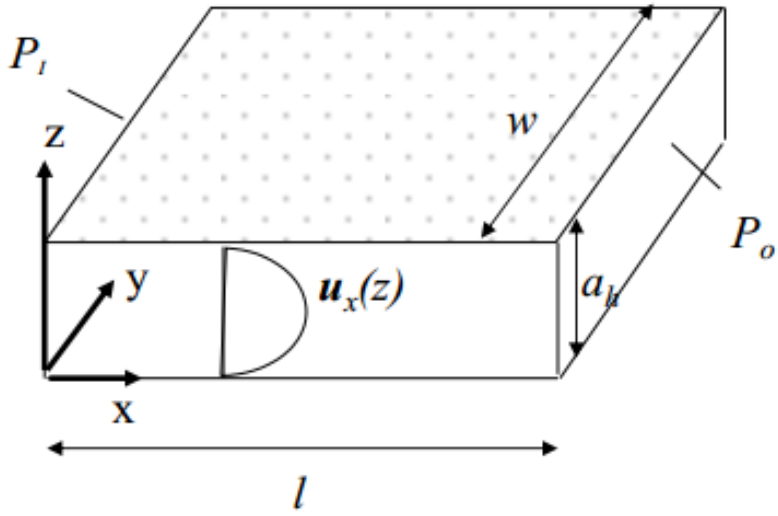

Figure 2.2: Simplified model of flow in fractures (Loew, (2013).

Realistically, fracture planes are not sufficiently represented by planar smooth parallel plates. By instead looking at rock mass as a permeable material with hydraulic conductivity K depending of fracture properties, one can estimate water inflow to a tunnel by utilizing equations of Prabhata et al. (2000) using the following function (Loew et al., 2010).

$$Q(t) = \frac{4\pi KL(h_e - h_t)}{2.3\log(2.25KL/S_r^2)}$$

where t is time, K is effective radial hydraulic conductivity, L is tunnel length of the evaluated section, h_e–h_t is difference in hydraulic head and S is the storativity, which after Loew et al. (2010) typically is set to $10^{-6}m^{-1}$ for crystalline rock mass. Figure 2.3 shows a sketch of the model.

Dripping will occur in most cases where one has water present in the rock mass. More severe water issues such as catastrophic inflows are usually encountered when bad quality rock mass is connected to surface water systems, often in shallow facilities, but

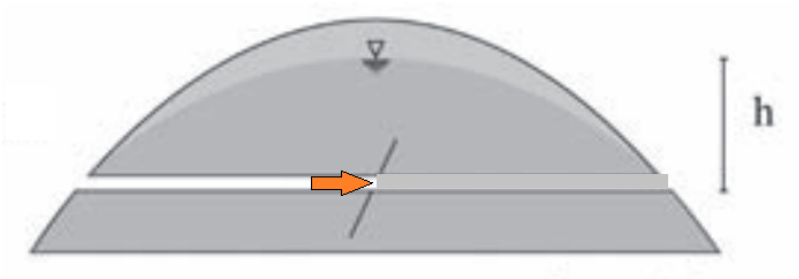

Figure 2.3: Simplified model for water inflow during construction phase. Modified after Loew et al. (2010)

can also be caused by highly conductive rock mass under enormous water pressures deep in the sub surface. During excavation of deep tunnels, high water pressures can cause problems with serious consequences in regards to progress and safety. An element to consider is that the cumulative amount of water inflow often is controlled by a few strongly conductive zones as observed during excavation of the Lötschenberg Base Tunnel (Loew et al., 2010).

2.6 Strength of rock

2.6.1 The Mohr-Coulomb criterion

Mohr-Coloumb criterion is a theoretical solution for the failure of brittle materials. In geotechnical engineering the Mohr-Coulomb criterion is the most common way to predict failure of brittle rock and is used in a variety of disciplines and for a range of materials. The criterion predicts that an intact material under stress experiences shear failure when shear stress exceeds the shear strength of the rock. The material experiences maximal shear stress before failure equal to half the difference between the two principal stresses as following Hooke's law (Myrvang, 2001).

$$\tau_{max} = \frac{\sigma_1 - \sigma_2}{2}$$

Where τ_{max} is the maximal shear stress.
$\sigma_{1,2}$ is the two principal stresses in a 2D stress situation.

The Mohr-Coulomb criteria regards rock as having inner friction. This results in that maximal effective shear stress in the failure plane is shifted from the plane with maximal shear stress because the normal stress σ_n in this plane is too large. The "weakest" plane in the Mohr-Coloumb criteria is thus defined as the plane with maximum shear stress plus the inner friction angle of the rock.

$$\theta = 45 \pm + \frac{\phi}{2}$$

where θ is the angle of the failure plane to the principal stresses.

Now the Mohr-Coulomb failure criterion can be defined as

$$\tau_{at\ failure} = c + \sigma_n \times tan(\phi)$$

and further

$$\sigma_1 = \frac{2c + \sigma_3(\sqrt{u^2+1} + u)}{\sqrt{u^2+1} - u}$$

Where $u = tan(\phi)$.
c is the cohesion, or the shear strength of the rock.
σ_n is the normal stress on the failure plane.
and ϕ is the inner friction angle of the rock.

The Mohr-Coloumb criteria is simple and easy, and is used as an option of predicting failure both in theoretical analysis and in numerical modelling. Usually one would use the criteria if one believes joints and fractures plays little part in the failure of a

material. Examples may be problems where small cross section tunnels are built at deep elevations, and that rock is anticipated to fail along an internal shear plane rather than in the pre-existing joints and fracture planes. In other problems where failure is expected in fractures and joints, one would usually tend to the Hoek-Brown failure criterion. Defining the Mohr-Coulomb criterion for a rock at different enclosed pressures makes it possible to create a failure envelope, and gives the ability to predict failure at different stress environments in your project.

2.6.2 The Hoek-Brown criterion

Since at the time in 1980 no suitable solution for obtaining estimates of fractured rock mass strength existed, Hoek and Brown (1980) proposed a failure criterion for jointed rock mass. It was initially based on failure in fracture planes and interlocking blocks, and internal rock failure was neglected. After several modifications a general criterion for jointed rock mass is proposed in Hoek et al. (2002), also including suitable correlation with Mohr-Coulomb parameters.

Even though the Hoek-Brown failure criterion is vastly used in the industry, a large part of software for civil engineering projects is based on Mohr-Coulomb theory (Hoek et al., 2002), and thus the Hoek-brown criterion today may be used as a tool to estimate equivalent strength parameters for a rock mass as one would define them for an intact rock. The following equation is evaluated as the failure criterion.

$$\sigma_1 = \sigma_3 + \sigma_{ci}(m_b \frac{\sigma_3}{\sigma_{ci}} + s)^a$$

where

σ_1 and σ_3 are the principal stresses.

σ_{ci} is the uniaxial compressive strength of intact rock.

m_b, s and a are material constants that can be evaluated from known rock

classifications schemes as follows.

$$mb = exp^{\frac{GSI-100}{28-14D}}$$

$$S = exp^{\frac{GSI-100}{9-3D}}$$

$$a = \frac{1}{2} + \frac{1}{6}(e^{\frac{GSI}{15}} - e^{\frac{-20}{3}})$$

where
GSI is the geological strength index.
D is the surface factor which is an adjustment for the quality of the rock surface.
This makes the Hoek brown failure criterion partly empirical and open for subjective opinions from the analysing engineer which may be considered a weakness. Keep in mind that the analysis will not be more correct than the input parameters, and thus the outcome of the criterion will encompass uncertainties in the empirical classifications schemes used to obtain the various parameters.

Because of naturally occurring variations in rock mass strength properties, no failure criterion can be considered absolute.

2.6.3 Rock mass strength

In most cases concerning moderately to highly fractured rock surrounding a cavern, failure will occur along fracture planes. In Scandinavia good quality rock is most prominent and rock strength regarding failure as described above can be called the "spalling strength" of the rock mass (Martin and Christiansson, 2009). As most failure criteria builds on rock mass strength, it is of great usefulness to have methods of estimating a rock mass strength. Martin and Christiansson (2009) showed in different experiments that rock mass strength would be approximately $0.58UCS \pm 0.2MPa$. However, as argued by Panthi (2012) the formula presented below based on further studies in the Himalayas to predict spalling strength was found better suited.

$$\sigma_{cm} = \frac{\sigma_{ci}^{1}.5}{60}$$

2.7 Common rock mass classification systems

2.7.1 Usefulness of classification systems

Worldwide there is a number of ways to classify a rock mass with regard to it as a building material. Rock mass will over large areas represent itself as a somewhat chaotic system, where ideal conditions and analytical approaches deem hard to benefit from alone with sufficient correctness. Knowing this, designing rock support for underground constructions has proven successful with empirical approaches. Today such approaches are used together with analytical foundations to design support measurements for underground openings and predict the behaviour of rock mass with desired level of satisfaction.

Classification systems can prove weak when applied wrongly. The weakness lies within the fact that one is defining an entire rock mass with usually only a few parameters that is easily defined in field. Its use is often restricted to surface exploration where the subsurface can prove to be both much better or worse than what is expected. Another criticized aspect is that instead of investigating the rock mass by utilizing engineering knowledge along with thorough interpretation of the geology, the classification schemes give a superficial and subjective report on geological conditions. Since the schemes are simple in nature, the danger of neglecting important problematic features in an area is present. A typical example is the Være-tunnel in Trøndelag where prediction of fair-good rock mass from surface exploration was done using mainly the Q-method. Conditions during excavation proved to be much worse. A possible explanation could be that intact and strong rock was visible at the surface with the weaker rock being weathered away overlain by soil cover, making it practically invisible. It could be that relying too strongly on the Q-method in this case caused surprises when actually excavating.

Figure 2.4: The Være-tunnel in Norway had stability issues both in constructional and operational phase due to difficult rock conditions. The picture is taken from the local newspaper after unstable rock mass had fallen on to the road (Adresseavisen[online], 2004).

2.7.2 Bartons Q-system

There are several systems available for the engineering geologist to help predict rock mass behaviour.

In Norway the Q-system plays a large part in the design process of underground excavations. It is based on 6 values assessed in field or on the tunnel face. The Q-value has been proven to correlate well with the need for rock support through data from over 200 underground excavations (Barton et al., 1974).
The Q-value for a rock mass can be obtained with the following formula.

$$Q = \frac{RQD}{J_n} \times \frac{J_r}{J_c} \times \frac{J_v}{SRF} \quad (1)$$

Where

RQD – rock quality designation
J_n = joint set number
J_r = joint roughness number
J_a = joint alteration number
J_w = joint water reduction factor
SRF = Stress Reduction Factor

When an engineering geologist has assessed the different input parameters the Q value is obtained from the formula above (1). The spectre of Q-values 0.001<Q<1000, embodies all rock mass qualities (Barton et al., 1974). With a thoroughly assessed set of Q- values one can predict the need for rock support from an empirical scheme. Figure 2.5 shows a sketch for support estimation from NGI Norway.

The Q-method accounts for additional elements in the SRF (Strength Reduction Factor), an empirical value determined from a list of typical rock mass behaviours (Loeseth and Kveldsvik, 1997). These categories take faults/weakness zones, stress factors, rock burst phenomena, sqeezing phenomena, and rock swelling in to account in order to predict more realistic results (Loeseth and Kveldsvik, 1997). The Q-system is criticised for not including joint orientation in the classification. Undeniably, several additional parameters and considerations could have been included in the Q-system. It is however believed that parameters Jn, Jr, and J_a plays a larger role in the stability by that resistance characteristics of joins exceed the importance of the orientation, and number of sets decides the freedom of blocks to move. By incorporating joint orientation as additional parameter the classification scheme could loose its essential simplicity.

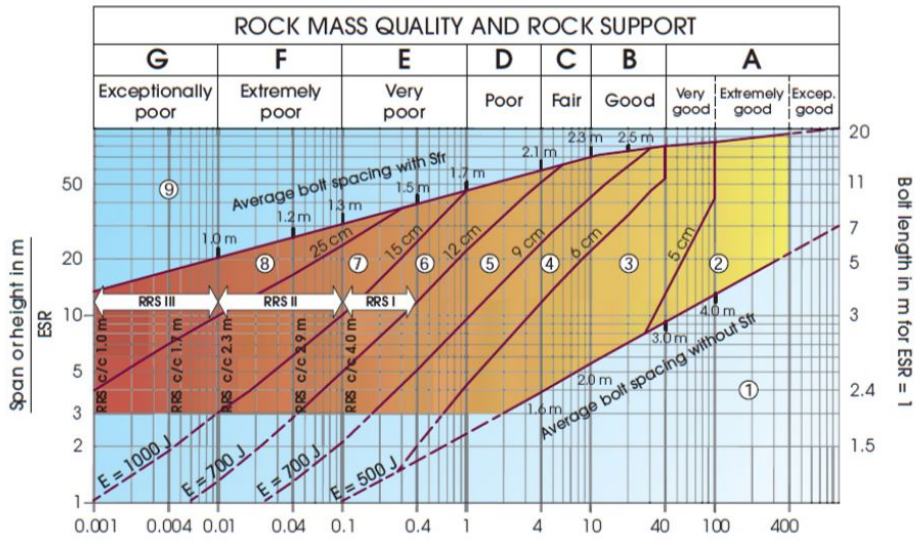

Figure 2.5: Suggested permanent rock support using the Q-system (NGI[online], 2013)

.

2.7.3 GSI system

The system was first introduced by Alfred Hoek in 1994, and later 1995 and 1998. It bases on the concept of identifying a state of the rock mass from field observations visually, and give a GSI value based on descriptions of different common rock conditions (Hoek et al., 1998). The system bases on rock surface visual traits and rock surface conditions.

In order to obtain a GSI value for a given geology one compares the rock mass to a chart in which different types known structural formations are sketched and explained. By visually classifying the rock mass in one of five categories, a GSI value range is given on basis of surface and weathering conditions. Figure 2.6 shows the updated version from Hoek et al. (1998). The GSI system are based primarily on investigations in South Africa. Accordingly the scheme may not be as representative

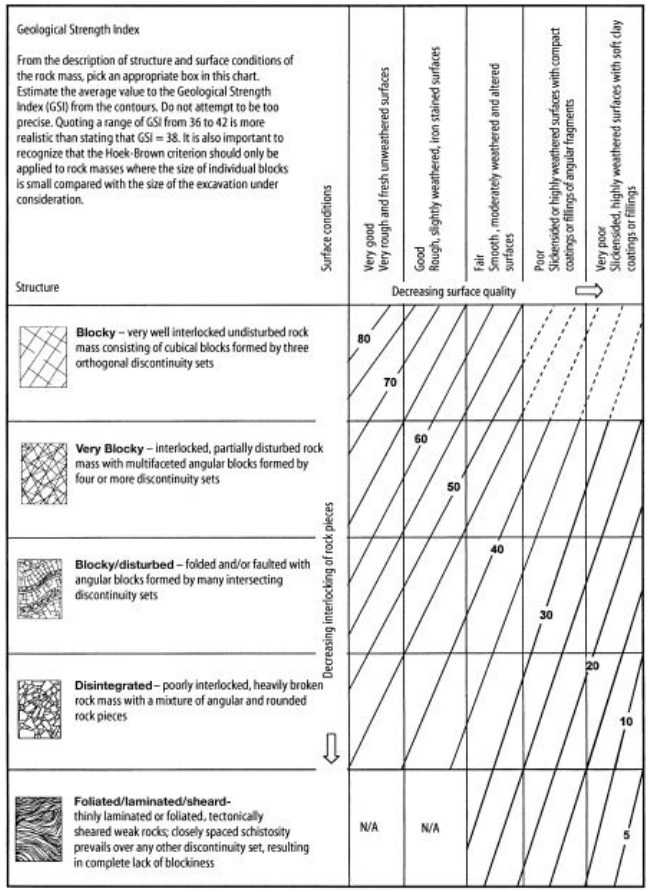

Figure 2.6: Application for the GSI classification (Hoek et al., 1998)

.

for geological conditions in other places of the world.

One of the main principles in the GSI system the correlation to Hoek - Brown failure criterion for rock mass. It is very helpful to be able obtain the strength of a rock mass similarly to defining intact rock strength in a lab. It is very important to keep in mind that parameters in field are not as precisely measured as in a lab, and in general one should give values in intervals. A big advantage is that most common rock engineering software incorporates it as a way of predicting rock mass strength. Some factors are important to consider if planning to use GSI as a method of predicting rock mass properties. Deciding if it is applicable is important and it should only be used for rock mass that you expect to fail in fractures and joints. It can be difficult assessing GSI

ahead of face or with only borehole information if the geologist is not of significant experience. In other words it is important that one practises objective and logical reasoning along with general geological knowledge when applying the system, and that limitations are kept in mind.

2.7.4 RMR system

Bienowski (1976) published what he called the Rock Mass Rating. It has later been modified and changed to fit new measurements and discoveries. Like the Q-system, it has six easily definable parameters assessable in field by a geologist.

- RQD - Rock Quality Designation
- UCS - Uniaxial compressive strength
- Spacing of discontinuities
- Condition of discontinuities
- Groundwater conditions
- Orientation of discontinuities.

Each input group is given a value from empirical descriptions and magnitudes of occurrence, and a final RMR-value is calculated by the sum of individual values.

One clear weakness of the RMR system is the lack of stress consideration, and under certain unfavourable stress conditions the RMR system would prove to be almost worthless in regards to predicting the stability of the underground opening. Using solely the RMR classification scheme one would have to include such considerations in the final evaluation which requires experience from the engineer or geologist performing the classification. Some support requirement correlation exists with the RMR system but application is specified for a pre-determined span width, and thus will not be explained further in this thesis.

2.8 Typical stability issues for shallow constructions

Several elements with shallow laying tunnels or caverns can potentially cause problems during construction or in operational phase. In general regarding water inflows and environmental impacts, is that surface near facilities will be more exposed to surface phenomena such as rivers and weathering.

According to Alvarez (2012) assuming isotropic stress conditions for shallow tunnels is inaccurate in many cases since vertical stress is low an horizontal stresses can vary around a large spectrum. Effects of this can prove both advantageous and disadvantageous. Types of phenomena one avoids in shallow facilities are rock burst and squeezing. These phenomena require great circumferential stress in the rock. However, tensile failure in roof can provide difficulties if horizontal stresses are low and extensive block failure occurs in bad rock mass not being properly "held together" in shallow localities.

2.9 Challenges of tunnelling in the Arctic

Underground excavation in northern regions presents special challenges related to climate. The location of Hammerfest at N70°exposes the city to sub-zero temperatures large periods of the year. Weather statistics from the Norwegian Meteorological Institute show average sub-zero temperatures lasting from November to late April. These conditions must be taken in to consideration when designing larger underground excavations. Neglecting frost issues can result in a range of problems with respect to both construction and operation of the facility. Problems related to frost concerns freezing of water and may induce instabilities such as block fall. Slippery conditions in road tunnels are hazardous, damage to electrical systems in railway tunnels, and accumulation and blocking of drainage channels are more examples of unfortunate outcomes.

Figure 2.7: Illustrative photo from a road tunnel ruined by ice, near Øksfjord in Finnmark. The Øksfjord-tunnel is deemed the "tunnel of shame" by the director of the Norwegian newspaper Altaposten. (Altaposten[Online], 2013).

2.10 Freezing in rock: Frost mechanics

Frost related problems in tunnels are largely dependent on the presence of water. Water expands 8-9% when frozen, and volumetric expansion continues until -22°C (Pedersen, 2002). Around the underground opening there will in many cases be pores containing water. Rock close to the opening will be sensitive to the temperature inside the cavern, and water lenses will start to form in the near laying rock as shown in figure 2.8. Expansion of water could destabilize blocks at the excavation surface.

Frost load F_{10}s (h*°C) is defined as the magnitude of frost that statistically will be exceeded once every ten years. Design of frost mitigation in Norway for tunnelling projects depends on the size of the frost load factor F_{10} defined as the negative temperatures integrated with respect to time throughout an average year and may

estimated with the simplified equation below (Pedersen, 2002).

$$F = 730 \times \sum(\upsilon_{month})$$

Where F is the frost magnitude in h*C°, and υ is monthly average temperature with the requirement $\upsilon_{month} \leq 0$ according to the definition (Pedersen, 2002).

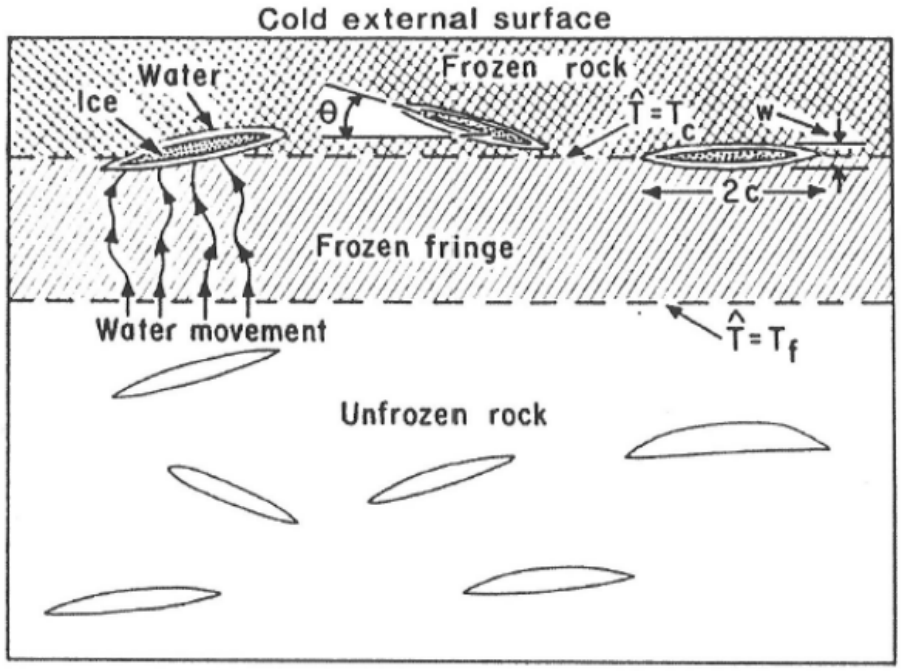

Figure 2.8: Illustration of frost lenses forming around underground openings (Pedersen, 2002).

Hammerfest has a frost magnitude of approximately F_{10} = 24 000 h°and F_{100}=34 000 h°C (Byggforsk and Meteorologisk Institutt, 2012). The latter indicates the magnitude of frost that will statistically be exceeded once every 100 years. As a rule of thumb the amount of frost inside the underground excavations is made equal to the frost magnitude outside at every time for short tunnels in Norway. If however it is possible to show that the amount inside will be significantly less, the design value for frost mitigation can be adjusted to a lower value representing the magnitude inside the excavation. For road tunnels in Norway shorter than 500m the frost mitigation is

always designed with respect to the frost magnitude coefficient F_{10} in the area due to the large insecurities related to frost intrusion in tunnels. Some localities are subjected to lower temperatures than what is typically given for a county or a region, and thus will design frost factor F_{10} also need to embody such variations.

In brief this means that one usually designs the frost mitigation as if outside and inside temperatures are the same for >500m tunnels.

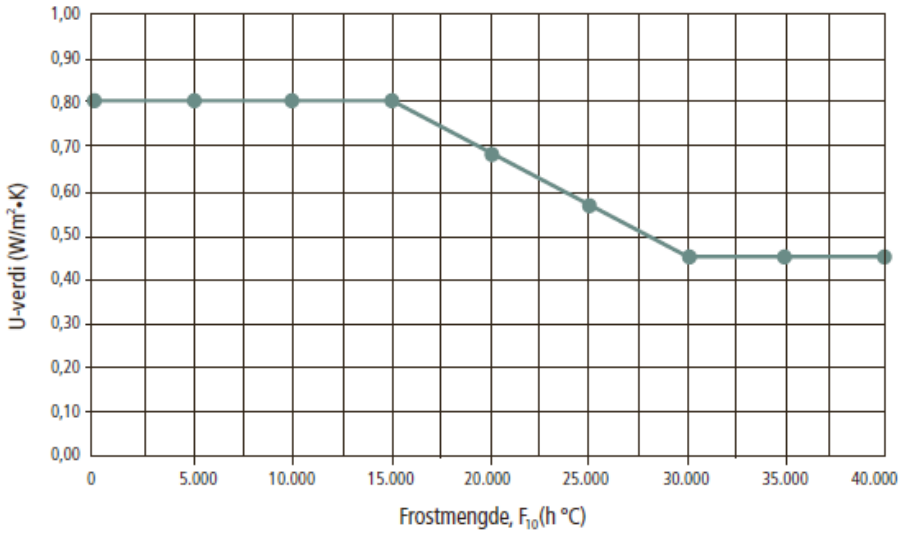

Figure 2.9: Limits for U-value or overall heat transfer coefficient, dependant on the frost magnitude F_{10} from the Norwegian road authorities (Statens Vegvesen, 2006).

The interaction between water and ice is of importance when designing drost mitigation in underground constructions. A drainage channel is most often leading water to a ditch along the tunnel lining, making it vulnerable to subzero temperatures. Frozen water in the drainage systems may damage the lining and may require extensive maintenance work. To avoid this the drainage system is made insulated if freezing temperatures are expected to exceed given limits. The limits are for road tunnels controlled by the road authorities (Statens Vegvesen, 2006) in Norway, and depends on the average frost magnitude F_{10} factor as discussed earlier. Figure 2.9 shows the given limits for maximum heat transfer through an underground facility by

giving a design U-value (W/m^2K). The design U value gives the thermal characteristic the frost insulation layer should have.

2.11 Frost control in tunnelling

All road tunnels in Norway requires frost- and water-mitigation according to standards of the national road service (Statens Vegvesen, 2010). This will most likely also apply to the Hammerfest parking cavern. Should frost magnitudes exceed the tolerated limits, mitigation will have to be designed.

Design of frost mitigation in Norway follows from Handbook no.163 by the road authorities; Statens Vegvesen (2006), and is based on two main aspects.

- The U-value ($\frac{W}{m^2} \times K$) or overall heat transer coefficient, is a measure heat loss through an object. This is calculated specifically for each object.
- The requirements and regulation for a certain construction.

In cold localities it is possible to construct so called frost gates in order to prevent extensive use of frost insulation inside the underground excavation (Statens Vegvesen, 2010). This type of mitigation is usually only suitable for facilities with low traffic, e.g >200 vehicles per day. For larger tunnels and certainly underground caverns the frost intrusion has to be evaluated specifically for each case. This is done by assessing local temperatures and experiences from previous constructions of similar geometry and surrounding conditions.

The ventilation of the parking facility in Hammerfest will approximate to 150 000 cubic metres of air exchanged with the surroundings each hour.

3. Review of cases

3.1 The 1994 Olympic Hall of Lillehammer.

3.1.1 Introduction

The decision to build a 61 m span cavern open for the general public, was in many ways a quantum leap for civil engineering (Broch et al., 1996). Typically, sports halls in Norway have generally widths around 25 m, which is considered the critical parameter, and lengths of around 50 m (Broch et al., 1996). In April 1993 the contract was signed, and two years later the cavern was successfully excavated and supported ahead of schedule (Broch et al., 1996). Excavation was done by first blasting a centre pilot tunnel and then excavating upwards to the roof. The full height was achieved by blasting benches in two steps. A sketch is shown in figure 3.1.

3.1.2 Geological conditions and investigations

In Gjøvik there was already situated an underground swimming pool in one of the neighbouring mountains so knowledge of the areas geology was extensive. The site is dominated by Precambrian gneiss, composed of granitic and quartzitic minerals. Rock mass quality was considered good, with Q-value classification of 70. Large variations in dip of fracture planes was characteristic for the area. Joints were medium rough and without clay minerals.

Knowing that there was large horizontal stress in the area was crucial for the

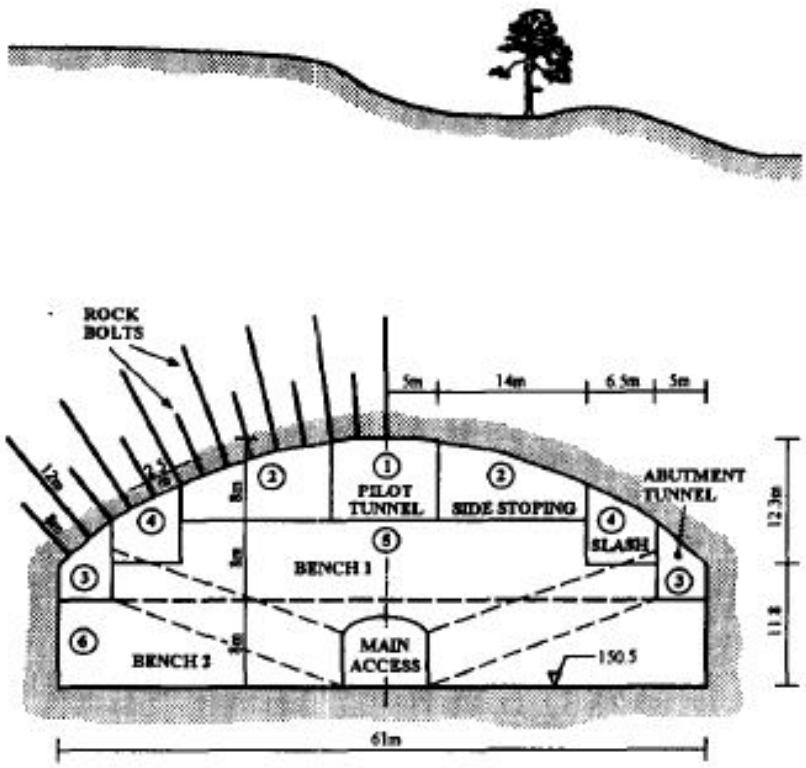

Figure 3.1: Sketch of excavation stages for the Olympic Gjovik Hall in 1993 (Broch et al., 1996).

discussion on building the cavern. Tests performed were hydrofracturing and 3D overcoring in order to obtain a 3-dimensional overview of the stresses. Other tests were conventional engineering geological investigations, lab testing of rock properties and core analysis. Stress tests unveiled a horizontal component of around 5 MPa. The overburden being 20-50 m the vertical stress component is very low (<1 MPa). In theory this is advantageous for large cavern spans; in that way the roof can be stabilized with sufficient compression.

3.1.3 Support measures and monitoring

As temporary support, decisions were made to install c/c=2.5 m, 4 m long mechanical shell bolts. In addition to the temporary support, the permanent scheme included c/c=2.5 m, 6 m long rebar bolts, as well as 12 m long c/c=5 m steel cables, as shown in

figure 3.2.

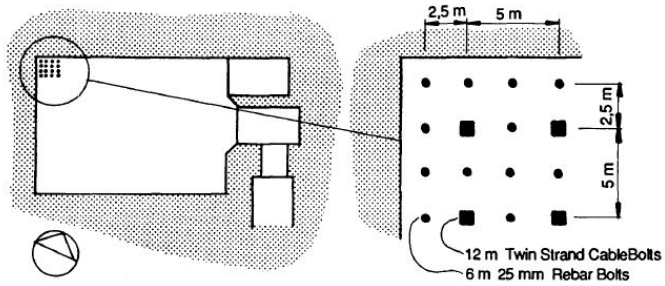

Figure 3.2: Sketch of bolting scheme for the Olympic Gjovik Hall in 1993 (Broch et al., 1996).

Bolting was accommodated by a section-wise application of two shotcrete layers of 50 mm thickness each.

Deformation monitoring was also installed. The roof design consisted of 7, 30-40 m long extensometers drilled from ground level and downwards, and three 15 m extensometers from tunnel roof and upwards. Additionally, 8 of the rebar bolts in the middle were fitted with strain gauges. To check the performance of the installed shotcrete, strain gauges were specially designed for the shotcrete surface.

Data from the extensometers showed upward deformation in the roof. This was predicted by numerous numerical models investigated beforehand. The maximum deformation was measured around 7 mm, which was in accordance with the anticipated magnitudes. Only little strain was observed in the rebar bolts. Pressure build up occurred in the part of the bolt nearest the cavern, and showed only small values of load (1-1.5 kN). and The small magnitude is explained by late installation (Broch et al., 1996). The performance of the shotcrete was somewhat affected by shrinkage effects indicating very low tensile stresses.

Previous experience with upward movement and stable conditions in other sports halls was important for the feasibility of the Gjøvik cavern, hence horizontal stresses contribute largely to the stability of large span caverns.

3.2 Construction of crusher hall at Rana Gruber Norway

3.2.1 Introduction

The case of the crusher hall in a mine in Mo i Rana in Norway was selected as a case because of the detailed description of the numerical approach used to estimate deformations and yielded elements before excavating the cavern. It was thought that it would be a valuable study with regards to the numerical analysis presented in chapter 7.

Rana Gruber is a mining company located in Nordland Norway, extracting iron one by sub-level stoping. Calculations have shown that profit could be gained by changing excavation type from stoping to block caving. Block caving is a relatively new mining method in Norway, which lets large ore blocks excavate themselves by making them unstable by blasting a cut (Keevil and Caldwell, 2012). The block will is excavated from bottom and up, so the ore falls into a transportation system located under the it, as shown in figure 3.3. Excavation efficiency is increased with higher horizontal stresses as the roof becomes unstable.

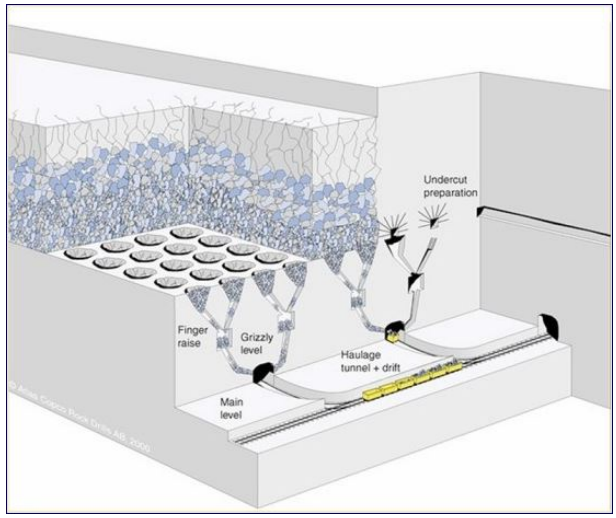

Figure 3.3: Schematic representation of block caving concept (Keevil and Caldwell, 2012).

3.2.2 Geological conditions and problem areas

The project area is characterized by high horizontal stresses around 10 MPa found at relatively shallow locations. At cavern elevation the largest principal horizontal stress was measured around 22 Mpa, and the vertical stress only about 8 MPa. Intact rock strength was by laboratory testing estimated as 80 MPa, and rock quality was characterized by GSI=70. From Trinh et al. (2010), phenomena occurring during excavation of infrastructure tunnels were intensive rock spalling in the walls, floor heave and rock burst at front face, see figure 3.4. Instabilities would occur after a few hours to several days after blasting with very little deformation beforehand, making instabilities hard to predict. This indicates a very brittle rock mass with little plastic deformation before brittle failure occurs. The rock mass thus behaves elastically, failing similar to an intact rock sample in an UCS test. It was concluded that a perfectly brittle model was the best way to represent the rock mass.

Figure 3.4: Stability issues during excavation of tunnels near the crusher hall in the mine. (a)Spalling in side wall. (b)Typical shape of spalling fallout. (c)Rock burst at front face. (d)Cracks in floor resulting from heaving (Trinh et al., 2010).

3.2.3 Support measures

Support installed during excavation is summarized in figure 3.5.

Exc. Stage	Parts	Bolt	Shotcrete layers			
			1st	2nd	3rd	4th
1	TH	Roof	Roof			
2				Roof		
3	1st b.	1st w.	1st w.		AF	
4				1st w.		AF
5	2nd b.	2nd w.	2nd w.		1st w.	
6				2nd w.		1st w.
7	3rd b.	3rd w.	3rd w.		2nd w.	
8				3rd w.		2nd w.

Note:
- TH is top heading
- 1st b., 2nd b., and 3rd b. are first, second, and third benching respectively.
- 1st w. is the wall within 1st benching, 2nd w. is the wall within 2nd benching and so on.
- AF is the footing area of the roof arch, where roof and wall are met.

Figure 3.5: Summary of required support (Trinh et al., 2010).

And failure of support is shown in figure 3.6.

Figure 3.6: Failure of shotcrete in different parts of cross section (Trinh et al., 2010).

For infrastructure tunnels support did not sufficiently stabilize the rock mass from the high underground stresses. The problems were initiated by factors not directly

distinguishable by investigation and geotechnical properties of the rock.

Numerical modelling was carried out to investigate the course of excavating the large crusher hall, and to propose support measures that would stabilize the rock mass surrounding the cavern. Results from the model are shown in figure 3.7.

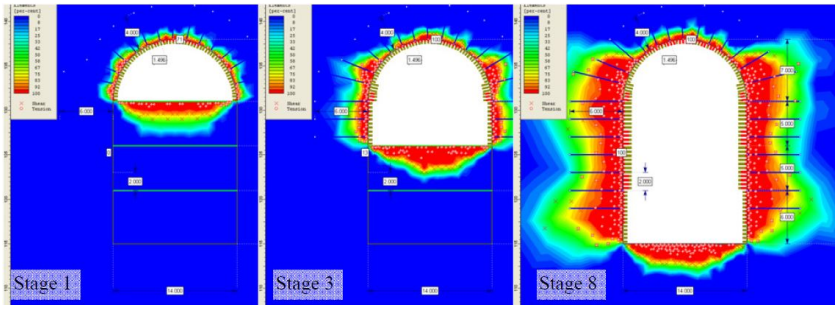

Figure 3.7: Numerical modelling visualizing yielded elements from stepwise benching from top pilot (Trinh et al., 2010).

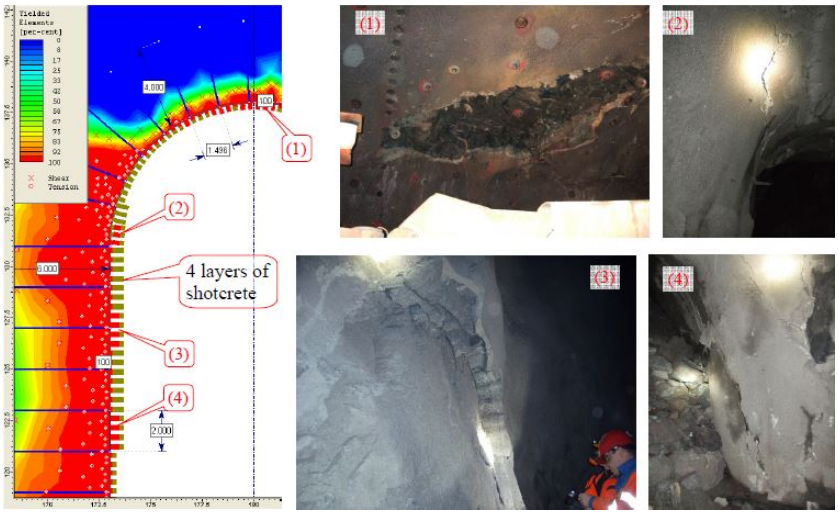

Figure 3.8: Comparison of numerical modelling and encountered conditions in the crusher hall at Rana Gruber (Trinh et al., 2010).

The analysis show the yielded zone expanding as benches are blasted out stepwise, see figure 3.8. One discovered that when allowing initial deformation to occur, the stress

on the support was greatly decreased. Further it was observed that because of the elastic behaviour of the hard rock, the application of shotcrete was best performed stepwise, with the necessity of 2 layers in the pilot tunnel before benching downwards. This principle is known from applying support in soft rock, where studies of the deformation of the rock mass is used to predict optimal installation of support. In principle letting rock mass deform a certain magnitude before support is installed, using the Ground Reaction Curve (Alvarez, 2012). It was also observed that rock mass deformation developed stepwise as benching was subsequently performed. By observing the general behaviour of the rock mass it was concluded that the use of CT bolts would be advantageous over normal end anchored bolts. This is partly due to the elastic behaviour of the rock mass where some deformation is wanted to reduce initial rock pressure. Movement in the wall would cause the pre-tensioned end-anchored bolts to loose tension. It was accordingly observed that bolt head lost contact with the rock surface. A combined approach by visual observations and numerical models, was the basis for the support design.

4. Project Description

4.1 Definition of project area

The project area includes part of the city centre and most of Salsfjellet (the local mountain) in Hammerfest which is located at latitude 70°north in Northern Norway. The investigated area stretches from the north eastern mountainside of Salsfjellet, south west to the cemetery located in Hammerfest city centre centre. From north-west, the area of study includes the the city centre from Strandgata and stretches south-east around 200 metres up and on to Salsfjellet. An overview of the area is given figure 4.1.

4.2 Location

The planned underground excavation is to be located in Salsfjellet. Location for the excavation is proposed in the pre-feasibility study developed by SWECO in may 2013. A slightly shifted design is presented in a project thesis developed by the author in the fall of 2013. The decision to choose any of the proposed alignments of the cavern are not yet made, hence all further analysis assumes the alignment described in the original pre- feasibility study carried out in May 2013. Figure 4.2 shows the locations of the two proposed geometric solutions for the excavation, (a) being the original suggestion, and (b) a slightly rotated alignment presented in the project thesis.

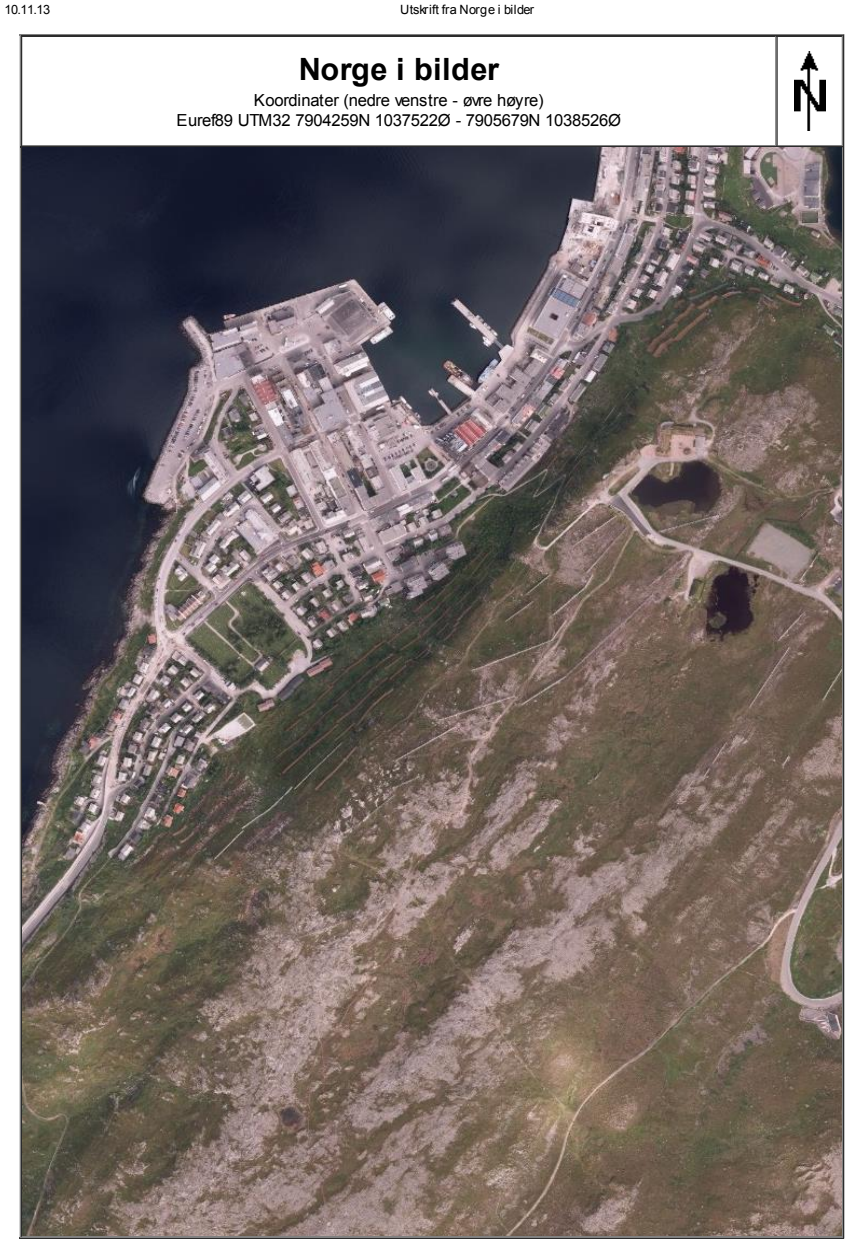

Figure 4.1: Overview of project area

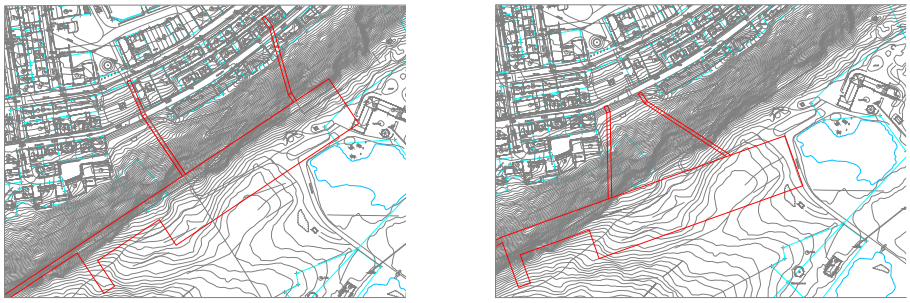

(a) (b)

Figure 4.2: Two proposed locations and orientations for the underground excavation.

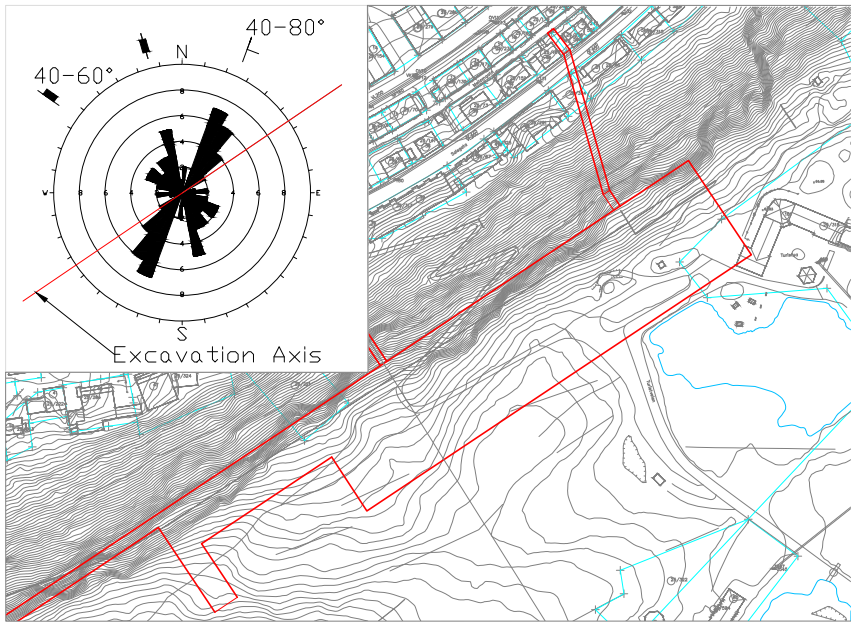

Figure 4.3: Caverns location shown together with fracture rose in the project area.

4.3 Size and geometry

In appendix C, D and E the proposed design for the three levels of the excavation is shown. The facility is planned to consist of two large parallel halls of about 240 meters long and a width of 20 metres. Between there will be five normal-running halls to

connect the two caverns with 10 metres width. The design will constitute a 240m x 60m cavern with four 20m wide pillars in the middle varying in length as shown in the appendixes. The pre-feasibility study suggested three options of construction. One where only 1 cavern would be excavated, one where both caverns would be excavated, and alternatively where both caverns are excavated but only one is supported and made operational. This thesis assumes that both caverns are excavated and supported in brief because this option poses the largest stability threat. The caverns will be connected to the future Rv40-road at the south-west flank which is to enter Hammerfest city through Salsfjellet west of the cavern. Connected the cavern will be two roughly 130 metre long pedestrian tunnels, making the cavern accessible by foot from the city centre from the north at ground level. The pedestrian tunnels are designed with a 4m width.

Cross section geometry of the main caverns consist 11m walls with arch top of roughly 16m above sole. Sketch of the cross section is presented in figure 4.4

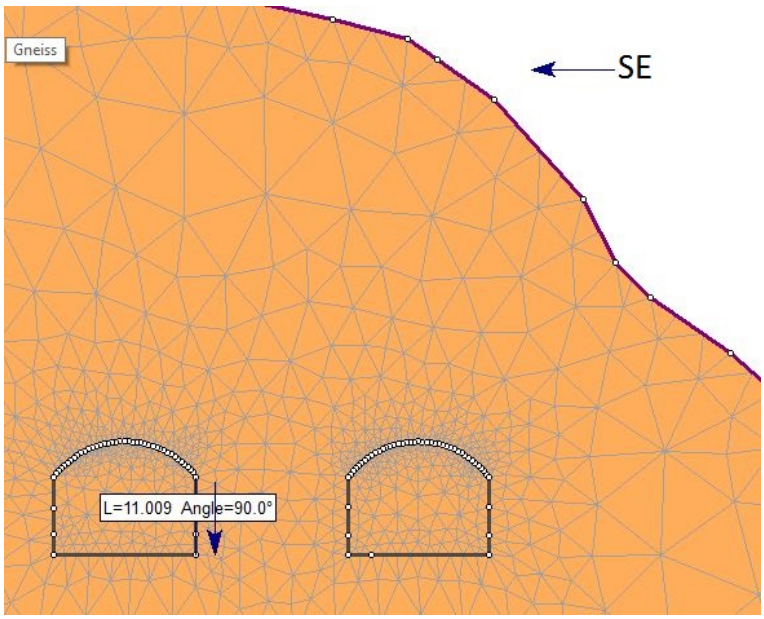

Figure 4.4: Cross section of the caverns with pillar.

4.4 Geological and tectonic background

Norway is geologically characterized by hard - massive rock conditions. Norway may roughly be divided in to three different units with respect to type and formation history as shown below.

- Carbon-Cretacious rock types which is found mostly in the Oslo region. They are of relatively new age and consists of a series of eruptive rock types. This component constitutes a rather small portion of the Norwegian geology, but is dramatically different in regard to formation from the rest of the country's rock types.

- Kambro-Silurian rocks constitute around one third of rocks types in Norway. They represent the metamorphosed Kaloedonian mountain range, and constitute mainly of mica-rich schist, phyllites, marbles, and greenstone.(Nilsen and Thidemann, 1993)

- Precambrian rock types constitute of almost two thirds of Norwegian rockmass. They are comprised of gneisses, granites as well quartzites, sandstone, amphibolites, and gabbro (Nilsen and Thidemann, 1993).

Hammerfest is located on the island Kvaløya which is a part of a detached Precambrian geological province. The island is surrounded by Kaledonian rock that together makes up a basal sliding plane (4.5). In turn one can divide Kvaløya into four different zones by geological features as can be seen in figure 4.6 (Oftedahl, 1974).

The northern part of the Island consist of a migmatized quartzite nappe of late-cambrian age as seen in figure 4.6. It stretches from the south past the island of Melkøya, and turns into migmatized feldspar-rich gneiss which constitutes the geology of the Hammerfest area. Moving south normal to the layering the rock changes into partly gneissified Muscovite-schist around the mountain of Svartfjellet. The south cap of the Island is made up by thin banded gneiss containing some amphibolite.

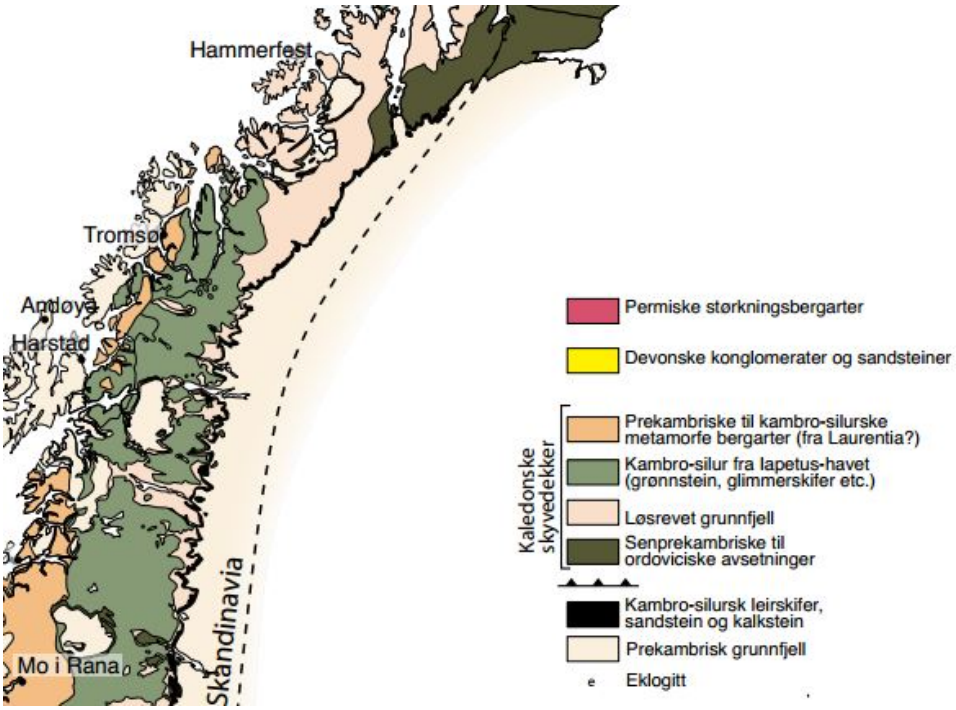

Figure 4.5: Geological overview of parts of Northern Norway (Unknown, 2013).

4.5 Geology in project area

4.5.1 Description of rock types

The project area includes two of the above mentioned rock types. Visible on map in appendix A the project area is distinguished with kalifeldspar rich gneiss containing apparent banding structures, together with a nappe of quartzite. The latter located north-west in the area and should not cross with the planned underground excavation. Folding structures can be observed on the image of the gneiss from location 14 (see Appendix A).

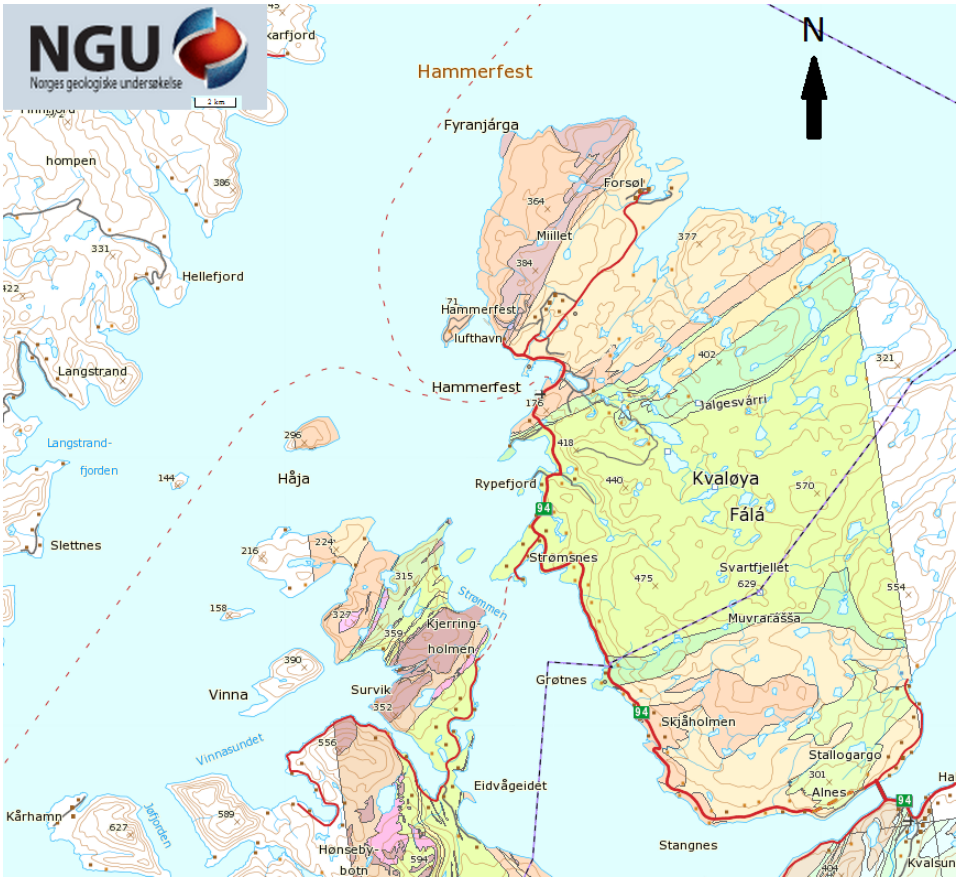

Figure 4.6: Geological overview of Kvaløya (NGU, 2014)

Figure 4.7: Picture of rock sample collected in Hammerfest. The rock show banding and distinct folding patterns.

Field observations unveiled some degree of surface weathering, but the rock is apparently massive just below the surface. This could be explained by rough weather conditions but massive and hard rock characteristics.

4.5.2 Weakness zones

Weakness zones are lineaments, zones of lower strength, zones of chemically alteration of minerals, or faults in the rock mass. They can extend from below 50 meters in length ranging up to several kilometres. If encountered and not dealt with properly it will mean costly delays for the construction.

Found in the project area are two clear weakness zones. As seen in appendix A in location 1 and 14 only one of the weakness zones can be noticed interfering with the excavation. Figure 4.8 shows how these zones present themselves at the surface. The weakness zones in figure 4.8(a) currently crosses the planned excavation. However, the propagation of the zone in to the mountain is highly uncertain. It could only be identified from the north face of the mountainside and could not be distinguished at the top of the mountain. Indeed it may not at all propagate in to the subsurface. However since it was observed its presence is assumed until confirmed with core samples. At field visit the presence of a 1-2 mm thick layer of epidote was confirmed. It is typical for in Norway to have chemically altered minerals close to the core of such zones Statens Vegvesen (2003).

Areas of increased fracturing are observed around the border between the gneiss and the quartzite, and could possibly be of significance in light of groundwater intrusion from the ponds located at the top of the mountain. Figure 4.9 shows one of these zones of more compact jointing.

(a) (b)

Figure 4.8: Picture *a* is taken towards south-east, and shows weakness zone in the planned cavern area at location A(Appendix A). Picture *b* is taken towards north-west and shows a weakness zone north of the planned cavern at location 10 (Appendix A)

.

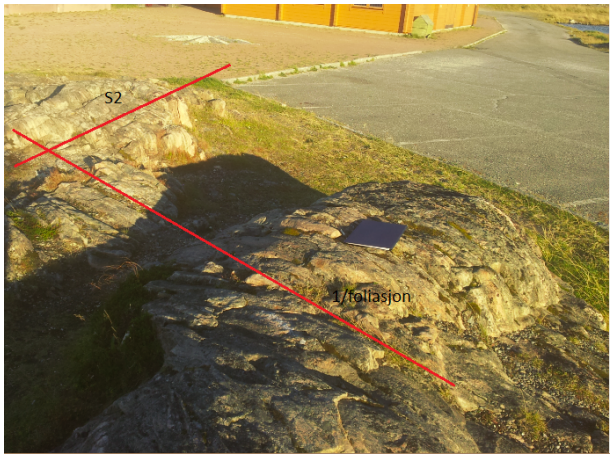

Figure 4.9: Zone with increased jointing. Picture taken towards east at location 10 (appendix A).

4.5.3 Description of discontinuities

The geology of the project area was mapped at field visit 23. September 2013 by the author.

Two major fracture sets were discovered in the project area, one as the foliation. Foliation is the planes of secondary origin in metamorphic rocks and is the most prevalent discontinuity set in the area. Secondly there is a near vertical fracture set cutting normal to the foliation, referred to as fracture set 2. Lastly there is locally a third set of fractures, though not as persistent as the two previously mentioned. Fracturing in the area is presented as a rose plot in figure 4.10.

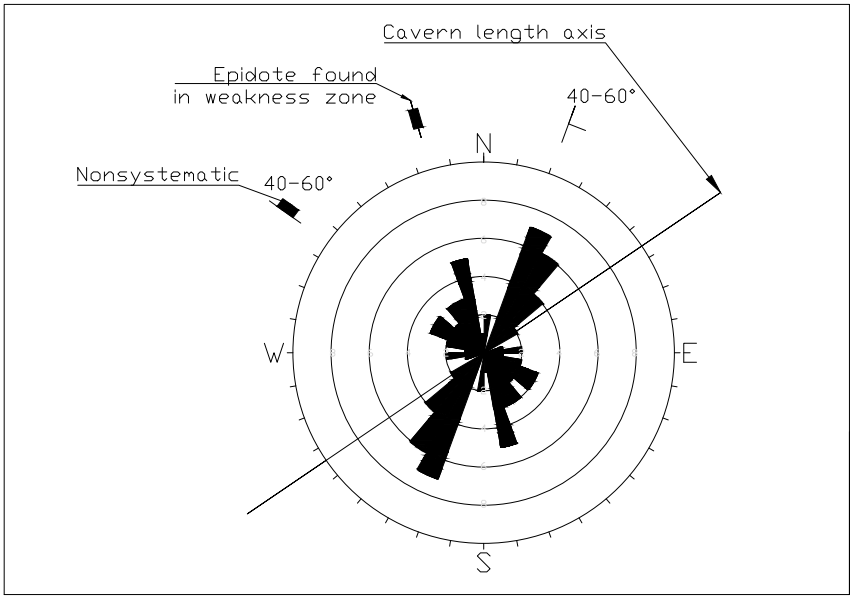

Figure 4.10: Fracture rose giving information on quantum and direction of the major fracture components of the rock mass. In addition, dipping information is added to the figure.

- Foliation: Strike varying between N20°-40°E, dipping generally steeply (70-90°), but some locations as little as 40°-60°southwards. The area around location 1 (Appendix A) showed shifted folation, with similar strike but dip towards north of 60°-80°. This is the result of local folding of the rocks.

- Fracture set 2: Dipping vertically or near vertical, striking N60°-80°E. Fracture set 2 is parallel to the weakness zone as described in the previous chapter.
- Non-systematic fracturing set: Striking in some locations N110°-130°E, dipping around 30-60°North.

Fractures are rough, wavy, and dry at surface. No observation is made of clay minerals except for on discontinuities on the heavily fractured rock at location 1. No fracture strength properties were obtained because suitable equipment was unavailable. Distance between fractures are often several metres, but zones of more dense fracturing were observed near the boundary to the quartzite (location 11) and around location 5, yet such zones may be caused by locally high exposure to weathering. Observations made in the entrance of a small tunnel at the foot of the mountain (location 17) showed wet fracture surfaces.

4.5.4 Stress conditions

In Pascala et al. (2005) the Finnmark region in Northern Norway is presented with regard to horizontal stress conditions. Figure 4.11 shows a simplified geological model with stress orientations in Finnmark. The paper presents research done on quantifying stress magnitude in west and eastern Finnmark by mapping over 90 axial stress relief fractures and gathering of over 20 borehole offsets in fresh cut road cuts. In brief the study shows data in general concludes with a NW-SE maximal compression. It thus contradicts the findings presented in Myrvang (2001) (see figure 4.12). Indications on maximum magnitudes of horizontal stress is rather moderate in the range of 0.1-1 MPa. Nevertheless, an average value of 2.8 MPa was found for horizontal stress magnitudes in Ferroscandinavia by Stephansson (1989), although the author stated that shallow stress magnitudes are largely varying. Further it is discussed that the main component of horizontal stress affecting Finnmark is the push force the North Atlantic oceanic ridge yields, and that rebound stresses from the latest ice age plays little role in the stress regime (Pascala et al., 2005).

Large uncertainties lie with the fact that large horizontal stresses can be found just

below sub surface (Myrvang, 2001) (Trinh et al., 2010) (Broch et al., 1996), and without measurements one can only extrapolate data from nearby locations. By looking at measurements obtained at Stjernøya about 60 kilometres from Hammerfest (Myrvang, 2001), a large horizontal stress $\sigma_H \approx 40MPa$, striking North20°South, and a smaller horizontal $\sigma_h \approx 20MPa$ normal to σ_H is found. The principal stress axis is not parallel to the proposed alignment of the parking cavern. By using Mohr circle, normal stress to the cavern would be 22 MPa normal to the main halls axis, and 38 MPa normal to the pedestrian tunnels. The magnitudes are very high and do most likely not represent conditions just below surface.

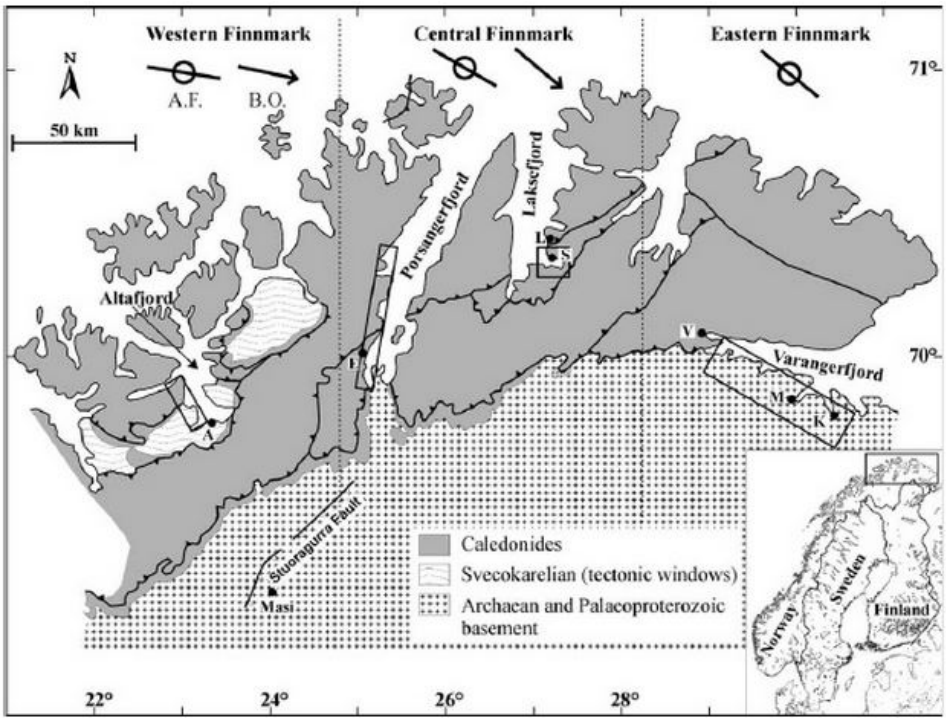

Figure 4.11: Simplified geological map of Finnmark. Boxes show where stress relief fractures are most abundant. B.O denotes borehole offsets, and are shown in the figure (Pascala et al., 2005).

The magnitude of horizontal stresses for the project area can not be stated with certainty for but research indicates magnitudes ranging from 0.1-2.8. With an

overburden of 60m, the conditions for the Hammerfest cavern is hard to quantify. Extreme magnitudes are however not expected since the small tunnels located in Salsfjellet does not show any large stability problems. Tectonic stress will be assumed in further analysis. Because little is known of the stress conditions currently present in the project area, one can use the Norway stress map presented in Myrvang (2001), to extrapolate measured stress in rock nearby the location of the project area.

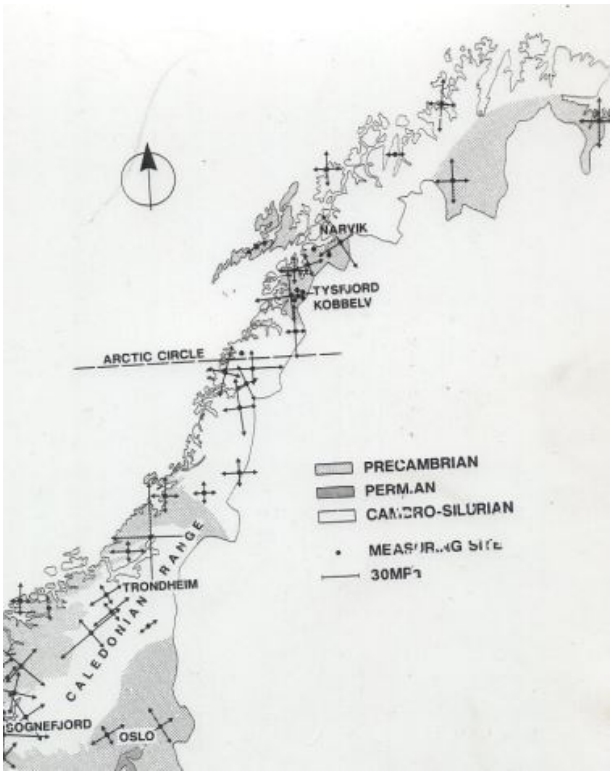

Figure 4.12: Norway horizontal stress map. From Myrvang (2001).

4.5.5 Hydrogeological conditions

Observations in a small tunnel at ground level in the mountainside at location 17 (Appendix A) showed constant dripping from the roof. The rock surface was wet and sound of heavy dripping was heard from deeper within the tunnel. It was not possible to enter into the main part of the tunnel at the site. An image from the wet rock surface is seen in figure 4.13. It had been sunny for 4-5 days at the time.

Figure 4.13: Image taken in the small tunnel in the mountainside just south of the city centre. Picture shows wet rock surface. It had not rained in the area in 4-5 days.

The surface above the cavern gently declines north-east and flattens out by two ponds. At the field visit it was possible to trace small creeks 25 metres in elevation upwards from the ponds and westward. West of location 6 the creeks were dried however signs of water activity could be followed further. Hence it is no doubt that there is groundwater present at the surface above the planned cavern and indications are that the level increases during rainy periods. It is a question if the this water table is connected to the dripping observed in the small tunnel and the cavern elevation. This is further discussed in chapter 5.

4.6 Laboratory tests

A series of laboratory tests were performed on rock samples from the project area. The qualities tested were the most common parameters describing rock strength, deformation properties, and drillability. The results show properties within moderate dimensions of what can be expected of the rock type tested. It can be concluded that several large scale underground caverns has been built in Norway in rock with

equivalent suitability as a construction material.

It proved hard to collect adequately fresh samples because surface weathering was widespread. Consequently it is important to perform further tests in order to gain sufficient knowledge of the geological conditions. In table 4.1 a summary of the results is shown.

Table 4.1: Presentation of lab results.

Parameter	Verdi	Enhet
Density ρ	2.68	g/cm^3
E-modulus E	24.6	GPa
ϕ_b	28.3	$^\circ$
Pointload index radial I_{s50}	6.2	MPa
Pointload index axial I_{s50}	6.2	MPa
Tensile strength σ_t	21.5	MPa
UCS σ_c	129	MPa
DRI	53	-
BWI	35	-
CLI	8.5	-
Sonic velocity	5370	$\frac{m}{s}$

An image of the samples is seen in figure 4.14.

Figure 4.14: Rock samples collected in Hammerfest for testing.

4.6.1 Tests performed

The following tests were performed on the Hammerfest Gneiss.

- Density
- Uniaxial compressive strength
- Young's modulus
- Sound velocity
- Brazilian test
- Point load test
- Drillability test

The tests were performed at the NTNU/SINTEF laboratory at NTNU Trondheim between 7^{th} and 11^{th} of October 2013. The laboratory supervisor was Gunnar Vistnes. The tests were performed by by Erik Martinelli, Agnethe Finnøy, Hallvard Nordbøren and Kaisa Herfindal, master students in engineering geology at NTNU.

4.6.2 Results

Anisotrophy

The point load test is performed both radial and axial and can indicate anisotropy in the rock sample. The lab results isotropic strength. However, as seen figure 4.9 anisotropic features are easily spotted. Noticeable is it that small scale folds make weaker planes randomly oriented which could explain the observed isotropy. Another possibility is that visual planar features do not represent zones of weakness in the rock. The number of tests is believed to give credible results.

Strength

The tests show a UCS (Uniaxial Compressive Strength) varying in the interval 100 - 150 MPa, with the average being 129 MPa. The samples may have been exposed to

weathering for some time, making the results lower than for a sample from the sub surface. The samples contained small scale folds (see figure 4.9), but these folds were not observed in the small tunnel north side of the mountain, where the foliation was observed to more predictable and continues. With empirical methods estimated compression strength from the point load index $I_{s50} \rightarrow \sigma_c \approx 136.4MPa$ may be compared with the values from the UCS test and show compliance

From the Brazilian test tensile strength of the rock samples were estimated. The test showed tensile strength of σ_t= 21.5 MPa. From literature, this parameter is often found to be between 10 and 20 times lower than UCS (Myrvang, 2001), and hence may indicate a too low UCS value for these particular samples. In general however, UCS is regarded as a more reliable than the Brazilian test.

Elastic properties

Traditionally the elastic properties of rocks are measured with Youngs modulus (E), and Poisson number (υ). Young's modulus is a measure of the relationship between stress and axial strain. The Poisson number is the relationship between axial and radial strain. Results from the test show generally values within expected area of gneiss, although the span of what is classified as gneiss is substantially large.

Drilliability and blastability

Drillability Index, Cutter Life Index and Bit Wear Index all show good values for underground excavation. Areas with larger quartz content were observed at the field visit and could possibly cause more difficult conditions during drilling. The testing is believed to be representative for the rock type, but again further testing will increase certainty.

Blasting quality depends on a number of rock characteristics. These include rock impedance, attenuation, tensile strength, anisotropy and resistance Nilsen and Thidemann (1993). Impedance is the product of density and sonic velocity. Those results can be found in table 4.1, along with an estimate of tensile strength. Resistance towards crushing, and degree of fracturing all show moderate magnitudes.

5. Stability Assessment

5.1 Geotechnical properties

Geotechnical properties are very important when performing analysis on stability. This chapter will discuss in detail important characteristics of the rock mass in the project area.

5.1.1 Hydraulic conductivity

When calculation water inflow to a tunnel it is necessary to know the hydraulic conductivity. Estimation of this parameter was done by assessing observed magnitudes of flow in field investigations and back calculating. This is presented in chapter 5.8.

5.1.2 Rock mass strength

There are several ways to predict the strength of rock mass. As discussed by Panthi (2012), the compression strength of a rock mass can be described as a material where failure is controlled by joints.

$$\sigma_{cm} = \frac{\sigma_{ci}^{1.5}}{60}$$

Where, σ_{cm} is the rock mass spalling strength, and σ_{ci} is the intact rock strength. This correlation is based on investigations from the Himalayas.

The Hammerfest gneiss was tested in laboratory and gave an UCS of 120 MPa. With

the intact rock strength known, an estimation of the rock mass compressional strength can be calculated as follows:

$$\sigma_{cm} = \frac{120MPa^{1.5}}{60} \approx 21MPa.$$

Further, Martin and Christiansson (2009) investigated fractured granites and granodiorites in Finland and found a correlation between rock mass spalling strength and intact rock strength of: $\frac{\sigma_{cm}}{\sigma_{ci}} = 0.44 - 0.5$.

However, rock mass strength generally depends on the quality of the rock mass, with regard to intensity of joints and fractures. Hence one can estimate rock mass strength as a function of empirical classification schemes. Genisa et al. (2007) presents the following relationship

$$\sigma_{cm} = \sigma_{ci}\sqrt{e^{\frac{RMR-100}{9}}}$$

which is based on a RMR classification of the rock mass. Since RMR values for the good rock part of the project area ranges from 40-70, the following estimations can be made:

$$\sigma_{cm} = 120\sqrt{e^{\frac{[]-50,-30]}{9}}} = [4.3-22]MPa$$

As discussed in the project thesis, most of the good quality rock was in the upper spectrum, and so a rock mass strength of roughly 20 MPa could be a fair estimation. Several authors have presented such relationships, also Sheorey (1997) did a RMR correlation to σ_{cm}, which gives following rock mass strength based on obtained RMR values

$$\sigma_{cm} = 120e^{\frac{RMR-100}{20}} \approx [15-20]MPa$$

The areas of more dense fracturing presents a change in rock mass strength, constituting 20% of the rock mass as described earlier. Barton (2000) gave the

following relationship of rock mass strength with the Q-value:

$$\sigma_{cm} = 5\gamma(Q\frac{\sigma_{ci}}{100})^{\frac{1}{3}}$$

Where γ is the density of the rock. With Q-values for the weakness zone at approximately 0.1 in the project area, the empirical relationship gives:

$$\sigma_{cm} = 5 \times 2.68(0.1\frac{120}{100})^{\frac{1}{3}} = 6.5MPa$$

In addition, an empirical GSI evaluation with intact rock strength can be used for the weakness zone. Genisa et al. (2007) presents results from phyllites and tectonic breccia, where GSI values around 25-30 showed corresponding Q-values of approximately 0.07-1.0. The code Roclab from Rocscience can then be used to estimate the rock mass strength. Input of intact rock properties and mi-value of 24, gives a rock mass strength of 5.4 MPa, correlating to the approach by Barton (2000).

5.1.3 Hoek-Brown parameters

Hoek-Brown parameters to use for instance in numerical modelling may be estimated using Roclab. Input of intact rock parameters from laboratory, an mi value of 24, and additionally no disturbance factor gave the results presented in table 5.1

Hoek-Brown parameters can additionally be obtained from various publications by E. Hoek amongst others, presented in Genisa et al. (2007), as

$$\frac{m}{mi} = 0.135(Q)^{1/3}$$

$$s = 0.002Q$$

$$\frac{m}{mi} = e^{\frac{GSI-100}{28-14D}}$$

$$s = e^{\frac{GSI-100}{9-3D}}$$

Where m and s are material constants for the Hoek Brown classification, and D the disturbance factor that depends on excavation quality and damage on surrounding rock.

Table 5.1: Estimation of Hoek-Brown parameters

Rock Quality	Approach	GSI	Q	m/mi	s (a)	mb
Good	GSI	75	-	0.4	0.06 (0.5)	9.4
Good	Q-method	-	10	0.3	0.02	8.4
Weak	GSI	25	-	0.06	0.0002(0.53)	1.58
Weak	GSI	35	-	0.08	0.0004(0.52)	1.88
Weak	Q	-	0.1	0.063	0.0002	1.7

The m_i parameter was obtained from the empirical databases of Rocscience for gneiss with a value of 24. In the numerical modelling averages will be used. By comparing values in table 5.1 it seems that numbers coincides.

5.2 Investigation class

The Norwegian road authorities published through a project called "Mijlø-og samfunsstjenelige tunneler" (Environmentally friendly- and society serving tunnels) a guideline on how to quantify the necessary pre-investigations for a project. The method is a classification system where a project is evaluated in form of size, area of use, anticipated problems, and effect on surroundings. The need for such a classification was discovered when the Eurocode 7 standard was introduced in Norway. The standard generally suggested what methods to use but not a quantifiable amount of them. In the project thesis this evaluation was performed for the project. It was concluded that there ideally should be performed pre-investigations at about 10%

of the cost of blasting and support. As discussed in the thesis this number is too high because the method is ideally meant for conventional road tunnels, thus the Hammerfest parking cavern would be very expensive per meter tunnel in comparison. It is therefore presented an interval in which investigation cost should lie in, between 2% and 10% of excavation and support cost. In addition, it is not recommended to spend less than 1% of blasting and support cost since experience show facilities having unsatisfying quality in such cases.

5.3 Analytical support assessment

Analytical approaches for stability assessment in underground excavations exist in various forms today and are used as preliminary methods of investigation on rock stability. Using analytical approaches to asses stability in underground excavations is most commonly based on the Mohr-Coulomb failure criterion.

According to conventional theory the stress at the depth of the cavern will be equal to the weight of the above laying rock mass e.g.

$$\sigma_v = \gamma_r \times h_{tunnel} \times g$$

where σ_v is the vertical stress at cavern elevation before excavation, γ_r is the unit weight of the rock, obtained in laboratory to be $2.68\frac{g}{cm^3}$, h_{tunnel} is the height from cavern elevation to the surface, and g is the gravitational constant$\approx 9.8\frac{m}{s^2}$. The vertical stress at cavern elevation is thus defined as:

$$\sigma_v = 2.68\frac{g}{cm^3} \times 60m \times 9.8\frac{m}{s^2} \approx 1.6MPa$$

Secondly, an estimate of gravitative induced horizontal stress is based on elastic theory from Hooke's law (Myrvang, 2001) using Poissons' ratio measured in laboratory of 0.09, results in (Myrvang, 2001).

$$\sigma_h = \frac{v}{1-v}\sigma_v = \frac{0.09}{1-0.09} \times 1.6MPa = 0,15MPa$$

As discussed earlier, the gravitationally induced horizontal stress may only constitute a tiny part of the horizontal stress regime if there is tectonic, or residual stress in the area.

The term "stability index" in constructing underground facilities has been described by several researchers. In massive brittle rock, the stability index "S" can be defined as:

$$S = \frac{\sigma_c}{\sigma_{\theta\ max}}$$

where
σ_c=the uniaxial compressive strength of a rock
$\sigma_{\theta\ max}$=the tangential stress along the periphery of the excavation

Failure will theoretically occur when the tangential induced stress around the opening exceeds the uniaxial compressive strength of the rock (Panthi, 2012)

$$\sigma_{cm} < \sigma_{\theta\ max}$$

The safety factor thus elaborates the relationship between the two parameters.

To investigate the peripheral stresses around the underground opening, one can utilise the equations of Kirsch, who in 1998 developed a solution for stresses on the periphery of a circular tunnel (Myrvang, 2001). He showed that for a circular opening, the tangential stresses would be:

$$\sigma_{t\ max} = 3\sigma_1 - \sigma_3$$
$$\sigma_{t\ min} = 3\sigma_3 - \sigma_1$$

In the Hammerfest cavern, this would result in the following tangential stresses, assuming that the opening is circular, and that only gravitative horizontal stresses are

present.

$$\sigma_{t\ max} = 3 \times 1.6MPa - 0.15MPa = 4.7MPa$$
$$\sigma_{t\ min} = 3 \times 0.15MPa - 1.6MPa = -1.15MPa$$

The maximum tangential stress would be of compression and in the side walls under these assumptions. In the roof, according to the analysis the result is tensile stress of about 1 MPa, which could be hazardous combined with a vertical fracture set. Presence of larger horizontal stress is not known at this stage in the analysis.

Further, a safety factor towards shear failure of intact rock in the roof can be calculated as followed

$$S = \frac{125MPa}{4.7} \approx 25$$

which is high safety factor. As described earlier, rock mass strength is lower than intact rock strength. An equivalent rock mass compressive strength can be found by empirical methods using the GSI system together with code Roclab based on standardized Hoek-Brown theory (Hoek et al., 1998). As discussed in the project thesis, GSI for the good rock quality in the area is estimated to be 75. m_i is estimated from databases of Rocscience to be 24. Surface quality is expected to be excellent. UCS is obtained from lab results at 120 MPa. The output rock mass compressive strength is $\approx 29MPa$, and accordingly a safety factor of:

$$S = \frac{29MPa}{4.7} \approx 6$$

In the weakness zone a lower GSI must be used, where impaired rock quality is expected. It can be argued based on above description and classification of rock mass,a suitable GSI value ranges from 25-35, with poorly interlocked and heavily broken rock mass and possibly worsened surface conditions due to weathering. In addition, clay minerals are present as discussed in the former chapter. Roclab code output from these simple estimations suggests a Rock mass compressive strength of

only 2.8 MPa, and according roof safety factor of

$$S = \frac{2.8MPa}{4.7} \approx 0.6$$

which indicates failure and is not satisfactory. In both cases tensile stress is developed in the roof because of low horizontal stress. This being the case block fall is expected to happen. It is though probable that some residual horizontal stress is present. One can investigate the stability under different circumstance with regards to horizontal stress magnitude before more information is gathered. The K-gradient is used to describe relationship between horizontal stress and vertical stress (Panthi, 2012)

$$k = \frac{\sigma_{H\,tot}}{\sigma_v}$$

$$\sigma_{H\,tot} = k\,\sigma_v$$

And further the total horizontal stress is defined as:

$$\sigma_h = \frac{\nu}{1-\nu}\sigma_v + \sigma_{residual}$$

In figure 5.1 the analysis is presented for different magnitudes of horizontal stress. In this case it is interesting to investigate at what point rock mass becomes unstable and could be exposed to spalling phenomena in the roof. Also, one may investigate at what point tensile failure would occur in the walls.

The key outputs from figure 5.1 are;

- Cavern walls become unstable with regards to tensile failure in the walls at 7 MPa of horizontal stress, when assuming a rock mass tensile strength of 1.7 MPa, a rough estimate based on Roclab software.

- Cavern becomes unstable with regards to spalling in the roof, at a horizontal stress of around 7 MPa.

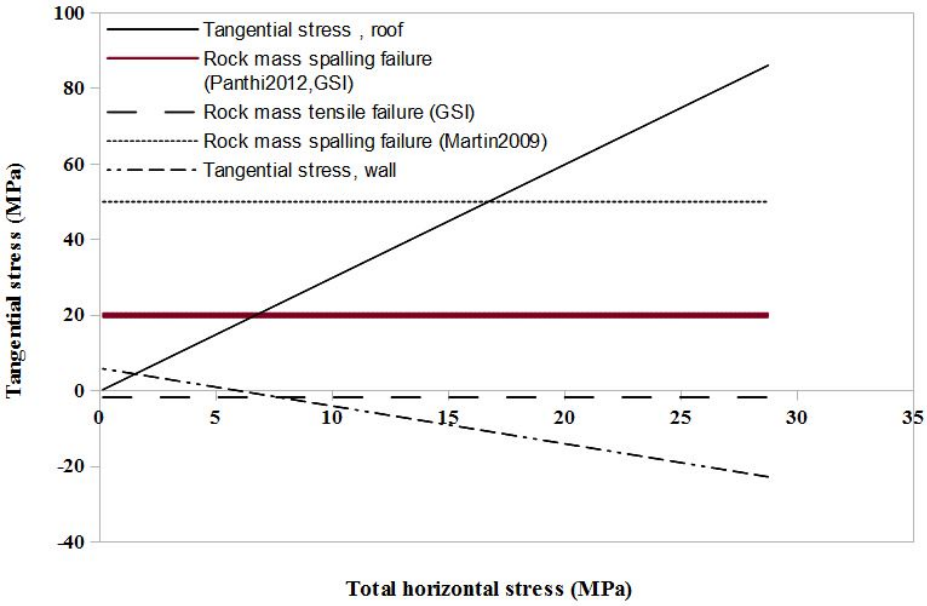

Figure 5.1: Graph showing ideal in-situ conditions under influence of different horizontal stress. Calculations are made for the Hammerfest cavern at 60 m below surface. Calculations are based on the Kirsch solution presented in Panthi (2012).

A weaker rock mass strength than suggested by Martin and Christiansson (2009) is supported by Panthi (2012) as shown below.

$$\sigma_{sm} = \frac{\sigma_{ci}^{1.5}}{60} = \frac{120MPa^{1.5}}{60} \approx 21MPa.$$

Where, σ_{sm} is the rock mass spalling strength, an σ_{ci} is the intact rock strength. Under the above mentioned assumptions, one would get spalling issues at a horizontal stress magnitude of 7 MPa or more. In order to design bolt lengths and type of bolts as support in case spalling would occur, it is possible to estimate the depth of spalling from Martin and Christiansson (2009) as follows

$$s_d \approx r\ (0.5\ \frac{\sigma_{\theta max}}{\sigma_{sm}} - 0.52)$$

where r is the radius of the tunnel, $\sigma_{\theta max}$ is the maximum tangential stress around the opening, and σ_{sm} is the spalling strength of the rock mass.

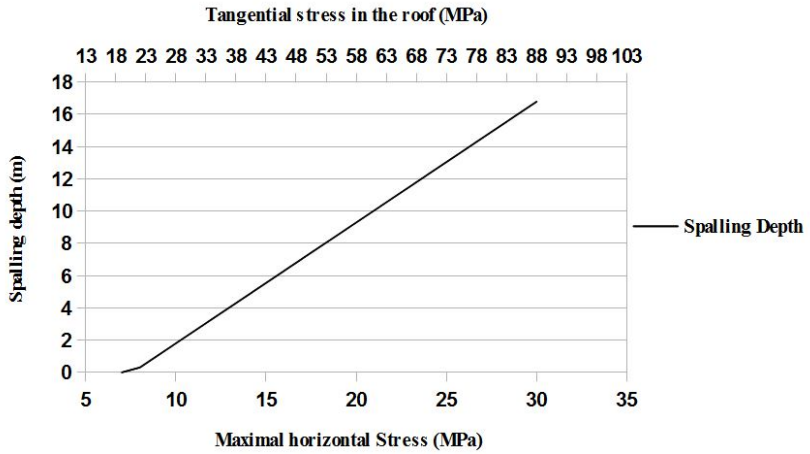

Figure 5.2: Graph of spalling depth under different horizontal stresses

In figure 5.2 spalling depth is presented as a function of horizontal stress in the subsurface at same stress magnitudes as figure 5.1. These calculations are done with rock mass spalling strength as predicted by Panthi (2012) and GSI≈ 70 e.g. $\sigma_{sm} = 20MPa$. The spalling depth will present itself as shown in figure 5.3 from Martin and Christiansson (2009).

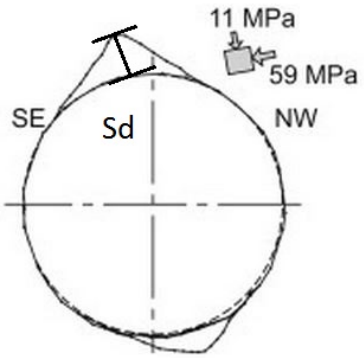

Figure 5.3: Sketch of spalling depth s_d. Modified after Martin and Christiansson (2009).

Presented in table 5.2 is a proposed bolt length scheme based on the above analysis. Here, it is assumed that the bolt length should have a safety factor of 1.3 compared to the length of spalling, e.g. $L_{bolt}/sd >= 1.3$. The key element is making sure the bolt

penetrates the unstable area, and yields force on the stable rock mass behind. It is assumed that maximal horizontal stress is perpendicular to excavation length axis.

Table 5.2: Segmental bolt length support scheme assuming $L_{bolt}/sd > 1.3$

Maximum horizontal stress, MPa	Bolt length in roof, m
..-9	2
10-13	6
14-17	>9
15-22	>14
>=15	Additional support

5.4 Graphical stability assesment

The code Unwedge proposes a way to investigate the joint orientations with respect to the tunnel and identify probable failing blocks along with calculating a safety factor for block failure. In addition, it is possible to estimate support needed for stabilizing blocks to a satisfactory safety factor. Unwedge is a limit-equilibrium code which bases on calculating forces acting on a block, including support forces (Rocscience, 2005). It is also a 3d tool available for investigate possible formed wedges in the tunnel. Additionally one can predict support at the tunnel face required for a stable cross section using block theory. These support schemes can later be compared to empirical support schemes and tested with a numerical model.

Joint strength parameters are estimated based on both Mohr-Coloumb and Barton Brandis approach.

- From Palmstrom (1995), the compressive strength of joints is equal to the UCS, in fresh samples. The investigated joints in the project area were not intensely weathered, and thus this assumption is considered valid.

- The basic friction angle ϕ_b, was found i laboratory tests to be 28°, and results are believed to be reliable as discussed in chapter 4.

- JRC is estimated from field observations. Joint surface character are generally consistent, mostly planar and some sign of large scale waviness, and a JRC value of 4-6 is suggested for the analysis. As a general rule, worst-case scenarios will be favoured in choosing from spectra of parameters.
- The analysis is done using three joint sets, though one of them was not present on mutliple locations.
- Joint persistence is >2m, as discovered in field observations, and joint spacing is performed with 1m and 2m for the general rock mass in order to make the model represent field observations in a good and simple way.
- Cohesion for the rock mass is estimated after Barton (1974). Clay filled joints in granite is meant suitable for the weakness zone int Hammerfest with values of 0-0.1 MPa and 0.24 MPa for regular discontinuities (see chapter 4). Joint characteristics is believed to be adequate between the two massive rock types in this case, since insecurities are quite large for this parameter.
- Tensile strength of fractures is assumed zero for the discontinuities. This is because regular joints were not observed to have any kind of cement and is believed to be easily pushed to tensile failure under its own weight.

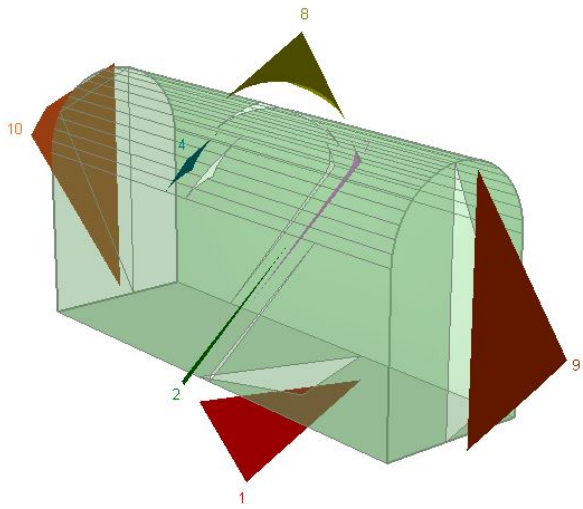

Figure 5.4: Wedges formed in Mohr-Coulomb analysis in code Unwedge by Rocscience. Unwedge assumes worst case, and wedges are here at maximal sizes.

As seen on figure 5.4, 7 wedges could possibly form under the given joint circumstances. Scaling to field observations results in smaller wedges as shown in figure 5.5.

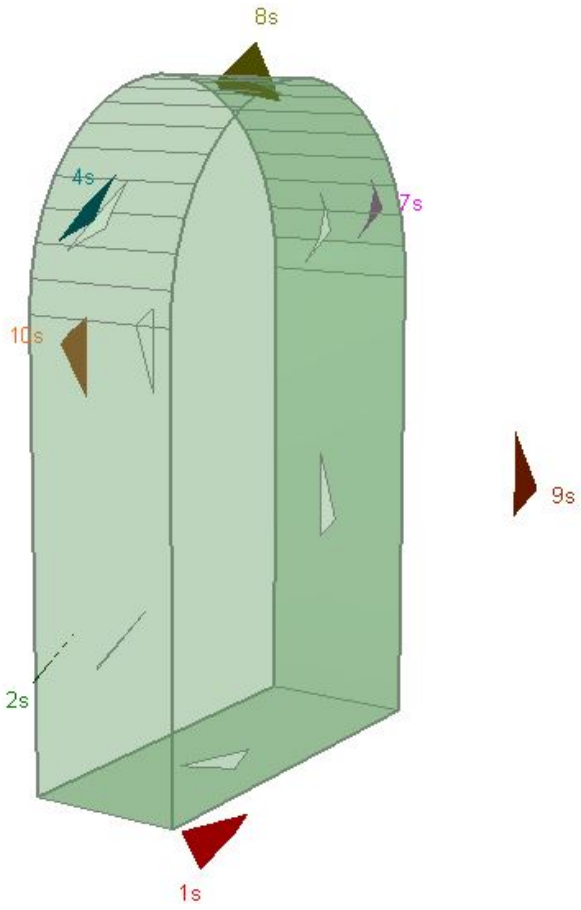

Figure 5.5: Scaled wedges formed in Mohr-Coulomb analysis in code Unwedge by Rocscience. The wedges are scaled after field observations on persistance and trace lengths.

As seen on figure 5.6, 3 wedges form in the roof, and 3 in the walls of the excavation. No field stresses has been added to the analysis because the code cannot use stress elements as weakening forces, and thus a field stress implementation would mean increasing the safety factor. The certainty of wedge sizes is small, but an area of fallout of $4-6m^2$ is believed possible from field observations.

Support will now be added to the analysis to try and reach a sufficient safety factor. An overview of the support can be seen in figure 5.6.

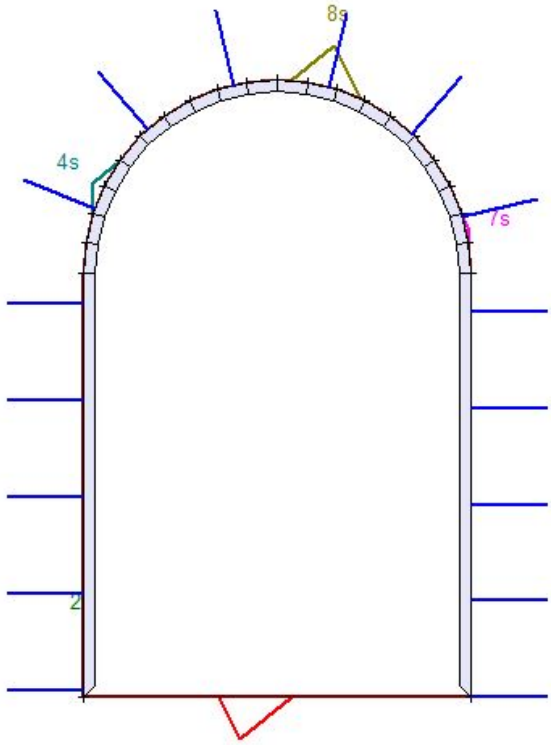

Figure 5.6: Sketch of supported cavern. The wedges are scaled after field observations on persistence and trace lengths. Lowest safety factor is at roof wedge (8s) at 1.3

Bolt pattern was added with c/c=2 m and with CT bolt properties from manufacturer. c/c=2 m seems sufficient to cover the formed blocks. Further, an 11 cm shotcrete layer was necessary to reach a sufficient safety factor for the roof wedge at SF=1.3. Shotcrete shear strength is put to $100\frac{t}{m^2}$. Table 5.3 summarizes the analysis for the wedges that could possibly create problems for the excavation. To compare with the Mohr-Coulomb model the same analysis was done using Barton-Brandis joint strength approach option. Geometric parameters are kept equal in order to be able to reasonably compare the different solutions. Essential parameters are chosen based on above discussion and the results are presented in table 5.4.

Table 5.3: Safety factors of support in code Unwedge using Mohr-Coulomb joint parameter approach.

Wedge	Volume (m3)	Support	Safety factor
Roof (8s)	0.327	c/c=2m bolts and 11cm shotcrete.	1.3
Roof (4s)	0.04	c/c=2m bolts and 11cm shotcrete.	2.6
Roof (7s)	0.007	c/c=2m bolts and 11cm shotcrete.	5
Wall (2s)	0	c/c=2m bolts and 11cm shotcrete.	22

Table 5.4: Safety factors of support in code Unwedge, using Barton-Brandis joint parameter approach.

Wedge	Volume (m3)	Support	Safety Factor
Roof (8s)	0.327	c/c=2m bolts, 12cm shotcrete layer	1.4
Roof (7s)	0.007	c/c=2m bolts, 12cm shotcrete layer	5.5
Roof (4s)	0.04	c/c=2m bolts, 12cm shotcrete layer	2.9
Wall (2s)	≈ 0	c/c=2m bolts, 12cm shotcrete layer	24.7

The output of the Barton-Brandis analysis is quite similar to the Mohr-Coulomb model. A 12 cm shotcrete layer is needed compared to an 11 cm in the Mohr-Coulomb model. Looking at previous constructions, 11-12 cm of shotcrete is usually needed for bad quality rock mass (Q=1-4) for large span excavations (Loeseth and Kveldsvik, 1997). Several reasons could be presented that make the blocks more unstable than in reality. First of all no stress is included in the model. In many cases stress would "clamp" the blocks together by yielding normal stress to planes and thus increasing the stability. Also, joints are here represented with no tensile strength so wedges in the model would fail instantly after blasting with no support. In reality this has proven unrealistic in fair-good quality gneiss. A water pressure equivalent of 60 meters is used in the model adding to driving forces for wedge failure, although this may not be the case in the project area.

The code Unwedge is not very suitable for modelling weakness zones. The joints would have less cohesion and slightly lower friction angle, but the main element would be the larger volumes of several blocks that could fail. The code is not very suited for estimating safety factors in such a case, a study could nevertheless be done

visually to help define bolt pattern. Also, heavy support such as concrete lining and shotcrete arches are not included in the code as support measures and would most likely be needed in the very weak rock mass portion in the Hammerfest cavern.

5.5 Limit-equilibrium assessment of weakness zone

As an analytical way of estimating support requirement in the weakness zone one can view the very fractured and jointed rock mass as a plastic material behaving like a soil (Hoek and Marinos, 2000). This allows analysis of deformation around a near-circular underground opening where the soil would behave elastic-perfectly plastic (Hoek and Marinos, 2000). There are several disadvantages that make this less suitable for studying the interaction between a weakness zone and support measures. First of all, it is assumed elastic-perfectly plastic behaviour of the rock mass. This would mean as soon as the strength of the medium is reach, it will deform plastically, and not brittle, as seen on figure 5.7.

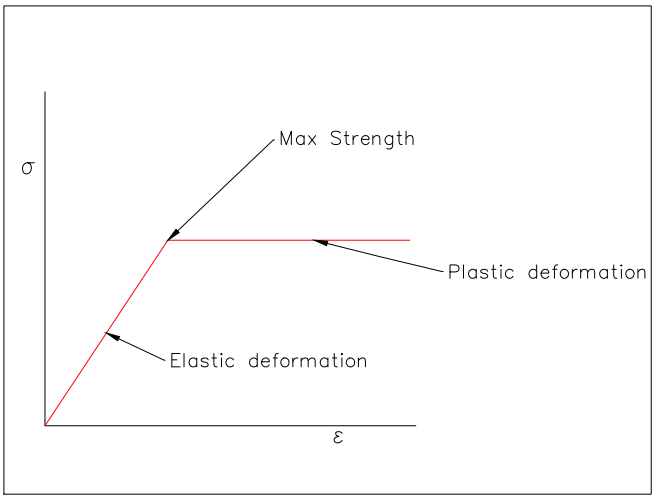

Figure 5.7: Sketch showing elastic-perfectly plastic behaviour of a material of in response to stress.

In reality, the weakness zone may behave brittle but also plastically. Nonetheless the

rock pressure would be the key element the support would have to withstand and the investigation could give valuable indications for this. The second unfavourable assumption is that the tunnel is perfectly circular, and that all support is installed continuously around the cross section. This results in a slightly elevated support pressure. A third disadvantage is that the stress field has to be homogeneous e.g. $k = \frac{\sigma_h}{\sigma_v} = 1$. This may not be the case as discussed earlier in both the Gjøvik sport cavern, and the crusher hall at Rana gruber. In Hammerfest the stress conditions are uncertain. Though these assumptions most likely create errors in the analysis it is still interesting to carry out investigation. Testing of parameters for the numerical modelling may come in handy. Additionally it suggests how to estimate support requirements for the weakness zone and compare the results to the empirical support scheme.

The following approach was selected in estimating model parameters:

- Tunnel radius is set to 10m, half of the cavern width.

- Rock mass strength is chosen for the weakness zone using Roclab. GSI value is based on earlier discussion with poorly disintegrated, poorly interlocked joints, heavily broken rock mass, and possibly poor surface conditions due to deep weathering of the weakness zone.

- Intact rock parameters are obtained in the laboratory investigations presented in chapter 4.

- In-situ stresses are simplified to hydrostatic stress condition of 2, 4 and 6 MPa, to compare different cases of stress in the subsurface. A minimum principle stress of 2 MPa is used because of the approximately 60 m depth.

- By Mohr-Coulomb rock mass envelope, a friction angle of 23 °is chosen.

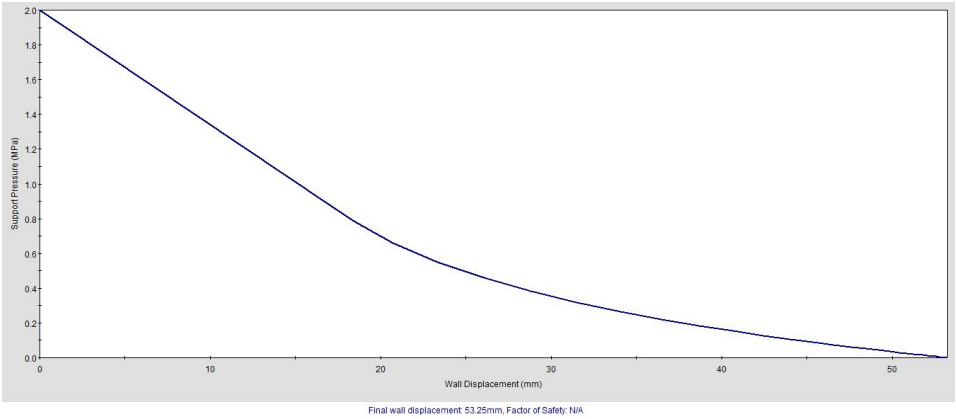

Figure 5.8: Ground reaction curve obtained with above mentioned parameters and a hydrostatic stress of 2 MPa. Final wall displacement is at 53 mm and plastic zone at 15 metres.

Figure 5.8 shows the ground reaction curve obtained with 2 MPa hydrostatic pressure and above mentioned parameters. In table 5.5 a support scheme is presented based on the support options available in the code. Tunnel convergence is kept restricted 20 mm at final displacement.

Table 5.5: Support needed to reach a SF of 1.3, for hydrostatic stress at 2 MPa in code Rocsupport.

Stress	**Unsupported final Deformation**	**Deformation before support**	**Support scheme**	**Supported final deformation**	**Safety Factor**
2 MPa	53mm	5mm	c/c=1.2m 25mm Rockbolts 15cm shotcrete 216mm steelsets	19mm	1.3
2 MPa	53mm	10mm	c/c=1.2m 25mm Rockbolts 10cm of shotcrete 162mm steelsets	25mm	1.33

To investigate what happens when pressure underground exceeds 2 MPa, the GRC for hydrostatic stress at 4 MPa is also performed. The outcome of the analysis is shown in figure 5.9.

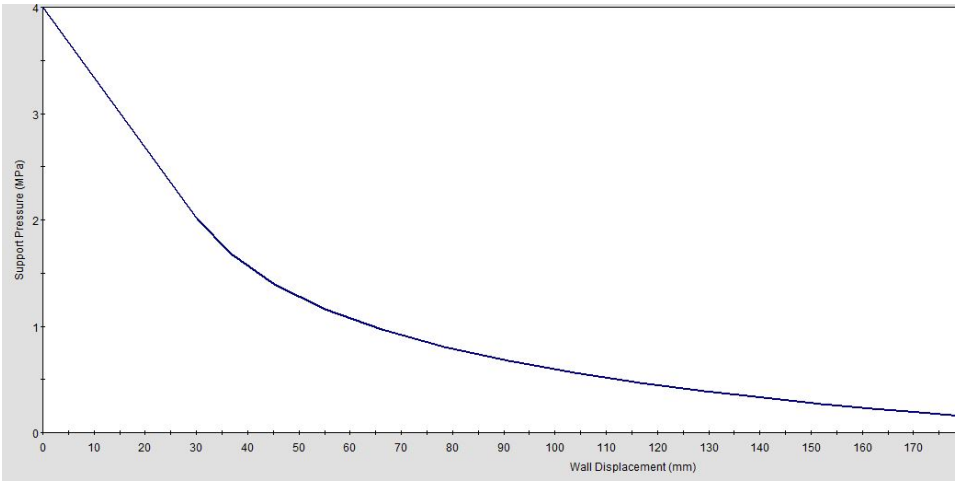

Figure 5.9: Ground reaction curve obtained with hydrostatic stress of 4 MPa. Final wall displacement is 230 mm and plastic zone at 23 metres.

The simulation indicates final wall displacement five times higher by doubling the stress. Hydrostatic stress at 4 MPa is believed to be unrealistic because of the low overburden, but tangential stress could rise to similar magnitudes for certain parts of the periphery under high horizontal stresses. In table 5.6 suggested support schemes gives safety factors >1.3 along with moderate displacements. The analysis indicates that deformations will take place under a very short time period. It would accordingly be hard to install support as fast as presented in the two schemes above. It is therefore recommended that support will be installed right after blasting and that the weak rock has to be sufficiently supported before continuing the excavation.

Table 5.6: Support needed to reach a SF of 1.3, for hydrostatic stress at 4 MPa in code Rocsupport.

Stress	**Unsupported final Deformation**	**Deformation before support**	**Support scheme**	**Supported final deformation**	**Safety Factor**
4 MPa	230mm	25mm	c/c=0.7m 33mm Rockbolts 30cm shotcrete 254mm steel ribs	40mm	1.3
4 MPa	230mm	19mm	c/c=0.7m 33mm Rockbolts 40cm of shotcrete 254mm steel ribs	34mm	1.32

5.6 Rock mass classification

The rock mass is evaluated with regards to the RMR and Q-method from previously performed investigations. There will be an additional classification according to GSI system for the rock mass.

Table 5.7: Rock mass rating of rock mass in project area.

Location	fracture distance	RQD	Water conditions	State of fractures	Strength
2	10	13	4	25	12
3	8	13	4	25	12
3	20	17	4	25	12
1	20	17	4	10	12
10	10	13	4	25	12
5	20	17	4	25	12
18	20	13	4	25	12
5	10	13	4	20	13
11	5	8	4	20	13

The RMR values are corrected for an unfortunate cavern orientation. By not including weak rock, the values lie in the range from 40-70. The majority of the rock mass has good quality (RMR<60), but locally the rock mass is more jointed, in addition to the weakness zone.

The rock mass has also been classified according to the Q-system on a field visit in may 2013, performed by SWECO Norway. The following Q-parameter distribution was found.

Fracture distance was more than 30 cm in the majority of the area.

- 80% of the rock mass is evaluated as Q>40 which in turn means good rock mass.
- 10% of the rock mass is in rock class D e.g. 1<Q<4 (bad).
- 10% of the rock mass is in rock class E e.g. Q<1(very bad).

5.7 Empirical stability assessment

As an empirical method of estimating support measures the Q-method is applied. Essential parameters were collected by SWECO in may 2013. The Q-values are accordingly evaluated as follows for the project area: 80% of rock mass in Class B(good), 10% in class D(bad) and 10% in class E(very bad). The support classes were evaluated as respectively class 3, 4 and 7.

It gives a basis for predicting support the measures presented below

- 80% (class B) of the rock mass i expected to need >5 m long, 25 mm in diameter systematic bolts with center distance 2.5 m, together with fibre-reinforced shotcrete of 6 cm thickness.
- 10% (class D) of the rock mass i expected to need >5m long, 25 mm in diameter systematic bolts with center distance 1.7-2.1 m, together with fibre-reinforced shotcrete with stiffness E700, and with 6 cm thickness.
- 10% (class E) of the rock mass is expected to need >5 m long, 25 mm in diameter systematic bolts with center distance 1.3-1.7 m, together with fiber-reinforced shotcrete with stiffness E1000 with >15 cm thickness. In addition, steel rib shotcrete arches are needed.

5.8 Mitigation concept based on performed investigations

For the good quality rock, bolt lengths can be estimated from the stability assessment in UnWedge, from the Q-method, and from the analytical spalling-depth approach as discussed earlier.

The Unwedge analysis show that bolt length of 2 m are sufficient in best case scenario. However, this scenario represents the smallest possible wedges. In reality wedges

could also fail on not the first, but the second or third fracture, should these be more unstable. Furthermore, since the span of the cavern is significant, bolt length of 6 m is assumed to be needed.

The Q-system can be used to estimate bolt length based on the span of the cavern or tunnel, and the ESR (Excavation Support Ratio). In this case, the ESR is 1, thus the empirical recommended bolt length would be 6 m.

Thirdly, the analytical approach is based on the stress regime and the magnitude of stresses around the cavern. Since this is crucial in estimating bolt length, more knowledge on stress conditions are needed before using this approach with certainty.

By comparing the different approaches, bolt length is suggested as 6 m for horizontal stress magnitude under 13 MPa. This is because the empirical investigations indicate that the large span would need such length. Should the horizontal stress be larger than 13 MPa, the bolt length would have to be increased according to table 5.2. Spacing described by center distance is kept at 2.2 meters as believed better suited than the 2.5 m Q system recommendation, according to the Un-wedge analysis.

Estimating the required shotcrete layer is done with the Q-system and by the Unwedge analysis. The Q-classification suggests that for good quality rock 6 cm of shotcrete is sufficient. Since Unwedge does not take any stresses into account, a more pessimistic prediction of 11-12 cm is necessary to reach a satisfying safety factor. Based on previous discussion, it is believed that Unwedge outputs are too pessimistic. It is accordingly believed that 6 cm of shotcrete is sufficient.

Looking at the bad quality rock part of the cavern, the tools of estimating support are Q-method and the Rocsupport code. Weakness zones or zones of severally jointed and weak rock mass are always hard to design support for without core samples. Often it requires ahead of face drilling to evaluate the true quality of the rock. It can be said that the Q-system based on Norwegian problems with weakness zones is better suited than the hydrostatic stress analysis done with the squeezing problem-designed

Rocsupport code. Rock quality in the Rocsupport analysis is estimated with GSI and may be less fitting than the Q-values actually obtained on site. However, the best solution would be testing the least extensive support scheme in the numerical model in order to save cost.

5.9 Water inflows

The cavern is planned with a maximal overburden of 60 m. It is thus not expected large waterpressure to occur during excavation. It is important to minimize the water leakage as discussed earlier. No precipitation had bin at field site the week before it being investigated. Despite, it was registered heavy drip in the small tunnel at the foot of the mountainside. In addition, groundwater is present at the top of the mountain found as high as 125 m.a.s.l. Accordingly, the height of the water column above the cavern is estimated to 60 m and results in an effective waterpressure as shown below:

$$p = \rho_w g h$$

$$p = 10\frac{g}{cm^3} \times 9.8\frac{m}{s^2} \times 60m = 0.6MPa$$

Should the cavern be in direct contact with the small water bodies on the surface, the possibility of draining them is present. The water inflow from a fracture in direct contact could be catastrophic. This is shown in the calculations below, based on discussion in chapter 2. It is assumed that viscosity of water is $9.7 \times 10^{-7}\frac{m^2}{s}$.

For fracure dilation $a_h = 0.1cm$

$$Q = \frac{9.81\frac{m}{s^2} \times (0.001m)^3}{12 \times 9.7 \times 10^{-7}\frac{m^2}{s}} \times 65m \times 3m = 0.16L/s$$

For fracture dilation $a_h = 1cm$

$$Q = \frac{9.81\frac{m}{s^2} \times (0,01m)^3}{12 \times 9.7 \times 10^{-7}\frac{m^2}{s}} \times 65m \times 3m = 164L/s$$

For fracture dilation $a_h = 10cm$

$$Q = \frac{9.81\frac{m}{s^2} \times (0,1m)^3}{12 \times 9.7 \times 10^{-7}\frac{m^2}{s}} \times 65m \times 3m = 164342L/s.$$

Another way of estimating water inflow as documented in chapter 2, is viewing the rock mass as an aquifer. This is possible when the scale is large and when assuming fracture systems give hydraulic conductivity to the mass as a whole making it act as an aquifer. To estimate hydraulic conductivity for the rock mass it is possible to back calculate the estimated amounts from the field visit, where a small tunnel by the foot of the mountainside was investigated. As mentioned earlier, heavy dripping was registered inside the cavern, with a roughly suggested magnitude of 30-60 $\frac{L}{min}$ per 100 m. Using equations described in Loew et al. (2010) and chapter 2 the hydraulic conductivity is estimated as

$$(Q) = \frac{4\pi K\frac{m}{s} \times 100m \times 60m}{2.3\log(2.25 \times K\frac{m}{s} \times 100m \times 1/(10^{-6}s^{-1})^2)} \approx 1\ L/s\ per\ 100m$$

which gives $K = 1 \times 10^{-7}$ for a inflow of 37 L/s per 100m. Compared with studies in the Alps presented by Loew et al. (2010), this number coincides to some degree. Uncertainties are acknowledged because the visual inspection was performed in rock mass with little overburden and the proposed magnitude is not measured with sufficient accuracy. More certainty in estimates of water inflows cannot be acquired before in-situ experiments such as the Lugeon test is performed at location.

5.10 Consequence of draining ponds

Should inflow from a water filled crack be hit during excavation, the water would drain out as a function of flow area in the crack as shown above. The total amount of water can be estimated with area of puddle, and an approximate average depth of 2 m, and is accordingly around $9000m^3$ when area of the puddle is $4538m^2$. Assuming fracture

diameter of 1 cm, the time to drain the pond would be accordingly

$$t_{drain} = \frac{V_{pond}}{Q_{drain}} = \frac{9000m^3}{0.164m^3/s} \approx 15\ minutes$$

An obvious disadvantage with draining the small pond Salsvannet on the plateau at Salsfjellet, would be the esthetic change it presents. Locals often frown upon such changes in scenery and can distrust or withdraw support from such projects in the future.

Figure 5.10: Image looking west, showing the pond on top of Salenfjellet. Directly above the west end of the cavern. Photo: Geir Jenssen

Experience of numerous tunnels in the Alps show that draining water table in crystalline rock mass may cause large scale settlement (Loew et al., 2010). Usually, the groundwater table in such high mountain regions lies several hundred meters below surface and that for instance springs in mountain slopes are fed by near surface groundwater bodies. In that manner, Loew et al. (2010) concludes that changes in shallow or phreatic water tables in crystalline rock not always has a direct impact on surroundings. Severe impacts one gets with draining the inner - deep water table. In high mountainous regions such changes can cause surface rock settlement of up to

tens of centimetres, and pose large problems for arch dams.

It is hard to predict the connection between the pond Salsvannet, and the groundwater table in Salsfjellet. Field observations show substantial proof of surface water being present in form of springs and ponds along with dripping inside the mountainside. There is no evidence concluding the connection between these two until more knowledge is gained on the water conditions inside the mountain. Should the springs and ponds be directly connected to the subsurface water systems the possibility of lowering the water table about 60 metres is possible. A risk of this could be destabilizing the already heavy supported mountainside that dips towards the city. Usually, a lowering of the water table would increase the stability of the slope, or parts of it. Several mechanics is behind this (Nilsen, 2012).

- Waterpressure on a sliding plane decreases resistance force.
- Waterpressure in a tension crack ads to driving forces in slope or block failure.
- No presence of water eliminates the possibility of frost expansion.
- Flow of water increases weathering.
- Water can produce swelling if certain clays are exposed to water.

Although removing waterpressure from the sliding surface of a possible failing block generally stabilizes it further, changes in waterpressure may interfere with natural systems within the slope thus causing failure of more complex compositions. An example could be lowering the weight of the overburden to an already dry fracture, and by doing so lowering the normal stress on the sliding plane. Thus frictional force decreases and gravitational forces would cause the block to fail. Of course this is unusual but similar events have happened in Italy at the Vajont dam (Duffaut, 2003). Though above mentioned events could happen, the general trend is that slope would be more stable by reducing water table since the presence of water in a slope generally adds to the driving forces for slope failure.

Lowering the head could generate problems to the surroundings. Chemical and

physical conditions can alter within the pond. In marshes, oxidation of iron sulphide minerals in the dried sediments can occur. The consequence could be acidic water draining to urban areas and disturb the Ph-value of the natural groundwater over a larger area (Statens Vegvesen, 2003). One has to assess the consequences both qualitatively and quantitatively when determining allowed impact. Qualitative elements are amongst others biological diversity, scientific and pedagogic importance, untouched value, value as hiking area and environmental pollution (Statens Vegvesen, 2003). Quantitative considerations embody direct economical interests such as agriculture, water resources, hunting and fishing, but tourism can also constitute a part of this.

It is not believed that settlements of any mentionable magnitude will occur should water table be lowered in Hammerfest. It is not believed that the change in waterpressure of 60 meters will be able to force the rock mass to settle. Such phenomena are additionally seen when water table lowering regards larger magnitudes. Field studies show that the soil cover on the surface above the tunnel is not thick, and is not likely to harm the building located at the surface. Nonetheless one should map how infrastructure is founded also at the foot of Salsfjellet.

5.11 Water mitigation

Most commonly used as mitigation for water problems in Norway is injection of cement or "grouting". The method proves sufficient to provide as low leakage as required even for projects with very strict requirements (Statens Vegvesen, 2004), the exception being areas with high overburden (high waterpressure), or rock mass not suited for grouting. Sometimes systematic injection is pre-determined where leakage has to be kept at a minimum. An other method is sporadically grout rock based on information from probe drilling. Sporadic grouting can be difficult because one risks excavating too far in to the leaking zone before grouting is initiated (Kluver and Kveen, 2004). Systematic grouting for projects with low leakage requirements is getting more common (Statens Vegvesen, 2004). For instance, a weakness zone in gneiss were systematically grouted, where minimum leakage could be 0.5-0.8 $\frac{L}{min}$ per 100 m for a

tunnel in Asker, Norway with OK results (Statens Vegvesen, 2005). Examples of successful grouting projects near vulnerable buildings are many (Kluver and Kveen, 2004). Grouting in front of face shows the best results as grouting behind face is not near as effective. It is important that information regarding groundwater conditions is obtained at an early stage, which practically means that information of pore pressure and groundwater levels should be available early in a project including data on seasonal change. Should settlement of nearby buildings or environmental impacts be considered extensive by change in pore pressure, a detailed testing program should be established. Leakage requirements can be divided in the following groups as suggested by the road authorities for a 100 m section of a tunnel (Kluver and Kveen, 2004)

- Extremely strict 1-3 L/min
- Strict 3-7 L/min
- Moderately strict 7-15 L/min
- Moderate >15 L/min

One can classify the rock mass according to a scheme, the classification follows descriptions given in Kluver and Kveen (2004) and will not be described here in detail. The class gives pointers and practical considerations on grouting in the rock. The rock mass in Hammerfest would best be considered in grouting class B. The following considerations follows the classification.

- Fractured rock with possibility of water carrying channels, often Precambrian gneisses, and possibly with clay filled fractures.
- Since the presence of clay can vary in a large degree, injection of cement mix has to be tailored or customized for varying rock conditions.
- The presence of clay often increases near weakness zones, where one would expect lower grouting capability.
- For a 8.5 m width, borehole length is suggested as 15-30 m with 15-40 boreholes in total.

- In densely jointed rock, it is suggested to use more boreholes, and less borehole length.

- Water/cement ratio is recommended to vary between 1.2 and 0.9 initially. Later reduction to w/c=0.5 and pressure build up to 60-80 bar. The last grouting sequence is recommended as a pressure build up top 90-100 bar.

Experience suggests that largest discharge occurs in steep dipping fracture planes (>55°) Kluver and Kveen (2004). In Hammerfest this is the case for much of the foliation and hence could be unfortunate for the excavation. Joint intensity is usually higher in the surface than in deeper in the subsurface. The project area is generally good quality rock, which may indicate that little water could penetrate deeply. An obvious point explained in Kluver and Kveen (2004) is fracture sets nearly parallel to cavern length axis increases discharge, and making areas of the rock mass sufficiently watertight could prove difficult. In brief, areas where grouting will be necessary, very close follow up together with continuous adjustments to the borehole set up will be decisive for a good result. In case of the weakness zone the observations made regarding the clay filling is beneficial in a hydrogeological aspect.

Crushing zones which often occur in Norway's mountain regions are usually deeply weathered, and have little permeability because of the clay material filling cracks. It is though possible o encounter problems with the rock mass next to the centre of the zone. Often heavily jointed and crushed rock with little chemical weathering has good conductive characteristics. If grouting is performed with bad care one might increase stability issues within the zone itself.

It is also worth considering leakage to the ventilation shafts. These structures can similarly to tunnels drain areas around. Leakage into a shaft could cause bad air quality inside the cavern if utility work is necessary. Water could also cause corrosive environment in the shaft, which again could cause damage to concrete constructions.

Performing grouting with good results does not solely depend on the water blocking

characteristics of the rock. Following the classification scheme above one is of high risk in injecting too much grout in to the rock. By doing so one uses too much resources compared to what is necessary. The injection pressure should rather be evaluated with regards to the pore pressure of the water in order to insure that no excess injection is performed where it is not needed. According to Panthi (2010), the need for grouting is first determined by ahead of face drilling. Packers are then used to evaluate the leakage of the rock by injecting water at pressure of 1.5 times the hydrostatic head and measure the water loss. The factor of 1.5 is used a safety factor assuring the penetration of water in to cracks. After discussion with supervisor Dr. Krishna Panthi it was decided that leakage should not exceed 0.5 L/m per meter borehole. Testing should be performed with three boreholes, one in the roof and two at the top of the walls. Testing should begin 20-30 meters ahead of the weakness zone with pipes length of 15-20 metres in to avoid excavating in to water carrying joints surrounding the zone. If grouting will be needed, the pressure of cement is controlled by the hydrostatic head as of Panthi (2010). Largest possible waterpressure is calculated to be restricted to 6 bar (or 0.6 MPa) as discussed above. Based on discussion on the unfortunate event of draining surface water it has been decided that a grout pressure at 2 times the hydrostatic pressure is recommended. This is increased from the case presented in Panthi (2010), the reason being that leakage requirements of the parking cavern would be stricter tan those of a headrace tunnel.

Assuming grout piping lengths of 15-30 m, two grout screens are recommended. The weakness zone is expected to strike normal to cavern length axis at approximately station 355 comparing appendix A and B. Hence grouting should be performed at station 335 and 375. Grout should initially have w/c-ratio between 1.2 and 0.9. Later w/c ratio should be decreased to roughly 0.5. The need for grouting in the good portion rock mass depends on the relationship between surface water and rock at cavern elevation. Investigations during excavation of the new tunnel to road RV40 should be considered. Should initial water tests show leakage in the good quality rock, the same principles as for the weakness zone applies. If tests show dry conditions

grouting is not necessary.

5.11.1 Constructional aspects and time estimates

Several methods in predicting construction time are available. In the project thesis an estimation was carried out using TUNSIM code. The code is a NTNU spreadsheet based code with various input parameters which calculates construction time from empirical numbers. It will here be compared to values from previous projects in Norway. Background for the estimate is excavation and support of both caverns.

Table 5.8 shows numbers of time for norwegian underground caverns from Rygh (1999).

Table 5.8: Time and size numbers for Norwegian underground caverns from start to completion (Rygh, 1999).

	Time (months)	Volume (m^3	m^3/month
Gjovik Olympic Cavern	24	140 000	5833
Holmlia Cavern	45	53 000	1178
Grottebadet	48	54 000	1125
Oddahallen	24	25194	1050
Skaarehallen	24	25600	1067

One notices the Olympic cavern of Gjøvik being an exception with some 5 times higher excavation rates than the rest. It correlates with the volume of the cavern suggesting rates increase in large projects when routines and efficiency are improved over time. Calculations in the project thesis gave volume estimates around 190 000 m^3. Based on average construction times the time for completion of the Hammerfest parking cavern would be 90 months. The number is very high, and by comparing to the Gjoevik Olympic hall with similar volume to be excavated, completion is expected in 13 months. Bollingmo (1974) presents data on the time required to solely excavate and support underground caverns in Norway. Comparison of the projects Olympic hall in Gjøvik, Froststorage in Jordalen, National archive in Kringsjå, and Høvik show strongly varying time in construction and completion ranging from 500 to 17 000 m^3 per month. However the average of around 4500 m^3 per month is believed to be achieved with the Hammerfest cavern assuming good planning and professional execution.

In accordance with the empirical numbers, time for excavation and support may be expected in and around 40 months. The Gjøvik Olympic hall stands out as significantly larger volume than the other projects. Further, time consumption is drastically smaller compared to volume. The data shows the time for completion is around 2.5 times higher than excavation and support. One may therefore suggest 15 months for excavation and installation of support.

6. Frost intrusion and mitigation

6.1 Approach

The goal of the investigation is to have data supporting empirical conclusions that the facility will be exposed to frost when ventilation is as described in the pre-feasibility study. Based on discussion in chapter 2 the design frost load in Hammerfest is F_{10}=24 000 hC°. From Statens Vegvesen (2006), all drainage system is to be frost insulated if frost load on location exceeds F_{10}=6 000 hC°.

6.2 Analysis tool

The excavation's special geometry and ventilation design makes ideal and theoretical approaches to temperature estimation difficult and impractical. Instead, a numerical approach is used through the code Ventsim. The software is generally used in predicting airflow in underground mining projects, hence it is ideal to investigate airflow and temperature exchange with the surroundings. The software can be used to give an indicator on how inside temperature will be affected by the ventilation design in terms of below-zero temperatures.

In corporation with master students with knowledge of the software the cavern was modelled as shown in figure 6.1.
The overburden is assumed 60m above sea level. This is only an approximation since not all of the cavern is at this elevation. However, the error is believed to be conservative by making temperature in the cavern higher. The model operates with a

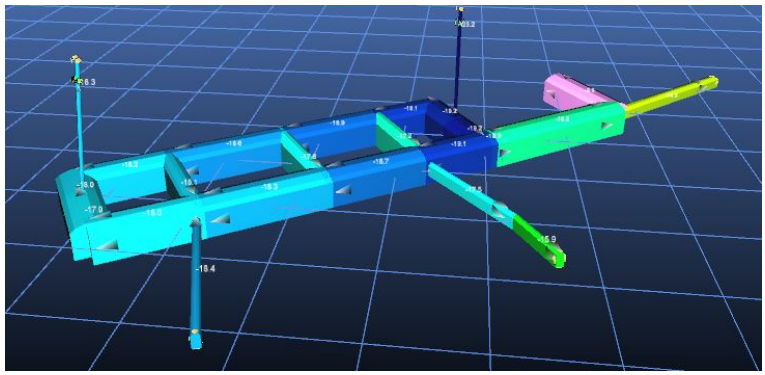

Figure 6.1: Geometric model of the parking cavern created in Ventsim.

simplified ventilation system where air is pumped through the eastern ventilation duct. The intake is modelled as having fixed flow at 34.3 $\frac{m^3}{s}$ suggested in the feasibility study, and the air drain with fixed pressure at 7 kW. A rock thermal diffusivity at $1.47 \times 10^{-6} m^2 s^-1$ was used as obtained in laboratory experiments done on similar gneiss types in Olkiluoto, Finland (Kukkonen et al., 2010). Inside temperature in the mountain is assumed steady at 4°C.

The model is ran for three different external temperatures at 10°C, -5°C and -20°C to represent seasonal changes and is presented in figures 6.2 to 6.4.

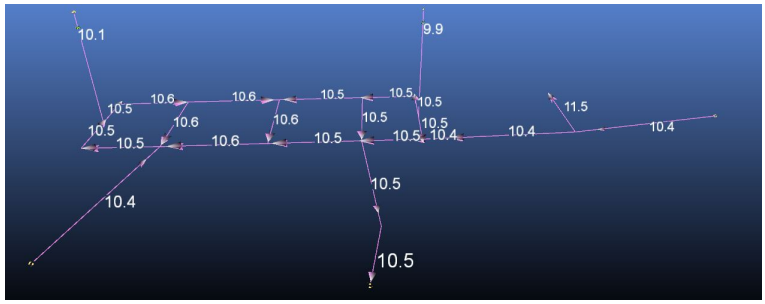

Figure 6.2: Model ran with external temperature at 10°C. The numbers indicate temperatures inside the cavern.

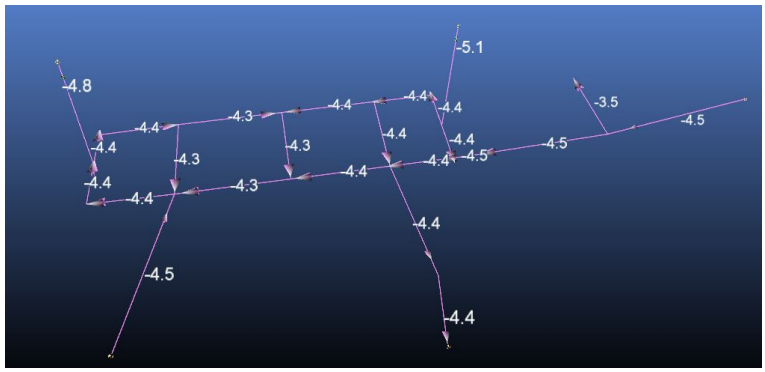

Figure 6.3: Model ran with external temperature at -5°C. The numbers indicate temperatures inside the cavern.

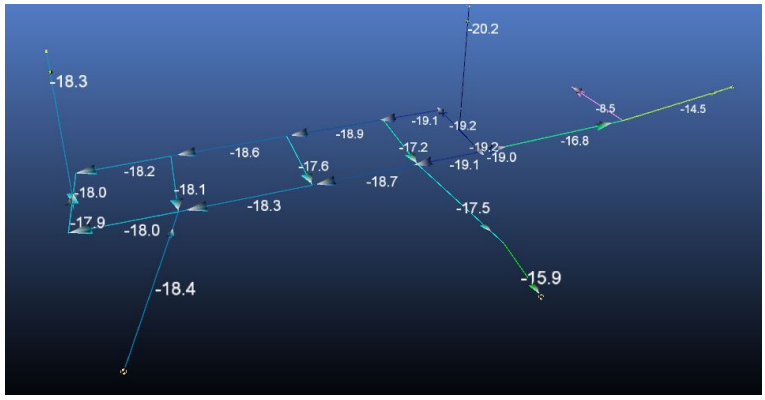

Figure 6.4: Model ran with external temperature at -20°C. The numbers indicate temperatures inside the cavern.

It is important not no have too much emphasis on the models magnitude outputs. Parameters used are not accurate for Hammerfest and the analysis should be used as an indicator if sub zero temperature will reach the cavern with the simplified ventilation concept described above. Results must be interpreted along with experience or possibly other approaches. This analysis indicates that during cold periods temperatures inside the cavern will be sub zero but slightly warmer than outside temperature. Thus the analysis implies the need for frost mitigation.

6.3 Frost mitigation

The investigation indicates that temperatures inside the cavern are slightly lower than outside, and since additional heat will be generated by cars, design frost load F_{10} is adjusted to a maximum value of $F_{10} = 20\,000$. The necessary thickness of the insulation is determined by the U-value as discussed in chapter 2. The required is given by the road authorities and depends on frost load as of figure 2.9. This amounts to a required U-value of 0.69 for the insulating material. The U-value for a material can be calculated as follows (Statens Vegvesen, 2006)

$$U = \frac{1}{d_1/\lambda_1 + d_2/\lambda_2}$$

where d_i denotes the thickness of material i andλ_i the heat number for material i. There are mainly two types of frost insulation to choose from in cold locations as in Hammerfest. The concrete plate arch has heat-number $\lambda = 0.2 - 0.25\frac{W}{mK}$, and should also have additional insulation if F_{10}>12000°Ch (Pedersen, 2005). PE-foam with systematic bolting (c/c=1.2) and fire mitigation such as shotcrete is another approved frost insulation method with $\lambda \approx 0.042\frac{W}{mK}$.

The thickness when using solely light concrete plate arches should be:

$$d = \frac{\lambda}{U} = \frac{0.22}{0.69} = 32cm$$

In order to reach sufficient level of insulation however, it is possible combine a layer of XPS-foam behind the concrete elements who should not usually be thicker than 150 mm (Statens Vegvesen, 2006). Assuming 150 mm thick light concrete plates the thickness of the XPS layer should be as follows:

$$U = \frac{1}{d_1/\lambda_1 + d_2/\lambda_2} \rightarrow d_{PE} = 2.26cm$$

Usually, extruded polystyrene is applied as a 5 cm layer (Pedersen, 2005) and accordingly, frost insulation will have a total thickness of 150 mm+50 mm=200 mm as sketched in figure 6.5. In addition, there has to be space behind the frost mitigation so that rock support may be accessible. It is normal to add +4000 h°C to the frost load as a material factor, because it is often colder near surface than a couple of meters up in the air. This gives a design frost load of 24000 h°C and accordingly a required U-value of 0.6. The according XPS layer behind the cocnrete plates should be:

$$U = 0.6W/m^2k = \frac{1}{d_1/\lambda_1 + d_2/\lambda_2} \rightarrow d_{XPS} = 3.3cm$$

XPS plates are usually installed with 5 cm thickness which means that the proposed mitigation qualifies. The theoretical frost load the concrete and XPS foam will withstand is

$$U = \frac{1}{d_1/\lambda_1 + d_2/\lambda_2} \rightarrow \frac{1}{0.15m/0.22\frac{W}{mK} + 0.05m/0.043\frac{W}{mK}d} = 0.45$$

which means that theoretically a frost magnitude of F_{10} = 40.000 h°C could be withstood using this insulation scheme based on figure 2.9 in chapter 2.

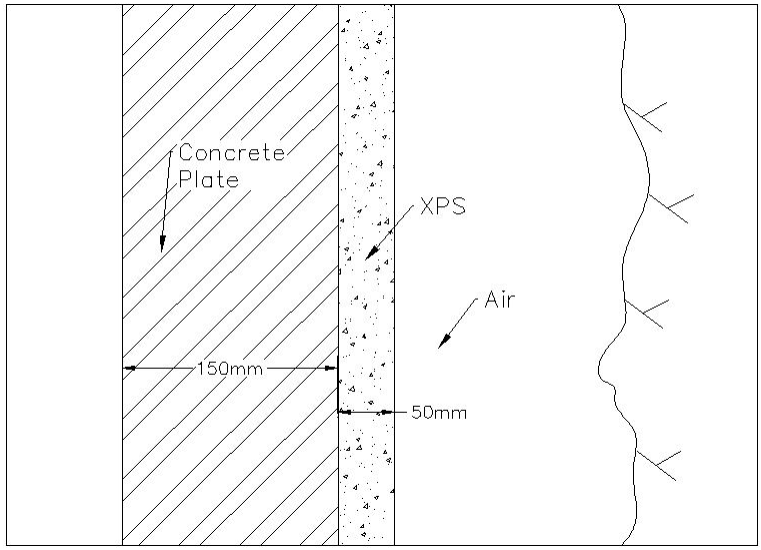

Figure 6.5: Sketch of the needed frost insulation if $F_{10} = 20000$ inside the cavern.

In comparison, the needed thickness using solely PE-foam is

$$U = 0.6W/m^2k = \frac{1}{d_1/\lambda_{PE}} \rightarrow d_{XPS} = 7cm$$

7. Numerical Modelling

7.1 Analysis tool

Numerical modelling is carried out using software Phase^2 from Rocscience. Numerical modelling is a powerful method of visualizing the dynamic behaviour of rocks mass. It has become a crucial tool in rock engineering, simulating the behaviour of rock or soil for an excavation, landslide, groundwater flow, rock foundation to name a few. The program is a finite element analysis tool based on 2D geometry inputs in addition to rock mass parameters and material properties. It computes stress and deformation around underground openings with either plastic or elastic criteria. Functions for rock bolts and other reinforcements are available for usage in the program. The software is suitable when presenting stability analysis of underground excavations, it produces results simplistic and understandably. It must be kept in mind that numerical modelling is an appropriate simplification of reality not the reality it self. It is important to be aware that the results of numerical analysis can never be more accurate than the input parameters suggests.

7.2 Main goals

The main goals of the numerical analysis are summarized in the following steps:

- Investigate proposed support measures and compare analytical with empirical support approaches for good rock quality conditions.
- Assess support schemes for bad quality rock (expected in the weakness zone), and determine stability measures to a satisfying safety factor.

- Investigate stresses in the subsurface. Determine the impact of varying horizontal stress on mitigation magnitudes.
- Finalize satisfying support measures for all rock conditions.

7.3 Model

Different tunnel geometries are investigated which require production of multiple sections in the model. Overview of planned excavations is presented in figure 7.1 with sections sketched.

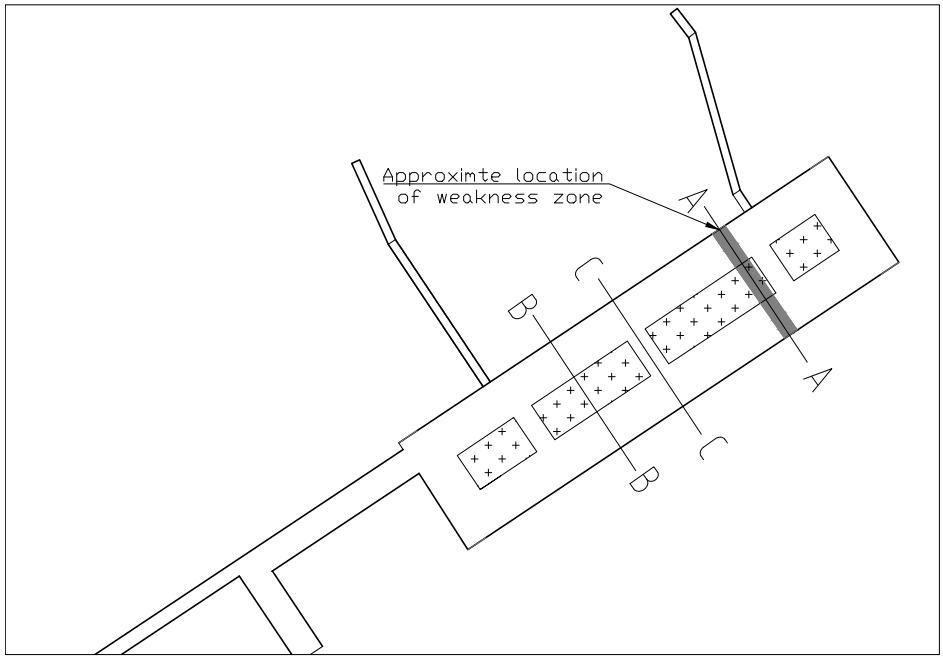

Figure 7.1: Overview of the cavern. The sections chosen for the model are marked on the sketch.

Subsurface characteristics of the weakness zone are not known however it assumed that they propagate into the mountain. Modelling the weakness zone is done in correspondence to figure 7.1.

Based on descriptions of the cavern the model for each section was created in $Phase^2$

and results are presented in figures 7.2 and 7.3.

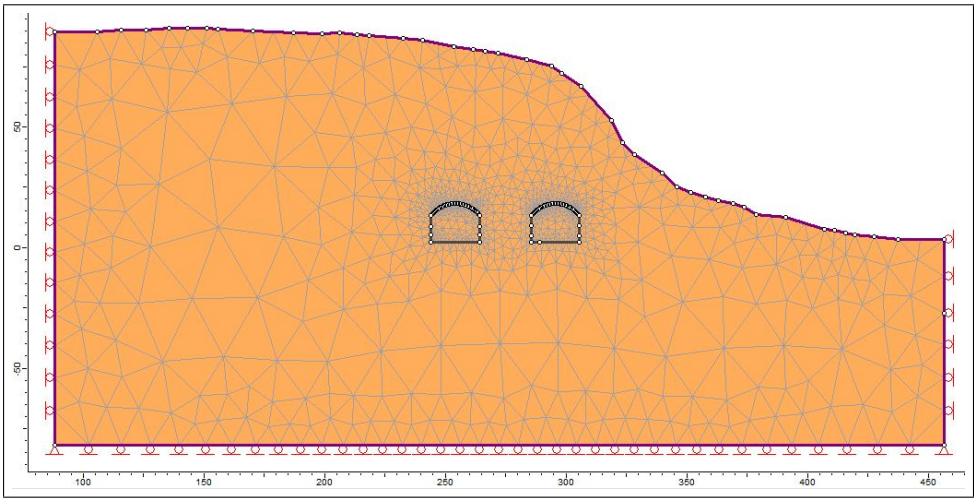

Figure 7.2: Scale correct model of the mountainside where the cavern is planned

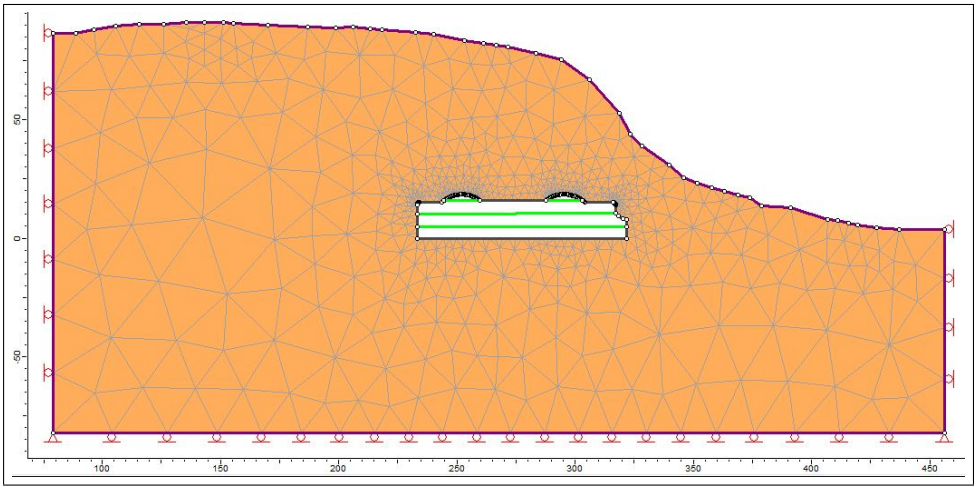

Figure 7.3: Scale correct model of the mountainside where the cavern is planned

As shown on figures 7.2 and 7.3 the lower boundary is vertically restrained (x-roller), and horizontal restraint (y-roller) on the left and right boundary. Lower corners are

restrained in all directions. The surface condition is "free surface".

The geometry of section C-C is demonstrated in figure 7.3. Mountainside geometry was carefully drawn in the model based on digital map data. Number of nodes are increased since distribution around excavation should be sufficient, this has been carried out in figure 7.2, but not 7.3.

7.4 Stress distribution around the cavern

As discussed in previous chapters there are no reliable data of stress distribution in the area. Modelling is therefore carried out under different stress conditions. Norway is special in regards to its distribution of horizontal stress, which are of large magnitudes shallow in the surface. Modelling the mountainside gives a good overview of the stress distribution within the rock mass. Listed below are the main conditions for the model:

- All rock parameters are based on discussion in chapter 5. A fitting GSI value for good quality rock is assumed to be 70-75.
- The model was carried out with $\frac{\sigma_h}{\sigma_v}$=0.075, 1 and 3. This assumes respectively no tectonic stress ($\sigma_1 = 2$, $\sigma_3 = 0.15$ at cavern elevation, see chapter 2), tectonic stress is equal to vertical stress, and horizontal stress is triple the magnitude of vertical the stress.
- The chosen failure criteria is Hoek-Brown because instabilities are believed to be dictated by joints.

Figure 7.4 shows the model with no horizontal stress component other than those occurring due to the rocks elasticity and the overburden, described with a K factor of 0,075. As seen on figure 7.2 vertical stresses in the model coincides with the analytical approaches with around 2 MPa in the roof. Part of the cavern is located under less overburden and shows lower magnitude of σ_v, see figure 7.2.

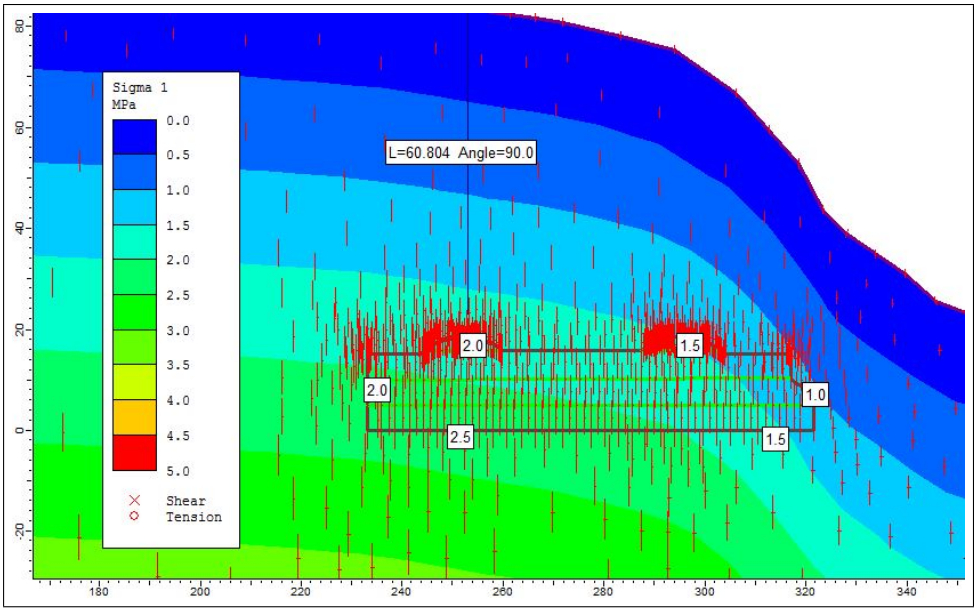

Figure 7.4: The model showing mountainside stress distribution with $k = \frac{\sigma_h}{\sigma_v} = 0.075$ before excavation. The largest principal stress is shown as text-boxes on the excavation boundaries.

Values of σ_3 varies between 0.1 and 0.2 MPa depending on the overburden. It is consistent with the predicted analytical values.

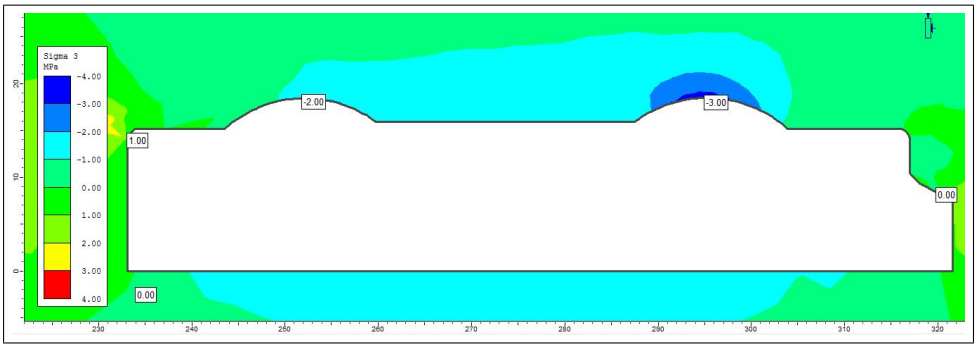

Figure 7.5: Model of section C-C (7.1) with $k = 0.075$. The model shows the occurrence of tensile stresses in the roof and critical tangential stress in the corners.

When excavating the Caverns the stress distribution will change and adapt to the opening of the cavern as shown in figure 7.5. The model implicates that the low horizontal stress causes the roof to be exposed of tensile stress as clearly visible in

figures 7.5 and 7.6.

It should be mentioned that modelling section C-C in this manner will generate some error. This is because $Phase^2$ assumes the cavern's geometry as being infinite out of the plane. The model in fact neglects all the effects of the pillars. Results concerning section C-C will not be taken as representative for the excavation, but used together with section B-B as indicator of stress and deformation tendencies.

Figure 7.6 show simulation of section B-B ideally presenting the cavern with no connecting tunnels between the two main caverns.

Under described stress state the model indicates that even though the span is considerably less than for section C-C, the roof will be exposed to low magnitude tensile stresses. Comparison of tangential stress and tensile/compressive strength of the rock can be visualized in figure 7.7. The model suggests that excavation will be stable with minimum strength factor along the periphery of the roof just above 1. However, the strength factor is too low to conclude that the structure would be stable without any support.

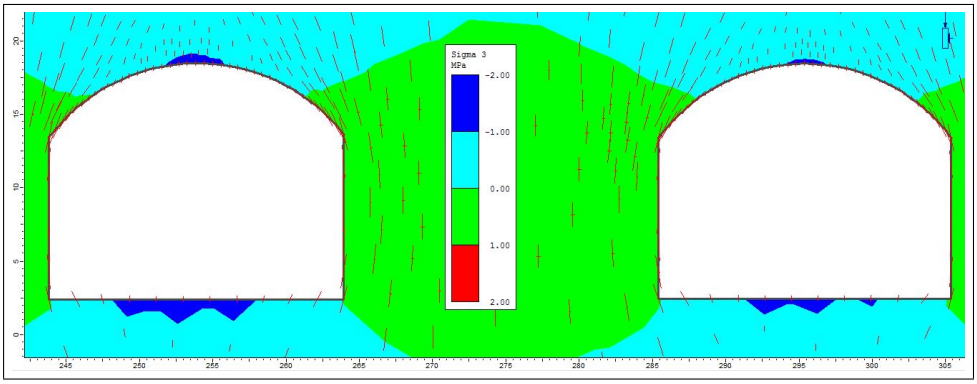

Figure 7.6: Model ran of cross-section B-B (Figure 7.1). k = 0.075, GSI=75. The model shows occurrence of tensile stresses in the roof. No critical tangential pressure can be found around the opening.

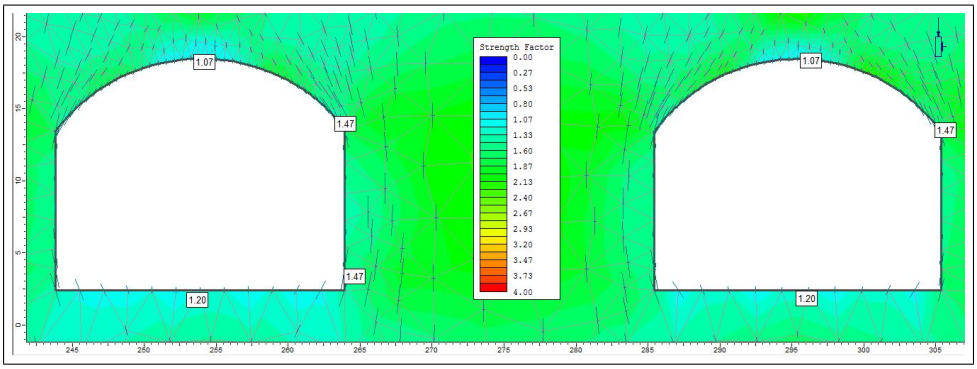

Figure 7.7: Model ran of cross-section B-B (7.1), visualizing relationship between rock mass strength and compressive/tensile stress. $k = 0.075$, GSI=75.

As discussed in previous chapters there is large uncertainty regarding magnitude of horizontal stress. Hence will simulations be performed with k varying between 0.075 and 3.

In figure 7.8 the model is ran with $k = \sigma_h / \sigma_v = 1$.

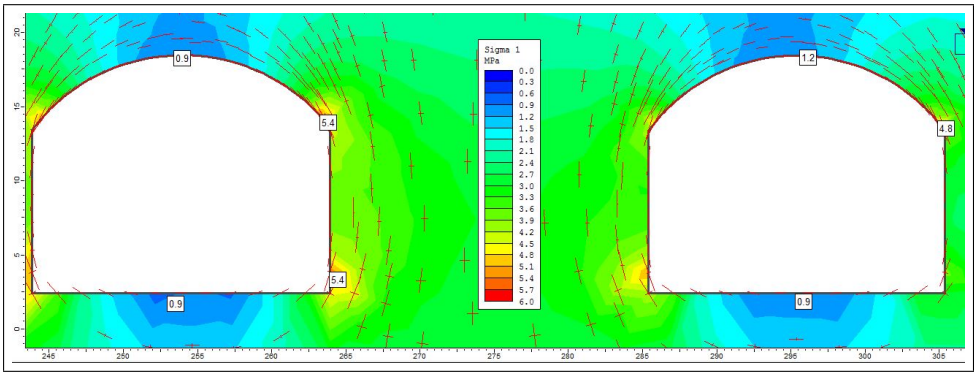

Figure 7.8: Model ran of cross-section B-B. $k = 1$, GSI=75.

It is clearly visible on figure 7.15 that stress ratio k= 1 is more favourable for this excavation. No tensile stress occurs along the periphery of the excavation. Also tangential stress does not come near the spalling strength which was estimated to 20 MPa computed using equations in Panthi (2012) and Hoek et al. (1998).

Low tangential stress in the roof is noticeable which could indicate problems with block fall if not unsupported.

Figure 7.9 shows the model when ran for k=3 before excavation of the caverns. Here the horizontal component is three times higher than the vertical component.

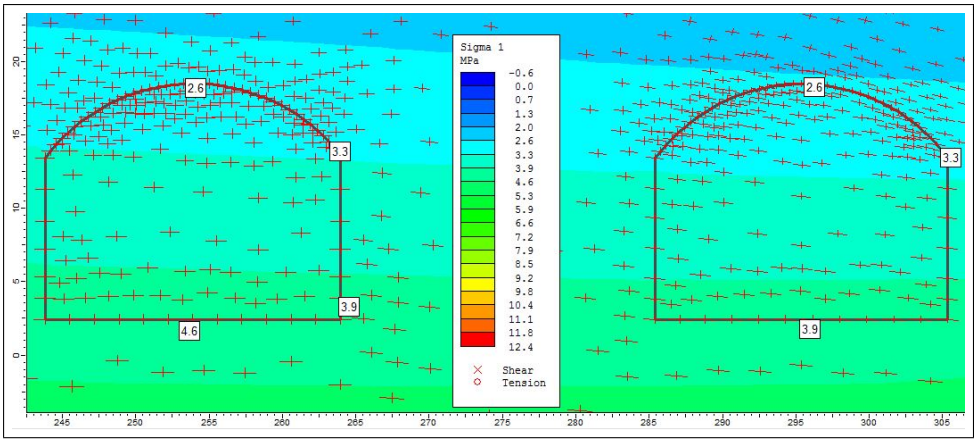

Figure 7.9: Model ran of cross-section B-B (7.1) visualizing σ_1 before excavating. $k = 3$, GSI=75.

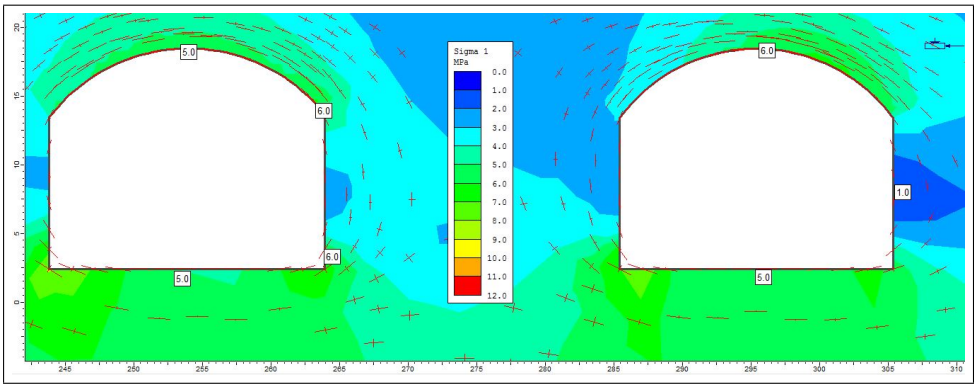

Figure 7.10: Model ran of cross-section B-B (7.1) visualizing σ_1 after excavation. $k = 3$, GSI=75.

Figure 7.10 indicates more favourable conditions than with k=0.075. This is typical for larger span caverns as discussed earlier in case of the Gjovik cavern which relies on

strong horizontal stress to keep the roof stable. However, low magnitude tangential stress are now found in the wall of the outer cavern.

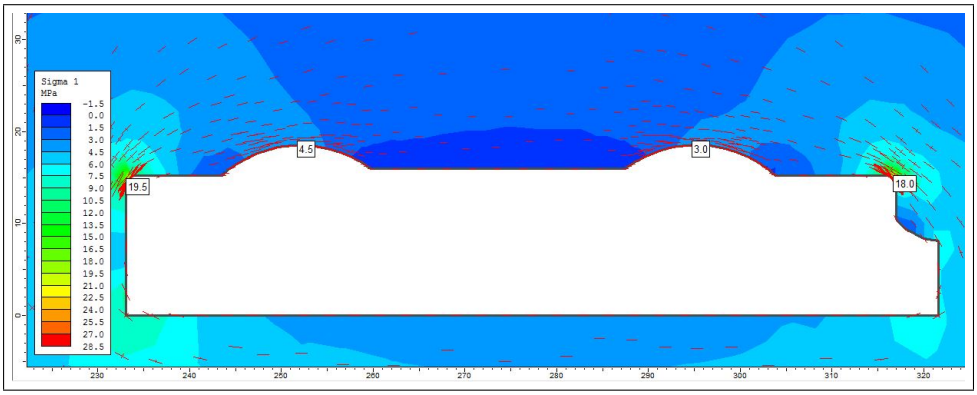

Figure 7.11: Model ran of cross-section C-C (7.1) visualizing σ_1 after excavation. $k = 3$, GSI=75.

Modelling section C-C with k=3 shows largest principal stress at cavern, it elevation is about 3-4 MPa before excavation. This stress magnitude does not result in unstable rock according to analytical analyses. However, because the caverns geometry is complex sharp corners are vulnerable to high tangential stress in the in the corners of the roof/wall, see figure 7.11. This differs from the analytical prediction by that stability problems could occur at smaller horizontal stress magnitudes.

7.5 Adding support measures

The following analyses use the same models as presented above but support schemes as discussed in chapter 5 will be added to the excavation. It is assumed the use of 25 mm CT bolts, whose support parameters is obtained from manufacturer (VIKorsta, 2014). In figure 7.13 section C-C is presented with suggested support for good rock conditions. Since bolt patterns are center-center distance based, there will be no difference in the modelling in regard to bolt pattern in the cavern and the normal running tunnel.

Figure 7.12 show plastic analysis depicting minor tangential stresses and yielded

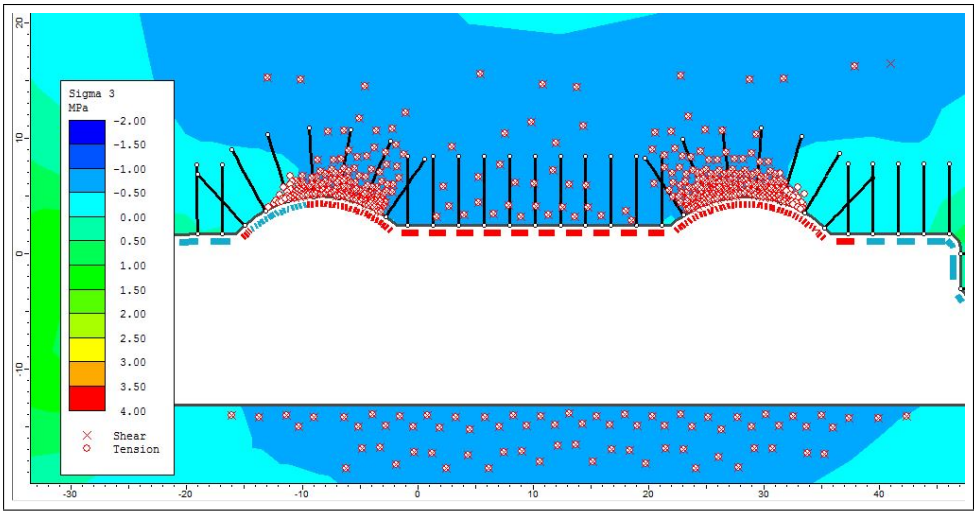

Figure 7.12: Model ran of cross-section C-C visualizing σ_3. $k = 0.075$, GSI=75.

nodes in the rock mass around the excavation for section C-C. As discussed earlier this geometry neglects effects of the pillars and thus shows significantly pessimistic conditions. Yielded elements extent beyond support length. If an element is yielded it means that the material fails in either shear, tension, or both. The percentage of yielding denotes the percentage of yielded elements connected to a node. Bolts are not yielded, and withstand sufficiently for the current condition. If compared to analysis of section B-B, one can reflect on the importance of the pillars for the roof stability.

Plastic analysis of section B-B shown in figure 7.13 depicts much more stable conditions than for section C-C. This model produces more accurate image of the pillar stability, figure 7.13. The model predicts that yielded elements extend a few meters from the roof at most, and that coverage of bolts are good. The results from the model indicate that support suggested by Q-system is sufficient. Elastic analysis show that the lowest strength factor, 1.3, is in the roof.

The same simulation is done for k=1 and presented in figure 7.14 and 7.15.

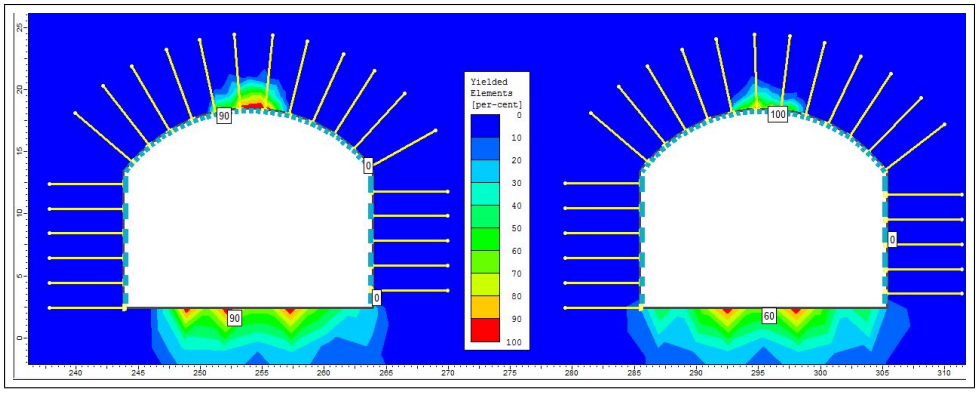

Figure 7.13: Model ran of cross-section B-B (7.1) depicting yielded elements. $k = 0.075$, GSI=75.

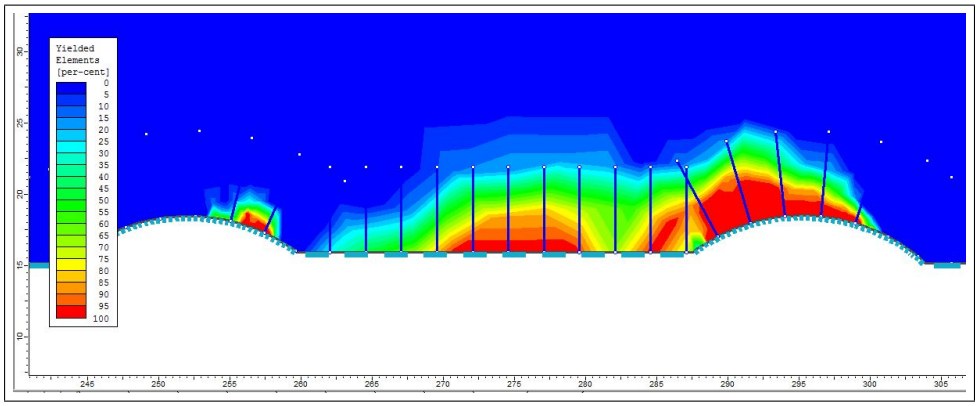

Figure 7.14: Plastic analysis of section C-C depicting yielded elements. $k = 1$, GSI=75.

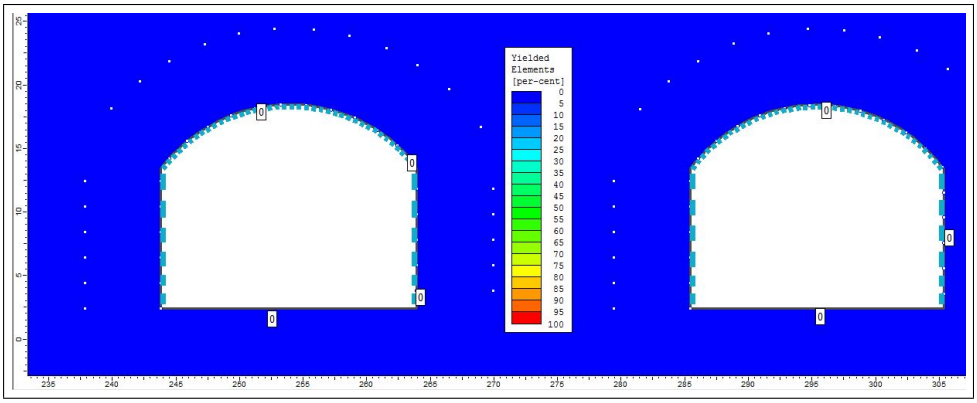

Figure 7.15: Plastic analysis of section B-B depicting yielded elements. $k = 1$, GSI=75.

In figures 7.14 and 7.15, indicate that support is sufficient, in hydrostatic stress state the rock support will hold without any problems. Results from plastic analysis where k=3 shows enhanced stability in the roof.

7.6 Strength factors

During elastic analyses there were an occasion where safety factor of below 1 was detected in section B-B. If strength factor is below 1, it indicates that the material strength is lower than the induced stress at a given point around the excavation. The case is showed in figure 7.16 where k=0.075. Viewing section B-B one does not take into account geometry of section C-C. General conclusion can be made from section B-B that additional support is needed when the cavern is not influenced by horizontal stress, see figures 7.17 and 7.16. The assumption of no horizontal stress impact, is not completely accurate when looking at results from chapter 4 where it is stated that some horizontal stress is present. It is believed that the stress originates from compression from drifting activity of the Mid-Atlantic ridge, quantified around 0.2-2.9 MPa

Since cavern elevation is 60 m deep it seems fair to assume that stress at cavern elevation lies in the upper part of the spectrum. These indications are most favourable

for the stability of the cavern with the current support scheme for k=1 and k=3.

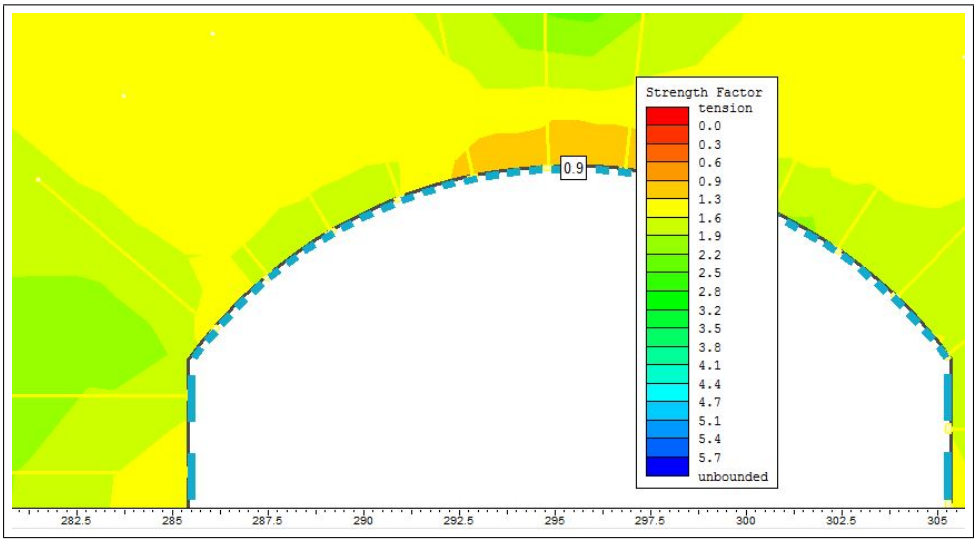

Figure 7.16: Section B-B showing low strength factor in the roof. K=0.075. Shotcrete thickness is 6 cm.

By adding an additional layer of shotcrete of 6 cm, the safety factor increased from 0.9 to 1.3, see figure 7.17. Analysis of section C-C is believed to be too imprecise for studying safety factors.

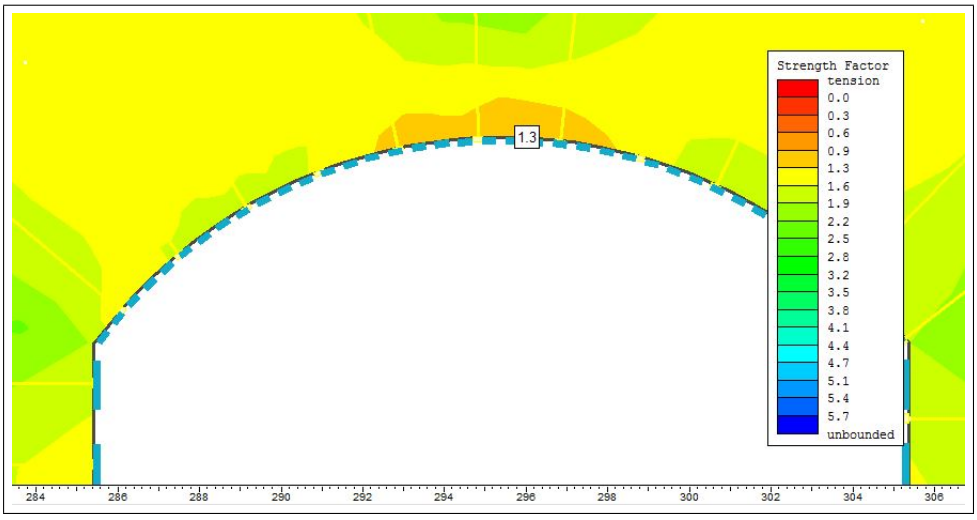

Figure 7.17: Sufficient strength factor in the roof for section B-B. K=0.075. Two shotcrete layers of 6 cm each is added

Deformation of the rock in the cavern was also modelled and showed almost no deformation (few millimeters), which matches to earlier discussions. This can be explained because of the low overburden and the rock's high elastic properties. Also in section C-C the model displayed little deformation, around 2 cm in the middle arc of the connection cavern. The magnitudes of the deformation is though over estimated since the effects from the pillars are neglected.

7.7 Modelling weakness zone

As discussed earlier the is one major weakness zone in the supposed excavation area. Observations about that zone is limited as no core drilling has been carried out in the area, as was discussed in detail in chapter 5. The weakness zone has an estimated GSI varying between 25-30 which has showed correlates a Q-value of 0.07-0-1. The reason the GSI system is emphasized in the analysis, is that the $Phase^2$ allows for a simple description of rock mass with regards to this classification system. Observations at surfapoint at high level jointing and small blocks. This strongly decreases the materials ability to absorb horizontal stress. It is therefore fair to assume a very small horizontal stress component in the zone described with k=0.075. Hoek-Brown parameters used are presented in table 7.1.

Table 7.1: Hoek-Brown input in the model

mb	s	a	ϕ (°)	c (MPa)	GSI
1.9	0.0004	0.522	33	5.7	30
1.58	0.0002	0.531	30	5	25

It is suggested as a rule of thumb that Poisson's ratio for rock mass is approximately 1.2 times that of intact rock e.g. $\upsilon_{rm} = 1.2\upsilon_{ir}$. Table 7.2 shows output of the estimated parameters.

Table 7.2: Hoek-Brown rock mass strength outputs

Compr. strength (MPa)	Deformation modulus (MPa)	Tensile strength (MPa)	GSI
2	976	0.026	30
1.5	720	0.018	25

Support measures for the weakness zone are suggested as radial 6 m long CT-bolts (c/c=1.2), and spiling bolts in combination with shotcrete and steel reinforced arches. Reinforcement used in the subway tunnel in Oslo is the 3-bar lattice girder, and is used in the analyses. 2D analysis of weakness zones have many disadvantages. Deformations will be overestimated as the weakness zone's thickness is assumed infinite. Effects from surrounding more massive rock is neglected. The model will show slightly optimistic results regarding the neglected effects of the connection tunnels since only section B-B is modelled. The effect of spiling bolts are hard to model in 2D because their yield is dependent on the shotcrete arches, and the improvement to rock mass they represent is very hard to quantify. Hence, they are neglected in the analysis.

As a supplementary investigation $Phase^2$ allows for 3D axisymmetric modelling. It bases on a tunnel profile drawn in 2D which is rotated symmetrically around an axis. The result will be a cylindrical representation a cavern in 3D. Geometrical errors will be largest in the lower half of the cavern where the periphery is not circular. The geometrical error will be lowest in the roof and hence best represent conditions here. The model will constitute a 100 meter section of the cavern including the weakness zone where it is anticipated to intersect. The main goal of the 3D model is to support deformation magnitudes obtained in the 2D analysis. It is not possible to add rock bolts in the 3D model but liners are possible.

2D elastic analysis of the weakness zone section A-A carried out with k=0.075 and rock mass quality GSI=25 is shown in figure 7.18.

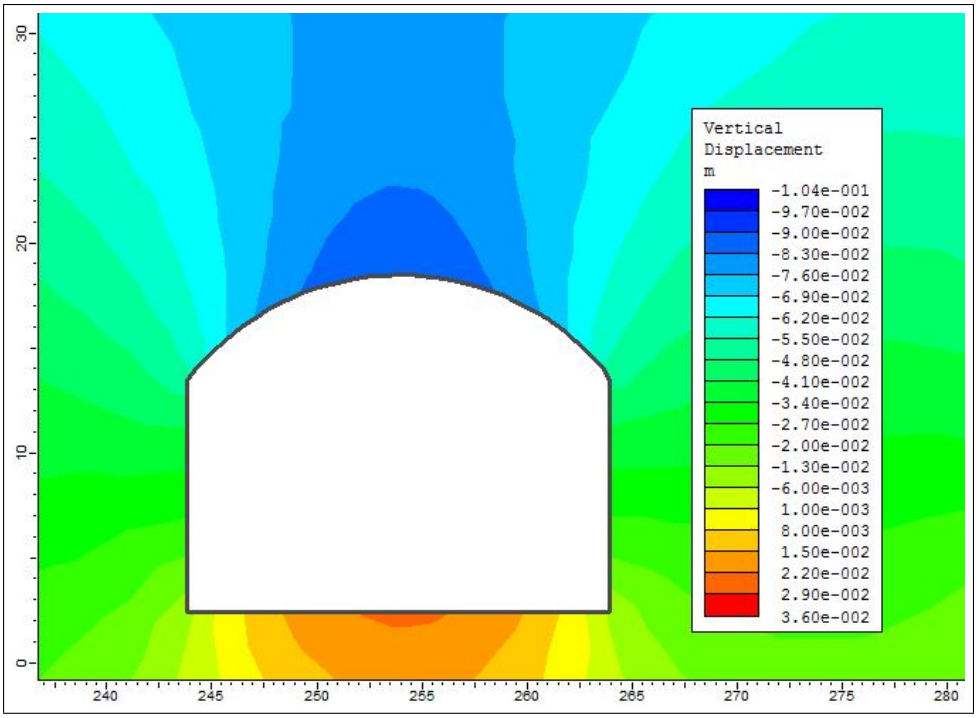

Figure 7.18: Elastic analysis of weakness zone with k=0.075

Deformation is indicated to be 8-9 cm downward motion in the roof, see figure 7.18. Compared to analysis in the code Rocsupport (chapter 5) the numerical model produces slightly higher deformation.

The most prominent reason for the difference between the models is the requirement of hydrostatic stress conditions in code Rocsupport. Both models will overestimate deformation as discussed earlier. Analysis performed with slightly better rock mass quality (GSI=30) does not represent any significant change in deformation. Uncertainty is considered larger that difference in output.

The 3D elastic model is shown in figure 7.19. Same parameters are used to compute the 3D model as for the 2D, see figure, see figure 7.20.

Magnitudes of displacement is about one third compared to the 2D model e.g. around

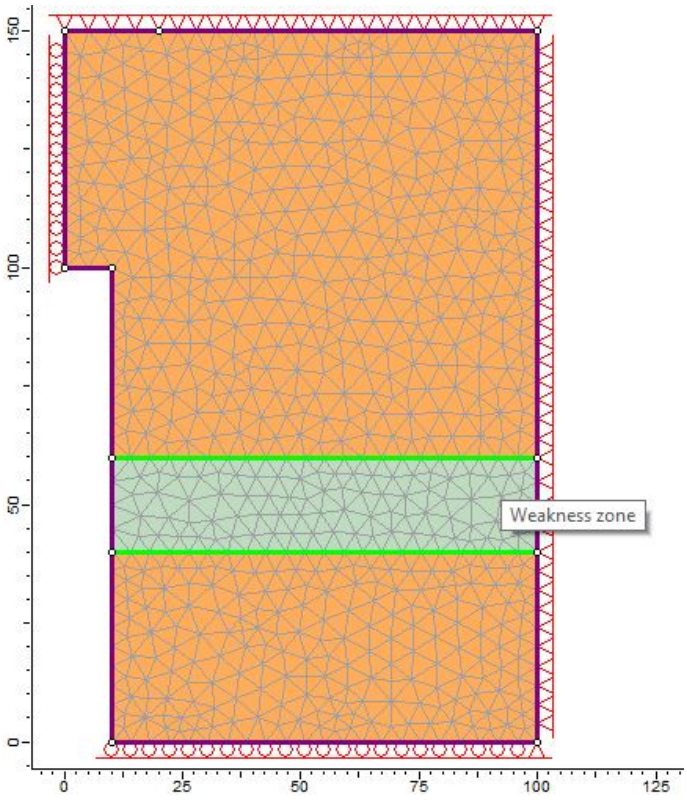

Figure 7.19: Representation of 2D geometry in axisymmetric elastic 3D modelling of the weakness zone problem. Rotation occurs around axis x=0.

2 cm towards the excavation. GSI value for worst case(25)was chosen. The axisymmetric model does not neglect the intact rock around the weakness zone. Error in the axis symmetric model would revolve around the geometry being represented as a cylinder. In addition the 3D model neglects effects of the second cavern which does according earlier analysis affect the stress state.

Based on the output, deformation in the order of 2-7 cm is expected as a minimum in the weak rock mass.

Requirement of liner thickness may be estimated from elastic 3D modelling. A sufficient strength factor was not obtained using solely liner suggested in the Q-system, see figure 7.21.

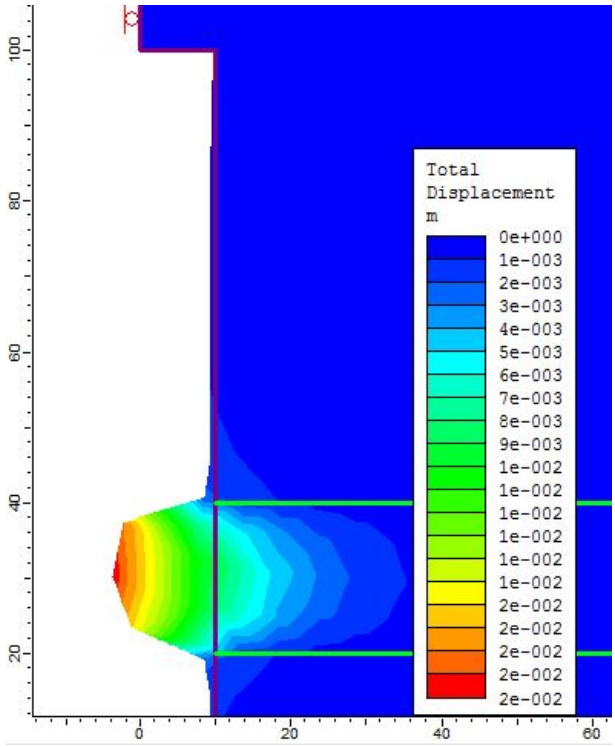

Figure 7.20: Simulation of axisymmetrical weakness zone problem.

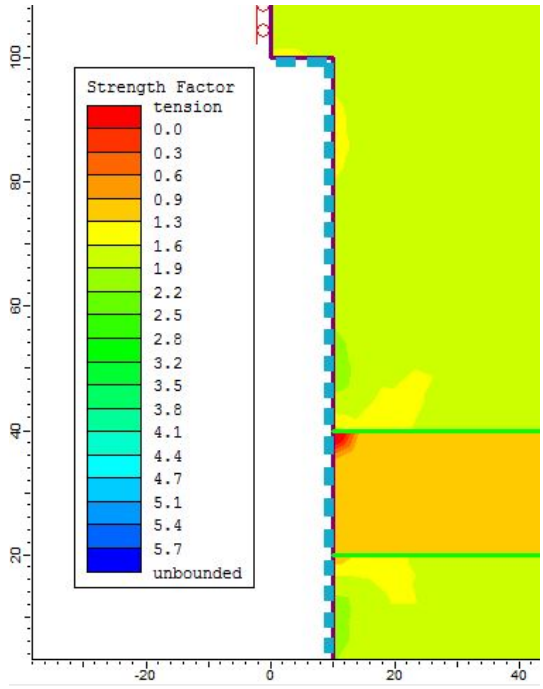

Figure 7.21: Simulation of axisymmetrical weakness zone problem.

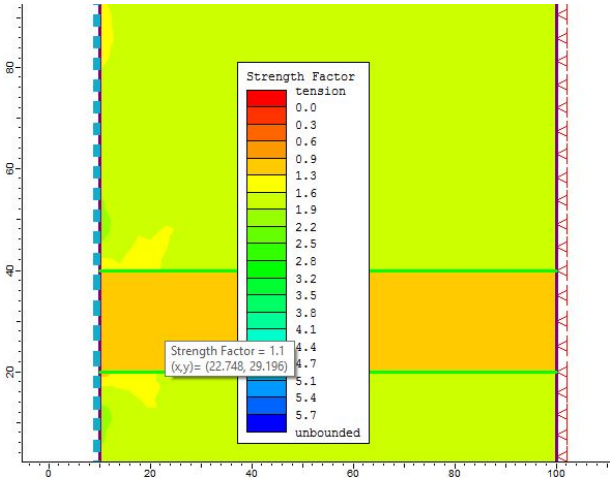

Figure 7.22: Simulation of axisymmetrical weakness zone problem.

By adding additionally 10 cm of shotcrete, a safety factor of 1.3 was reached shown in figure 7.22. Keep in mind that no rock bolts are allowed in the 3D analysis.

Plastic analysis of the weakness zone is modelled in 2D with same support scheme. GSI value is assumed worst case (25). Loading is carried out with above mentioned assumptions e.g. k=0.075.

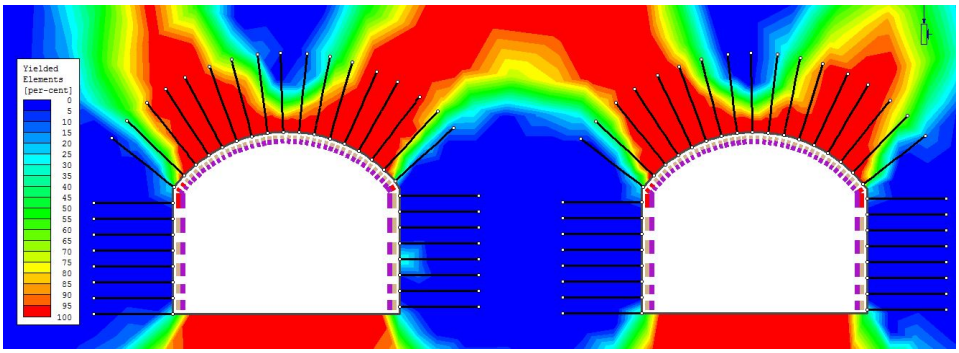

Figure 7.23: Plastic analysis with support scheme presented in Q-system

Figure 7.23 shows yielded elements extending in some places beyond the bolts. Bolts do not fail which indicates that support is sufficient. The inner layer of 15 cm shotcrete fails in the corners of the excavation. The steel rib shotcrete girder seems to be sufficient to stabilize the excavation.

The analysis indicates deformation between 2-9 cm in the weak rock zone. It is concluded that support suggested by the Q-system will hold for the excavation. The analysis deals with lots of uncertainty. Block fall can be assumed a problem in a weakness zone, and spiling bolts ahead of face are used to stabilize the it. Spiling bolts have not been modelled, and could have positive effects on final stability. Since $Phase^2$ 2D analysis neglects the width of weak rock zone, deformation is assumed to be slightly over estimated. 3D analysis with the axisymmetric model show about 3 times less deformation but neglects the effect of there being two caverns close to each other. Since yielded elements extend beyond bolt length in low stress regimes (k=0.075) it should considered to use c/c=5 m, 15 m long steel wires, as used in the Gjøvik cavern. In good rock conditions the model indicates that the suggested support schemes will hold, and little deformation will occur, if there are present some horizontal stress.

8. Concluding remarks

Determining required rock support for the excavation is done analytically and empirically and investigated numerically. It was found that the cavern would be sufficiently supported by rock bolts with c/c distance 2.5 m and 6 cm of shotcrete for good quality rock conditions. Additional shotcrete is is required should there be no tectonic horizontal stress in the project area. A bolt length of 2 metres is sufficient for best case scenario however, empirical schemes backed up by numerical modelling indicate that bolt length should be increased to 6 m for excavation spans of 20 metres. If horizontal stress exceeds 14 MPa longer bolts are required as suggested in chapter 5 however, these magnitudes are believed to be unrealistic. Good rock quality conditions show deformation of only a few mm of downward movement in the roof, and a few mm inwards in the walls.

In the weak rock mass (in the weakness zone) both analysis in code Rocsupport and Q-system show that sufficient rock support would consist of 6 m c/c=1.3 m rock bolts in addition to 15 cm of shotcrete reinforced with steel arches either T-bar type or 3-bar lattice girder as used in the Oslo subway tunnel. Spiling bolts are believed required if the weakness zone cross the excavation to ensure face stability. Numerical modelling confirm that support is sufficient based on the estimated parameters. Although uncertain, numerical modelling suggests 2-9 cm roof deformation in weak rock conditions.

There is expected to be water present at cavern elevation. It is however not anticipated large inflow in good rock quality, but some drip. It is concern that rock mass near the

weakness zone may contain more water, for instance highly conductive cracks connected to ponds at the surface. Consequences could be large inflow and possibly draining of ponds. Thus it is concluded that ahead of face probe drilling is necessary one "cavern width" before intersection with weak rock. Water loss test needs accordingly is to be performed with three boreholes, one in the roof and two at the wall/roof corner. Grouting will have to performed systematically by injecting grout up to pressure to twice the hydrostatic pore pressure should loss of water exceed 0.5 L/min per meter borehole length. Water in good rock conditions should be investigate before construction additionally. Experiences from the new Rv40 road through the mountain should be used to save cost in regard such investigations.

Simple analysis of frost intrusion to the cavern is carried out. It is concluded that frost will enter the cavern under ventilation concepts assumed in the model but temperatures are expected slightly lower inside than outside during cold periods. Accordingly, it the cavern will have to be mitigated for frost. Suggested frost mitigation using light concrete plates and XPS or PE-foam, is presented in chapter 6.

Bibliography

Adresseavisen[online] (2004). Ras i vaeretunnelen[online]. Available at $http$: $//www.adressa.no/nyheter/sortrondelag/article$350575.$ece$.

Altaposten[Online] (2013). Skammens tunnel.

Alvarez, D. L. (2012). Limitations of the ground reaction curve concept for shallow tunnels under anisotropic in-situ stress conditions. *Master thesis*.

Barton, N. (1974). A review of the shear strength of filled discontinuities in rock. *Norwegian Geotech. Inst.*, No. 105.

Barton, N. (2000). Tbm tunnelling in jointed and faulted rock. *Balkema, Rotterdam*, page 167pp.

Barton, N., Lien, R., and Lunde, J. (1974). Engineering classification of rock masses for the design of tunnel support. *Rock Mechanics by Springer-Verlag*, 6:189–236.

Bienowski, Z. T. (1976). Rock mass classification in rock engineering. *Exploration for rock engineering, proc. of the symp*, 1:97–106.

Bollingmo, P. (1974). Ingeniorgeologiske erfaringer fra prosjektering og bygging av haller i fjell. *Fjellsprengningsteknikk, Bergmekanikk*.

Broch, E., Myrvang, A., and Stjern, G. (1996). Support of large rock caverns in norway. *Tunnelling and Underground Space Technology*, 11, no.1:11–19.

Byggforsk and Meteorologisk Institutt (2012). Klimadata for termisk dimensjonering og frostsikring. *Buggforskserien, byggdetaljer*, May.

Duffaut, P. (2003). The traps behind the failure of malpasset arch dam, france, in 1959. *Journal of Rock Mechanics and Geotechnical Engineering*, Volume 5 issue 5.

Genisa, M., Basarirb, H., Ozarslana, A., Bilira, E., and Balabanc, E. (2007). Engineering geological appraisal of the rock masses and preliminary support design, dorukhan tunnel, zonguldak, turkey. *Engineering Geology*, 92:14–26.

Hoek, E. and Brown, E. T. (1980). Underground excavations in rock. *London: Institution of Mining and Metallurgy*.

Hoek, E., Carranza-Torres, C., and Corkum, B. (2002). Hoek-brown failure criterion. *Proceeding North American Rock Mechanics Society Meetting*.

Hoek, E. and Marinos, P. (2000). Predicting tunnel squeezing pproblem in weak heterogenous rock masses. *Tunnels and Tunneling International*, Part 1 November 2000, Part 2, December 2000.

Hoek, E., Marinos, P., and Benissi, M. (1998). Applicability of thegeological strength index(gsi) classification for veryweak and sheared rockmasses. the case of the athens schist formation. *Bull Eng Geol Env SpringerVerlag*, 57:151 160.

Keevil, N. B. and Caldwell, J. (2012). Block caving. *INstitute of mining engineering, University of British Columbia*.

Kluver, B. H. and Kveen, A. (2004). Berginjeksjon i praksis. *Miljo og samfunnstjenelige tunneler*.

Kukkonen, I., Kivekas, L., Vuoriainen, S., and Kaaria, M. (2010). Thermal properties of rocks in olkiluoto in finland: Results of laboratory measurements.

Loeseth, F. and Kveldsvik, V. (1997). Ingeniorgeologi - praktisk bruk av q-metoden. *Norges Geotekniske Institutt*. 592046-2.

Loew, S., Barla, G., and Diederichs, M. (2010). Engineering geology of alpine tunnels: Past, present and future. geologically active. *Taylor and Francis Group, London*. Williams et al. (eds). ISBN 978-0-415-60034-7.

Martin, C. D. and Christiansson, R. (2009). Estimating the potential for spalling around a deep nuclear waste repository in crystalline rock. *International Journal of Rock Mechanics and Mining Sciences*, 46, issue 2:219–228.

Myrvang, A. (2001). Bergmekanikk. *Institutt for Geologi og Bergteknikk,NorwegianUniversity of Science and Technology*.

NGI[online] (2013). Q-system. *NGI.no*. Available at :$http$: $//www.ngi.no/en/Contentboxes-and-structures/Main-page/Feature-articles-/Q-system-update/$. Assessed 24.03.2014.

NGU (2014). Ngu bergrunnskart fra kvaloya. $[ONLINE]Availableat$: $http$: $//geo.ngu.no/kart/berggrunn/.Assessed$19/102.2014..

Nilsen, B. (2012). Stabilitet av fjellskjaeringer. *Lectures in the course Ingerniorgeologi Grunnkurs, NTNU*.

Nilsen, B. and Thidemann, A. (1993). Hydropower development rock engineering. *Norwegian Institute of Technolog, Division of hydraulic Engineering,*, N-7034:5–50, 7–110. Trondheim Norway.

Oftedahl, C. (1974). *Norges Geologi*. Sit Tapir. ISBN:82-519-0089-1.

Palmstrom, A. (1995). Rmi:a rock mass characterization system for rock engineering purposes. *PhD thesis, Oslo University*, page Appendix 3. METHODS TO QUANTIFY THE PARAMETERS APPLIED IN THE RMi.

Palmstrom, A., Nilsen, B., and Borge, K. (2003). Miljo og samfunnstjenelige tunneler: Riktig omfang av forundersokelser for berganlegg. *Statens Vegvesen*, 101.

Panthi, K. K. (2010). Uncertainty analysis for assessing leakage through water tunnels: A case from nepal himalaya. *Rock Mech Rock Eng*, 43:629–639.

Panthi, K. K. (2012). Evaluation of rock bursting phenomena in a tunnel in the himalayas. *Bull Eng Geol Environ*, 71:761–769.

Pascala, C., Roberts, D., and Gabrielsen, R. H. (2005). Quantification of neotectonic stress orientations and magnitudes from field observations in finnmark, northern norway. *Journal of Structural Geology*, Volume 25 issue 5:859–870.

Pedersen, K. B. (2002). Telehiv i vegtunneler:. Internal memo. Acessed: $http://www.vegvesen.no/_attachment/290288/binary/512552?fast_title = Frostinntrengning + og + frostdimensjonering + av + tunneler.pdf$.10.02.2014..

Pedersen, K. B. (2005). Frosttekniske problemer i norske vegtunneler. In *Frost i jord*.

Prabhata, K., Swamee, Govinda, C., Mishra, Bhagu, and Bhagu, C. (2000). Simple approximation for flowing well problem. *Journal of irrigation and drainage engineering*, january february.

Rocscience (2005). Phase2 version 6.0 - finite element analysis for excavations and slopes. www.rocscience.com. *OntorioToronto, Ontario, Canada*.

Rygh, J. A. (1999). Publikumshaller i fjell gjennom 25 aar - fra oddahallen til gjoevik olympiske fjellhall. *Fjellsprengningsteknikk, Bergmekanikk*.

Sheorey, P. (1997). Empirical rock failure criteria. *Balkema, Rotterdam*, page 176pp.

Snow (1965). Groundwater inflows during tunnel driving. *Engineering Geology*, 2-1:39–56.

Statens Vegvesen (2003). Undersokelser og krav til innlekkasje for aa ivareta ytre miljo. *Miljo og samfunnstjenelige tunneler*, 103.

Statens Vegvesen (2004). Injeksjon - erfaringer fra hagantunnelen. *Miljo og samfunnstjenelige tunneler*, 31. Internal report.

Statens Vegvesen (2005). Injeksjon - erfaringer fra jong - askertunnelene. *Seksjon for geo- og tunnelteknikk*. Teknologirapport nr. 2424.

Statens Vegvesen (2006). *Haandbok163: Vann- og Frostsikring i tunneler*. Statens Vegvesen. ISBN 82-7207-597-0.

Statens Vegvesen (2010). Haandbok021: Vegtunneler. In *Statens Vegvesen Haandboker*.

Stephansson, O. (1989). Stress measurements and modelling of crustal rock mechanics in fennoscandia. *Mathematical and Physical Sciences*, vol. 266.

SWECO NORGE avd. Narvik. Ingenioergeologisk rapport - parkeringsanlegg i fjell - hammerfest. 2013.

Trinh, Q. N., Myrvang, A., and Sand, N. S. (2010). Rock excavation and support for a crusher hall at rana gruber, norway. *Copyright 2010 ARMA, American Rock Mechanics Association*, 1.

Unknown (2013). Kaledoniden - den moderne fjellkjedes dype roetter. *GEO*, February 2013.

VIKorsta (2014). Ct-bolt m20. *Technical specifications*. N-6151 Orsta AS, www.vikorsta.no.

A. Fieldwork map

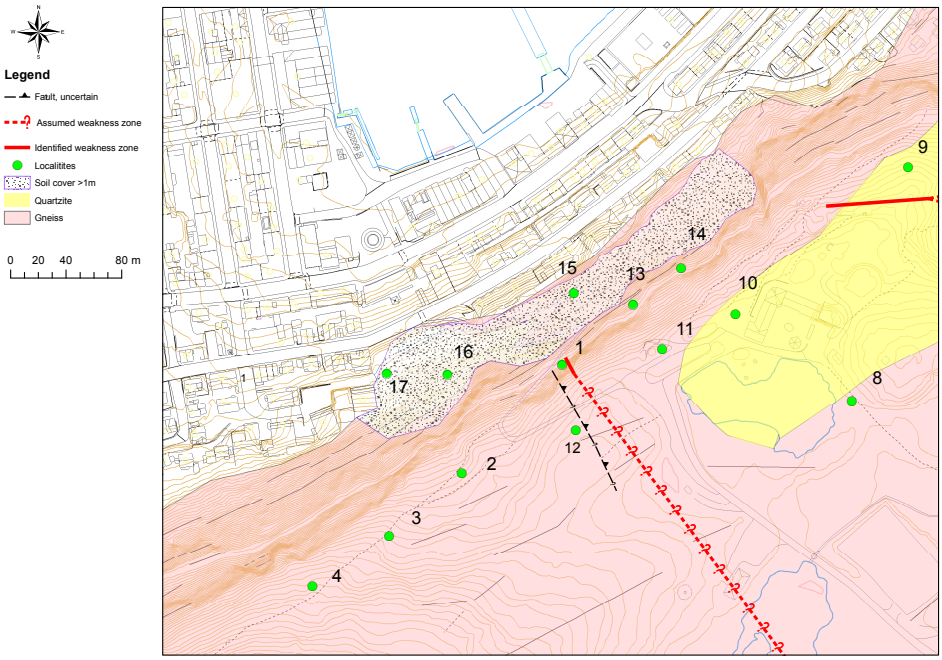

B. Cavern overview

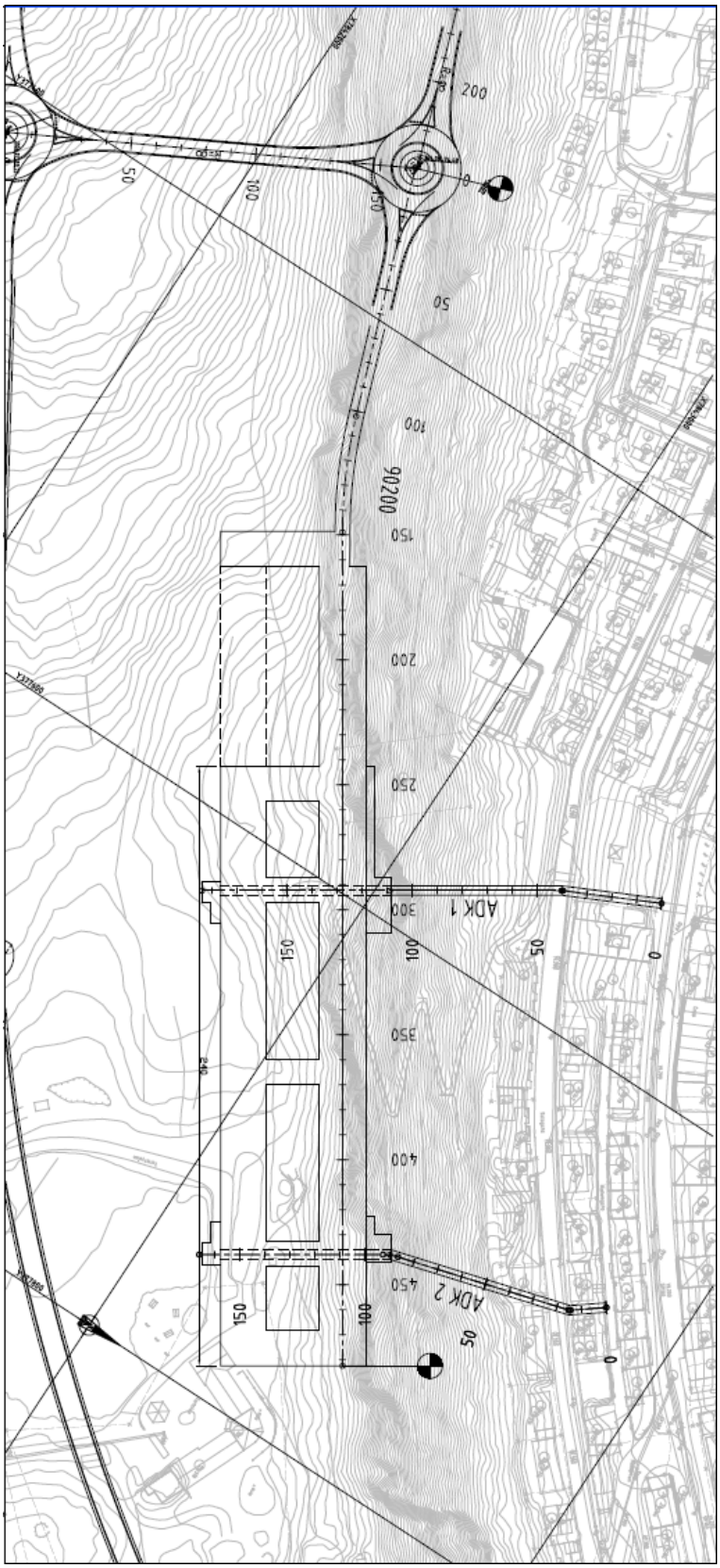
90200
ADK 1
ADK 2

C. Lowest level of cavern

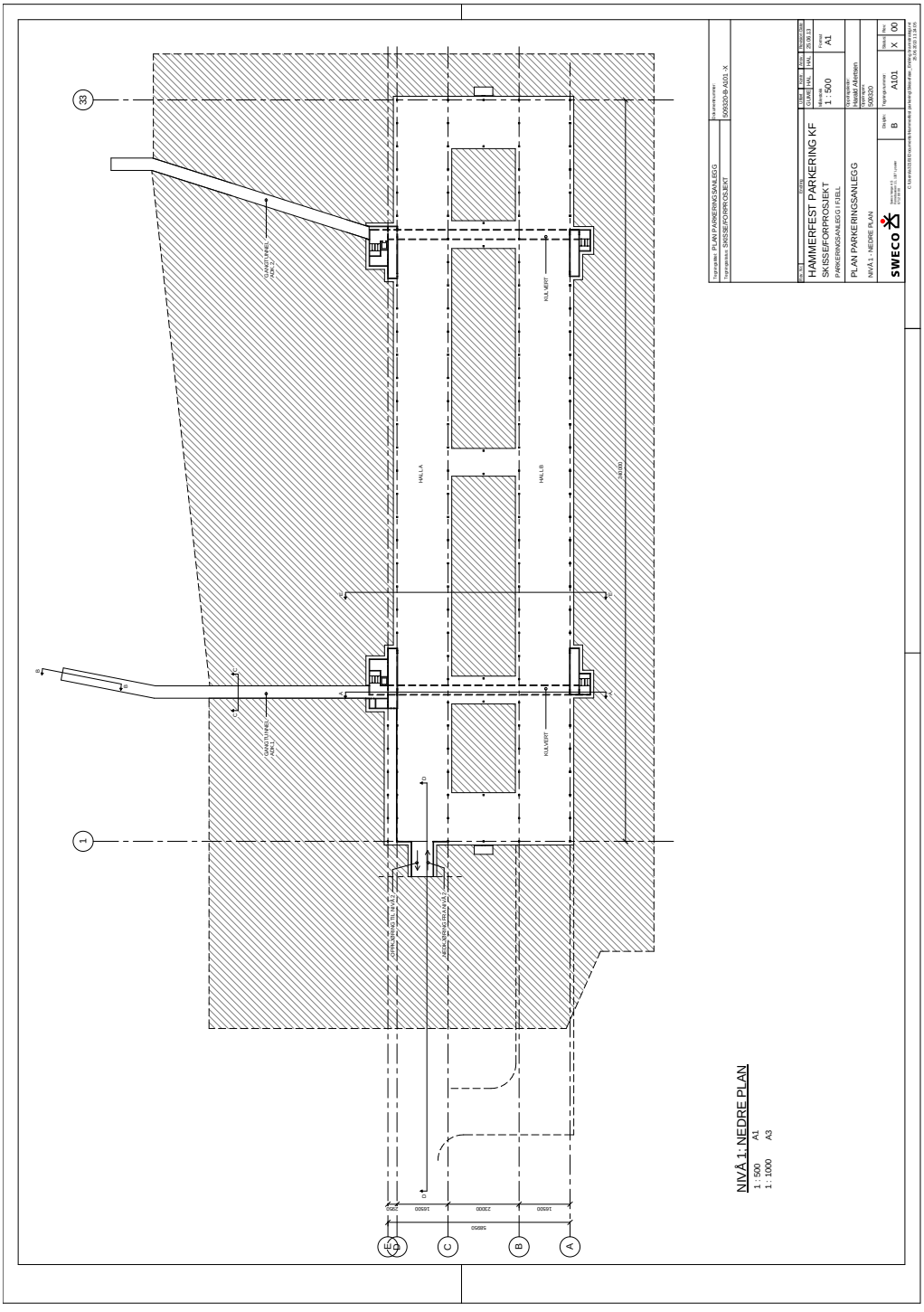
HAMMERFEST PARKERING KF
SKISSEFORPROSJEKT
PARKERINGSANLEGG I FJELL
PLAN PARKERINGSANLEGG
NIVÅ 1: NEDRE PLAN
SWECO
HALL A
HALL B
KULVERT
GANGTUNNEL
NIVÅ 1: NEDRE PLAN
1 : 500 A1
1 : 1000 A3

D. 1.st floor of cavern

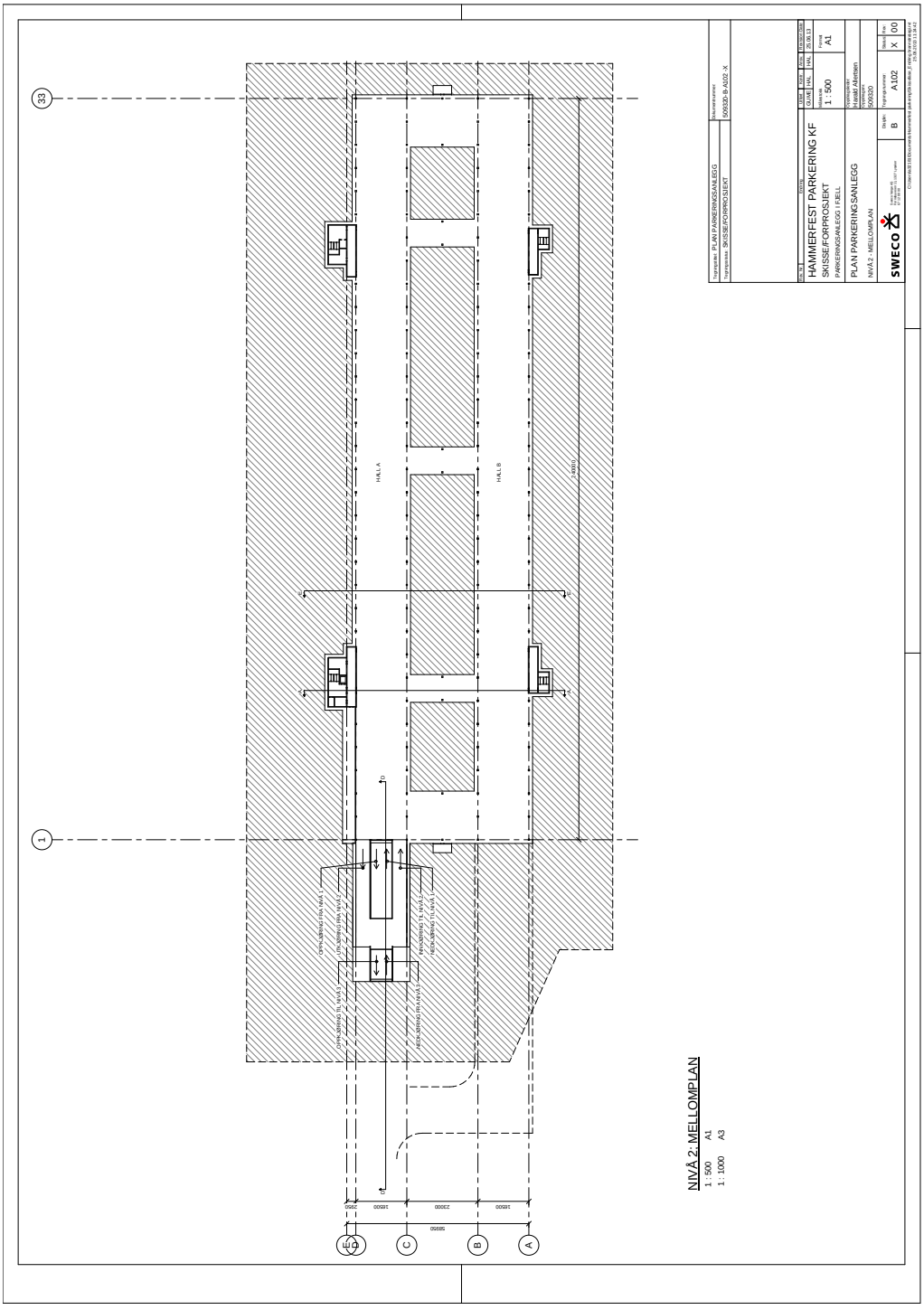
HALL A
HALL B
NIVÅ 2: MELLOMPLAN
1 : 500 A1
1 : 1000 A3
HAMMERFEST PARKERING KF
SKISSEFORPROSJEKT
PARKERINGSANLEGG I FJELL
PLAN PARKERINGSANLEGG
NIVÅ 2 - MELLOMPLAN
SWECO
A102

E. Top level of cavern

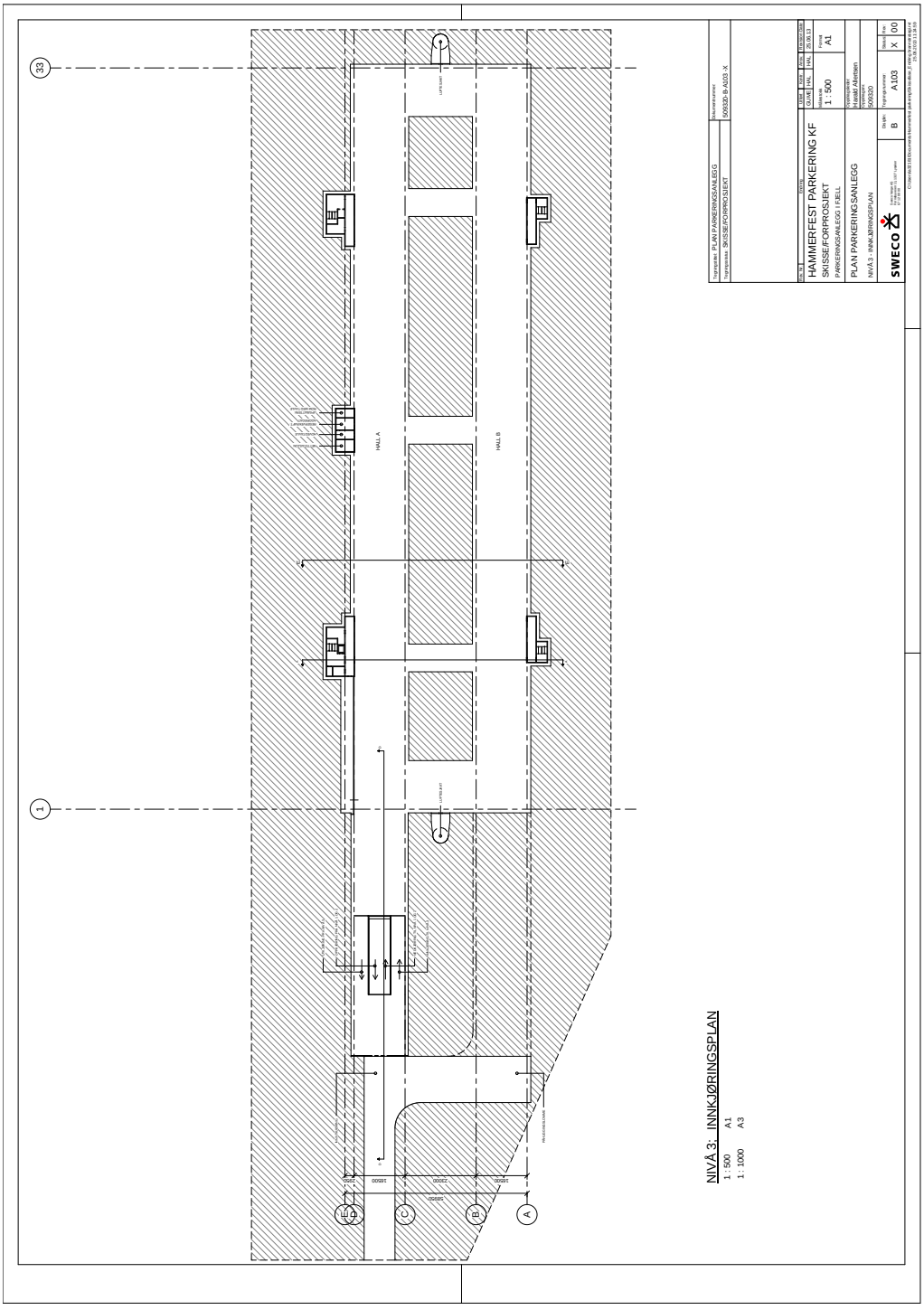
HALL A
HALL B
NIVÅ 3: INNKJØRINGSPLAN
1 : 500 A1
1 : 1000 A3
HAMMERFEST PARKERING KF
SKISSEFORPROSJEKT
PARKERINGSANLEGG I FJELL
PLAN PARKERINGSANLEGG
NIVÅ 3 - INNKJØRINGSPLAN
SWECO
A103
1 : 500
A1
B
X
00

F. Fracture rose diagram